Gas Absorption in Pulsating Liquids

James Howard Garstang

Presented for the Degree of Doctor of Philosophy

University of Edinburgh

1970

Acknowledgement

The Author would like to express his gratitude to Dr. M. H. I. Baird and Dr. D.M. Wilson for their help and encouragement in the preparation of this thesis, to his colleagues in the Departments of Chemical Engineering of the Universities of Edinburgh and Heriot-Watt for their assistance and advice, and to the Science Research Council for financial support.

Summary

During the present investigation the effect has been studied of bulk liquid pulsations upon the rate of absorption of oxygen into water from air bubbles.

The power input to the dispersion was measured from observations of the pressure/volume characteristics of the enclosed gas spaces of the absorption column. The absorption rate was measured in terms of the volumetric mass transfer coefficient ($k_L a$) by following the response of the column to a step change in the inlet gas composition. The oxygen concentration in the liquid was measured by means of a small polarographic cell.

Both the fractional gas holdup in the column and the volumetric mass transfer coefficient were found to depend upon the 0.33 power of the power input, the 0.53 power of the superficial gas velocity, and the 1.0 power of the pulse velocity, for values of the latter in excess of a critical value of 0.8 to 1.0 ft./sec. The inferred linear correlation of '$k_L a$' with the gas holdup suggests that there was little effect of pulsation upon the mean bubble size above the critical pulse velocity.

Improvements in the volumetric mass transfer coefficient of up to 230% of the unpulsed value were noted. Comparison with reported absorption equipment indicates that the pulsed column (as used in this investigation) is somewhat less efficient than the stirred tank from the aspect of power utilisation, but that this could be improved by the use of more efficient gas dispersing units, for example sieve plates.

It is considered, however, that the capability of countercurrent operation of the pulsed column should show considerable advantages over conventional agitated equipment.

Index

List of Illustrations

Chapter 1

Introduction

One of the most important branches of chemical engineering is that concerned with interphase mass transfer, which may be separated into two major subdivisions of industrial importance: liquid extraction, the transfer of a soluble species from one liquid solvent to another across a liquid/liquid interface, and gas absorption or stripping, the transfer of a gaseous species from a gas to a liquid or vice versa across a gas/liquid interface.

A useful model to illustrate the mechanism of mass transfer across a phase interface is the two-film theory of WHITMAN (56) described by COULSON & RICHARDSON (57).

This theory postulates that in the bulk phases material is transported by convection currents, and that concentration differences of any magnitude occur only in the region of the interface. The theory assumes the existence of a stagnant, thin film on either side of the interface, across which mass transfer must occur by molecular diffusion. The process is clarified by reference to Fig. 1.1, which is drawn from Coulson and Richardson. The diagram refers to the process of gas absorption, but the process of liquid extraction is analogous. Thus we have a constant concentration of the solute gas in the bulk gas phase approaching the interface, concentration gradients across the stagnant gas and liquid films, and again constant concentration in the bulk liquid phase.

In practically all gas-liquid contacting systems

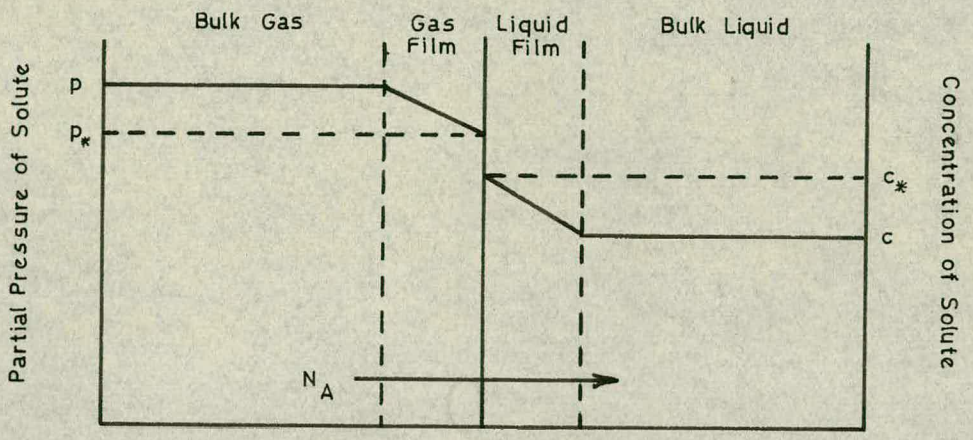

Fig. 1.1

the rate of mass transfer is controlled by the liquid film resistance (49); CALDERBANK (58) has shown that the concentration gradient in the liquid film is at least 44 times that in the gas film. Furthermore the ratio of the diffusivity of, for example, oxygen in air to that of oxygen in water is 7.12×10^4. The mass transfer model may accordingly be simplified to that shown in Fig. 1.2 below:

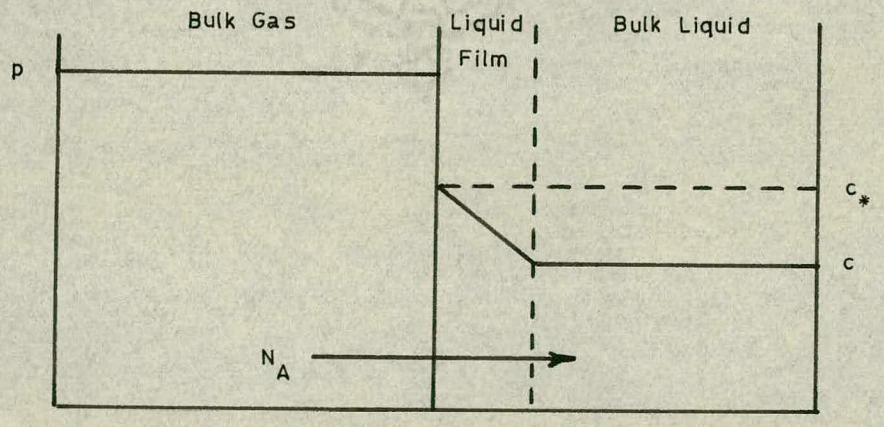

Fig. 1.2

Under steady state conditions the total rate of mass transfer across the interface in an ensemble of bubbles is given by:

$$N_A = k_L a(c_* - c) \qquad (1.1)$$

A somewhat different relationship applies to the absorption conducted under unsteady conditions:

$$N_A = \frac{dc}{dt} = k_L a(c_* - c) \qquad (1.2)$$

In this case 'N_A' and 'c' are dynamic, while 'k_L' and 'a' remain time invariant. It is self-evident from equations 1.1 and 1.2 above that in order to increase the rate of mass transfer in a given system we may (theoretically) increase on the right-hand side of equation 1.1 any of the three system parameters 'k_L', the film transfer coefficient, 'a', the specific interfacial area, and $(c_* - c)$, the concentration driving force.

In practice the concentration driving force is usually fixed, either by the required product solution concentration or by economic considerations of the quantities of solvent required. The film transfer coefficient and the specific interfacial area, on the other hand, are subject to external influences applied to the fixed system.

It is convenient when assessing the performance of gas-liquid contacting equipment to consider 'k_L' and 'a' together as $(k_L a)$, the 'volumetric mass transfer coefficient' (49,39).

'$k_L a$' is affected by the input of power to the system in two ways. The film transfer coefficient 'k_L' can by improved by increasing the turbulence in the liquid, and 'a' is enhanced by increased holdup in the system, and by the decreased size of the bubbles.

Gas absorption is carried out industrially in

several types of equipment, which may be generally divided into two classes; those in which mechanical agitation is applied to the system, and those in which it is not.

Non-agitated equipment includes:

1.- Packed towers, in which the liquid forms the dispersed phase distributed over the packing, and the interfacial area is partly that due to the interstices of the packing;

2.- Sieve plate columns, in which the gas is dispersed as bubbles in the liquid in several stages by means of perforated plates;

3.- Spray towers, where the liquid is dispersed as falling droplets in the gas;

4.- Venturi absorbers, where the gas is accelerated to a high velocity in a venturi throat. Injection of the liquid at the throat produces a fine dispersion of droplets;

5.- Simple bubble columns, in which the gas is dispersed in a column of liquid as free-rising bubbles, and

6.- Wetted wall columns, where the liquid forms a film on the wall of the column, and is contacted as such with the gas stream.

The latter is principally of laboratory interest, as its operation is simple and amenable to mathematical analysis.

Industrially, agitated gas-liquid contacting equipment is limited to the stirred tank, the performance of which has been thoroughly investigated (18). Other forms of agitated equipment, as will be seen in Chapter 2, have been investigated but have not gained acceptance commercially.

Absorption towers of the various kinds

(1,2,3,5,6 above) have the advantage of countercurrent operation, while to approximate this using stirred tanks requires a stage-wise operation of several units. On the other hand absorption towers suffer the disadvantage of large size, which is overcome in the case of stirred tanks by the input of power, creating relatively large interfacial areas in comparatively small volumes.

In the field of liquid extraction the advantages of countercurrent operation and external agitation have been combined in agitated packed and sieve plate columns (4,5), agitation being applied to the dispersion by means of cyclic pulsations of the liquids, via axial rotors in the column, or by vibration of the sieve plates. The effect of this 'hybridisation' has been to reduce the size of column necessary to carry out a given operation, an advantage which has led to the acceptance of pulsed extraction columns industrially, particularly in the field of radioactive fuel processing for obvious reasons.

The purpose of this work is to investigate the effects of power input to a gas-liquid contactor of the bubble column type. The choice of range of operating variables and gas-liquid system are discussed in subsequent chapters.

Chapter 2

Review of Previous Work

2.1 Introduction

Previous investigations into the effects of pulsations and vibrations upon gas-liquid systems may be divided generally into two categories suggested by the above terms, i.e. those in which the effects of low frequency pulsations of relatively high amplitude have been studied, and those concerning the effects of vibrations in the sonic and ultrasonic range of frequencies, of small amplitude.

This segregation of the two ranges of frequencies is of some importance, as the physical effects of the pulsations or vibrations upon the gas-liquid systems are dependent upon the range into which the applied frequency falls.

In order to clarify this point, it is reasonable to say that, whatever the system under investigation, the maximum effect of any applied cyclic disturbance will be observed at some inherent resonant frequency of the system. In the case of vibrations in the sonic range of frequencies, the system characteristic of prime importance is the resonant frequency of the bubbles, and in the case of low frequency pulsations, that of the column of liquid.

2.2 Effects of Vibrations in the Sonic Range

That a vibrating bubble may be subject to a force opposing that of buoyancy was first proposed by BJERKNES (3), who developed a theory to describe the effect in the hypothetical case of a balloon in a vibrating liquid.

The phenomenon of vibrating bubbles was first investigated by MINNAERT (1) during the course of his studies of the sounds produced by running water. Minnaert observed that the frequencies of the sounds produced by bubbles forming at an orifice were considerably lower (2000 Hz) than could be explained by treating the bubble as a resonant cavity (100,000 Hz), and demonstrated that the measured frequencies were consistent with a theory that the bubbles vibrated radially. Frequencies of vibration were found to be approximately inversely proportional to the radius of the bubbles for a specific system. SMITH (2) subsequently investigated the effects of applied vibrations on bubbles, and noted the violent activity of resonant bubbles. Smith confirmed that the resonant frequency was inversely proportional to the diameter of the bubble, using frequencies in the range 1000 - 1,000,000 Hz.

Interest in the possibility that vibrations may have an enhancing effect upon the rate of mass transfer between gases and liquids was first aroused in the late 1950's, although prior to this time pulsation of liquid-liquid extraction columns had already gained a footing in industrial practice (4,5,6).

BRETSZNAJDER & PASIUK (10) investigated the effects of vibrating a countercurrent bubble column in the range of frequencies 5 - 66 Hz, and constant amplitude 1 mm., using the system carbon dioxide/water. The percentage improvement in the mass transfer coefficient over that in the unpulsed case was found to be a function of frequency, and independent of the height of the water column and the concentration of carbon dioxide in the gas phase except for one particular case (27% CO_2, 120 mm. bed height). No attempt was made to explain this

anomaly. The maximum improvement in the absorption coefficient was found to be nearly 99%.

Concurrently with Bretsznajder and Pasiuk at this time, HARBAUM & HOUGHTON (7,8) were working with a similar system, but using vibrations in the range of frequencies 20 - 2000 Hz and amplitudes in the range 0.001 - 1.0 mm. These workers noted peaking in the rate of mass transfer/frequency relationship, attributed by them to resonance effects. The maximum improvement in the mass transfer rate obtained was 70%. The investigations showed that increases in the volumetric mass transfer coefficient ($k_L a$) were due primarily to increases in the gas holdup (ϵ), and that the mass transfer coefficient 'k_L' was in general decreased. Some attention was paid to the visual appearance of the bubble bed under conditions of vibration, and at high frequencies (c. 1000 Hz) the bubbles were seen to take on a 'frothy' appearance, indicating a highly agitated state of the gas-liquid interface. It was also observed that at frequencies below 40 Hz '$k_L a$' was decreased to below that found in the unvibrated case. It was suggested that this may have been due to the violent vibration at the lower frequencies having induced coalescence, and therefore decreased the overall interfacial area.

BRETSZNAJDER & PASIUK (11,12,13,14,15,16,20) in continuation of their previous work (10), investigated the effects of vibrations on gas absorption at the free surface of a liquid (11) using frequencies in the same range as their previous work, but somewhat higher amplitudes (8.3 mm.). The maximum improvement obtained in this system was 7600% at 17 Hz, 8.3 mm., decreasing at higher frequencies. The peaking phenomenon was proposed by Bretsznajder and his co-worker to be due

to a resonance effect in the system. In a further investigation (13) of the absorption at the free liquid surface, an improvement of 13,500% was obtained at a frequency of 17 Hz and amplitude 5.5 mm. This indicated to the authors the probability that an optimum amplitude existed for their system in the range 4.0 - 5.5 mm. It was shown by Bretsznajder and Pasiuk, by comparison of the results obtained in the above papers, that in their experimental conditions the improvement of absorption from bubbles is relatively insignificant in comparison to the improvement of absorption at the free surface of the liquid, and that the overall improvement in absorption in the bubbling system is principally due to increased absorption at the free surface. The column used by the authors, however, was neither baffled nor packed.

Bretsznajder and Pasiuk subsequently (29) carried out an analysis of the mechanism of absorption in their equipment, distinguishing the absorption in the bubble bed from that at the free surface of the liquid.

BAIRD (17) developed an expression to predict the resonance frequency of a gas-liquid dispersion:

$$f = \left[\frac{2n-1}{4}\right] c/H_L = \left[\frac{2n-1}{4H_L}\right] \left[kp_o/\rho_L \quad (1-\epsilon)\right]^{\frac{1}{2}} \qquad (2.1)$$

where $n = 1,2 \ldots$ is the mode of resonance

p_o = static pressure in the system

c = velocity of sound

k = constant for a given gas

The author found reasonable agreement between his theoretical expression and experimentally observed frequencies, and further was able to postulate that the porosity of a vibrated gas-liquid dispersion tends to adjust

itself so that the bed is always in resonance with the applied frequency.

BUCHANAN, TEPLITZKY & OEDJOE (18,19) utilised in their experiments the effect postulated by Bjerknes (3), namely the force opposite to buoyancy experienced by a vibrating bubble. These workers found that using frequencies in the range 20 - 50 Hz and amplitudes in the range 0.05 - 1.0 cm., gas bubbles were seen to be entrained at the free surface of the liquid, migrate to the bottom of the column and coalesce to form a slug which then returned to the top. The system used for the evaluation of the mass transfer rates in this equipment was oxygen/sodium sulphite solution. Since the apparatus was not sparged with gas, it was not possible to make any comparison with an unvibrated case. '$k_G a$' was found to be independent of the liquid rate, and proportional to the 0.33 power of the gas rate and the 1.1 power of the vibrational acceleration ($\omega^2 A$).

BAIRD (21) investigated stationary, resonant single bubbles in the frequency range 40 - 1050 Hz, and found that in viscous liquids a resonant bubble could be obtained which would fill the diameter of the column. The resonance frequency of such a slug could be predicted by the expression:

$$f = \left[\frac{K}{2\pi}\right] \left[\frac{\gamma p_o}{\rho_L h G}\right]^{\frac{1}{2}} \qquad (2.2)$$

where p_o = bubble pressure in static system.

G = height of gas slug at equilibrium.

K = correction factor.

Rigorous mathematical analysis has been applied to

the behaviour of gas bubbles in vibrating liquids by HOUGHTON (22), JAMESON & DAVIDSON (23,24), and RUBIN (25). For bubbles vibrating in phase with the applied pulsation (i.e. where the applied frequency is less than the Minnaert natural frequency) it was found that at low Reynolds numbers the condition for no nett displacement of the bubble was:

$$M = \frac{f^4 A^2 \rho_L h}{2g p_o} = 1 \qquad (2.3)$$

where M = dimensionless force ratio.

p_o = static pressure in the liquid.

while for higher Reynolds numbers, $M = 1.4$ was found to be a good approximation. Rubin confirmed these findings.

GORODETSKII, OLEVSKII, LEVITANAITE & LEGOCHKINA (27) investigated the effects of vibrating packed and tray absorption columns with frequencies up to 40 Hz, and found that in most cases, the effectiveness increased with increasing frequency. The height of transfer unit was found in the absence of vibration to be 0.8 m. and at 40 Hz to be 0.1 m. The pressure drop across packed columns was also found to increase with increasing frequency.

JACKISCH (28) applied acoustic vibrations in the frequency range 1500 - 2500 Hz to carbon dioxide bubbles dissolving in water at an orifice, and obtained improvements in the mass transfer coefficient of up to 180% or 1400%, depending upon the mode of oscillation of the bubbles. However, these large improvements relate to stagnant conditions in the absence of pulsation.

In an apparatus similar to that of Buchanan et al

(18,19) embodying the principle of Bjerknes (3), JAMESON (30) investigated the effects of vibrations in the frequency range 20 - 40 Hz and amplitude 3.8 mm. - 8.1 mm. on the absorption of oxygen into sodium sulphite solution in a bubble entrainment-type absorption column. Jameson again noted the peaking effect in the absorption rate/frequency function. He further correlated the rate of absorption, the frequency and the amplitude as:

$$N_A \propto f^6 \; A^{3.5} \qquad (2.4)$$

for the portion of the absorption rate/frequency function in which the absorption rate was rising. An attempt was also made to correlate 'N_A' with the vibrational acceleration, '$f^2 A$', but the scatter in the experimental points on this plot made the deduction of any correlation difficult, other than that the absorption rate generally increased with increasing vibrational acceleration. The absorption rate was found to be independent of the bed height, up to a point at which a stagnant layer of liquid was formed in the bottom of the column.

VEVIOROVSKII, DIL'MAN & AIZENBUD (37), working with a bubble column, confined themselves to the investigation of the hydraulic characteristics of a vibrated system, using vibrations of frequency 0 - 37 Hz and amplitude 1 - 10 mm. Resonance frequencies were measured for the various columns used, and peaking of the gas holdup of the vibrated bubble bed was found at the resonant frequency. Increases of up to 1000% were obtained in the holdup.

2.3 Effects of Pulsations in the Subsonic Range

The amount of work carried out in the field of low

frequency, high amplitude pulsations has been relatively limited, and has been applied to a number of differing types of equipment.

TUDOSE (31) pulsed the gas phase of a wetted-wall column in the range of frequencies 0 - 20 Hz and of amplitudes 5 - 29 cm., and obtained increases in the overall absorption coefficient of up to about 300%. A peak-type variation of absorption coefficient was found with respect to frequency, with a maximum at 9.33 Hz, but the coefficient was found to vary linearly with amplitude. Tudose subsequently (35) applied gas phase pulsations in the frequency range 0 - 20 Hz and amplitude range 2.5 - 15 cm. to both wetted-wall and packed columns, obtaining absorption coefficient increases of 210% and 110% respectively. In contrast to the findings of Ziolkwski and Filip (26,33), Tudose found that the initial increase of rate of absorption with amplitude was sharp, and then the value of the coefficient approached a constant value assymptotically. The absorption coefficient was found to depend weakly upon the liquid phase Reynolds number, but strongly on the gas phase Reynolds number.

BEEK (32) used a similar system, but pulsed the liquid phase, forming waves in the liquid film with frequencies ranging from 0 - 20 Hz. Improvements in the rate of mass transfer of up to 60% were found.

ZIOLKOWSKI & FILIP (26,33,36) applied vapour phase pulsations to both a packed absorption column (33,36) and a packed distillation column (26). In the case of the distillation column the pulsations applied were in the range of frequencies 8 - 17 Hz, and of amplitudes 0 - 5.5 cm. The best effect obtained was a doubling of the number of transfer units. In their experiments with the absorption

column, the frequency was held steady at 6.6 Hz and the amplitude was varied through a range of 0 - 5.6 cm. (pulsator amplitude). A logarithmic plot of the overall mass transfer coefficient against pulsator amplitude showed a slow linear rate of increase of the coefficient for amplitudes less than about 2 cm. followed by a significant increase in the coefficient for amplitudes greater than this figure (up to 300%). The improvement obtainable was apparently limited only by the inability of the equipment to generate amplitudes greater than 5.6 cm. The increase obtained in both the above series of experiments was attributed by the authors to an increase in turbulence, and therefore surface renewal, due to the constant acceleration and deceleration of bodies of fluid within the column packing.

BAIRD (34) developed an apparatus in which high amplitude, low frequency pulsations were generated by means of a compressed air injection/exhaust system. Preliminary experiments showed that an increase of 50% in the rate of mass transfer could be obtained by the use of pulsations of frequency 1.3 Hz and amplitude 5 cm. in a baffled column.

The experimental conditions, apparatus and investigations of the workers mentioned in this survey are summarised in Table 2.1.

TABLE 2.1: Summary of previous work

Parameters Investigated	Range of Experiments		System		Type of equipment	Means of Pulsation (gas, liquid, whole column)	Reference
	f Hz	A mm.	Liquid	Gas			
f_r	2000	-	water	air	single bubbles	natural vibrations (g)	Minnaert (1)
f_r	10^3 - 10^6	-	water	air	not reported	not reported (1)	Smith (2)
I	5 - 66	1.0	water	CO_2/air	bubble column	mechanical piston (1)	Bretsznajder (10)
k_La,A,ϵ,d,a	20 - 2000	0.001 - 1.0	water	CO_2	bubble column	electrodynamic piston (1)	Harbaum (7,8)
I	3 - 62	0.9 - 8.3	water	CO_2/air	free-surface entrainment column	mechanical piston (1)	Bretsznajder (11,12,13,15,16)
Behaviour of surface	2 - 92	0.9 - 2.0	water methanol aq. glycerol	none	column	mechanical piston (1)	Bretsznajder (14)
I	5 - 67	0.5 - 10.5	water	CO_2/air	bubble column	mechanical piston (1)	Bretsznajder (20)
f_r	22 - 120	-	glycerol	air	bubble column	electrodynamic piston (c)	Baird (17)
K_Ga	20 - 50	0.5 - 1.0	sulphite	air	free-surface entrainment column	mechanical piston (c)	Buchanan (18,19)
f_r	40 - 1050	-	glycerol	air	single bubbles	electrodynamic piston (c)	Baird (21)
f,A,d	0 - 50	0 - 8	water/ glycerol	air	single bubbles	eccentric weight (c)	Jameson (23,24)
HTU	0 - 40	15	water	CO_2/air	sieve tray column	vibrating trays (1)	Gorodetskii (27)
I	80 - 1500	0 - 0.8	water	CO_2	single bubbles	electrodynamic piston (1)	Jackisch (28)
N_A	20 - 40	4 - 8	sulphite	O_2	free-surface entrainment column	mechanical piston (c)	Jameson (30)
f_r, ϵ	0-37	1 - 20	water	N_2	bubble column	mechanical piston (1)	Veviorovskii (37)
k_p	0 - 20	50 - 290 25 - 150	water	NH_3/air CO_2/air	wetted-wall column packed column	mechanical piston (g)	Tudose (31)(35)
N_A	0 - 20	-	water	CO_2	wetted-wall column	mechanical piston (1)	Beek (32)
K_ga	6.5	0-60	NaOH aq. water	CO_2 NH_3/air	push-pull packed columns	mechanical piston (g)	Ziolkowski (33,36)
f,I	1.3	50	sulphite	air	baffled column	air spring pulsator (1)	Baird (34)

Chapter 3

Apparatus and Experimental Procedures

3.1 Choice of Apparatus

The choice of apparatus to be used in this investigation was influenced by the desire to show that the process could be applied successfully to industrial scale equipment. It was therefore decided to build the equipment on a pilot scale basis.

It is well known (7,37) that the transmission of sonic vibrations, even at high power inputs, is rapidly attenuated in bubble dispersions, and hence the use of such vibrations is limited to bed depths of the order of 1 m.

It was decided therefore to investigate the effects of low frequency, high amplitude pulsations upon the rate of absorption of a gas from a bubble bed.

It was further decided that the equipment should work at its resonant frequency, since the maximum effect for a given power input could be expected under these conditions.

3.2 Means of Pulsation

Several methods of pulsing or vibrating a column presented themselves from the work of previous investigators, the most common of these being the mechanical or electrodynamic piston. Pulsations have been applied to the process (a) by direct impact of the piston upon the fluids (7,8,31,35,36), or (b) via a flexible membrane in contact with both the process fluids and the piston (27,28,32) or (c) by vibrating the entire column (17,18,19,21,23,24,30).

The first of these methods (a) would have involved

the sealing of the piston, the difficulty of which would have been aggravated by the high amplitudes envisaged. For the same reason the second method (b) was discounted. The third means (c) of generating pulsations was also rejected by reason of the large size of the equipment envisaged.

Two further methods of generating pulsations are given in the literature. The first of these was developed by Ziolkowski and Filip (33,36) for pulsed absorption in packed columns, and involved switching of the gas-phase flow into alternate legs of a double column. Baird (34) developed a method of pneumatic pulsation by which a column of liquid was maintained in oscillation by alternate injection and exhaust of compressed air at a side arm. The latter method was chosen by reason of its simplicity, lack of moving parts, (the only such part involved being the spool of the solenoid valve used to inject and exhaust the compressed air), and because it operated necessarily at the resonant frequency of the system.

3.3 Final Form of Apparatus

The form of apparatus eventually decided upon was that of an oscillating U-tube, driven by Baird's method (34) of the injection and exhaust of air. The double column configuration was chosen since it was considered that this would show a better economy of power than Baird's single column, there being a proportion of the kinetic energy of the column of liquid recovered as potential energy in the transfer of liquid from one leg to the other in the course of one cycle. Furthermore, the compressed air consumption would be essentially steady, facilitating the measurement of air flow.

The absorption column is described in detail in

Section 3.5.1.

3.4 Choice of Methods of Measurement

3.4.1 Power Consumption

The means by which the power consumption within the column was measured was adapted from the method known as the 'indicator diagram', used in the testing of mechanical piston engines of various types. In the traditional apparatus used for this purpose a diaphragm is deflected against a spring by the pressure developed within the cylinder of the engine, and a system of levers is deflected by the longitudinal movement of the piston. These two deflections are applied at right-angles to one another to a pen, which scribes a trace of the resultant movement. The trace obtained from this apparatus represents a pressure-volume relationship for the gas within the cylinder for one cycle, and the area of the trace is proportional to the power developed (or absorbed) by the engine during one cycle.

In this investigation, the pressure and volume signals were obtained in the form of electrical analogues by the means described in Section 3.6.1 and Appendix I.

3.4.2 Absorption Rates

Methods for the measurement of absorption rates are widely reported in the literature. Some of the systems in more common use are air/carbon dioxide/water, air/carbon dioxide/sodium hydroxide solution, and air/oxygen/sodium sulphite solution. The last of these is commonly used in industry for gauging the performance of gas absorption equipment, in particular fermentation plant.

However, chemical methods of measuring absorption

rates by analysis are laborious and time-consuming, from three to four hours being required to obtain sufficient data to calculate one absorption rate. Furthermore, the O_2/sulphite reaction has recently (39,59,60) been called into question as a means of measuring transfer rates due to uncertainty in the reaction kinetics caused by catalysis by trace impurities.

An elegant and direct method for the measurement of oxygenation rates in a channel has been developed by a colleague of the author (38). The method recommends itself by its simplicity and speed, the time taken to measure one absorption coefficient being of the order of fifteen minutes in the pulsed absorber.

In this method a small polarographic cell is inserted into the absorbing liquid, and direct read-out of an electrical signal proportional to the concentration of oxygen in the liquid is obtained. The method was successfully adapted to the requirements of this investigation. A paper has recently been published by GAL-OR, HAUCK & HOELSCHER (39) in which a similar method was reported as having been applied to the absorption process in a stirred tank.

The method of measuring rates of absorption is described in detail in Section 3.6.3 and Appendix I.

3.5 Description of Apparatus

A general view of the equipment is presented in Plate I.

3.5.1 The Absorption Column

The principal part of the apparatus as it appeared in its final form consisted of a U-tube constructed of 3 in. nominal bore Q.V.F. glass pipe sections, as detailed in Fig. 3.1, consisting of two

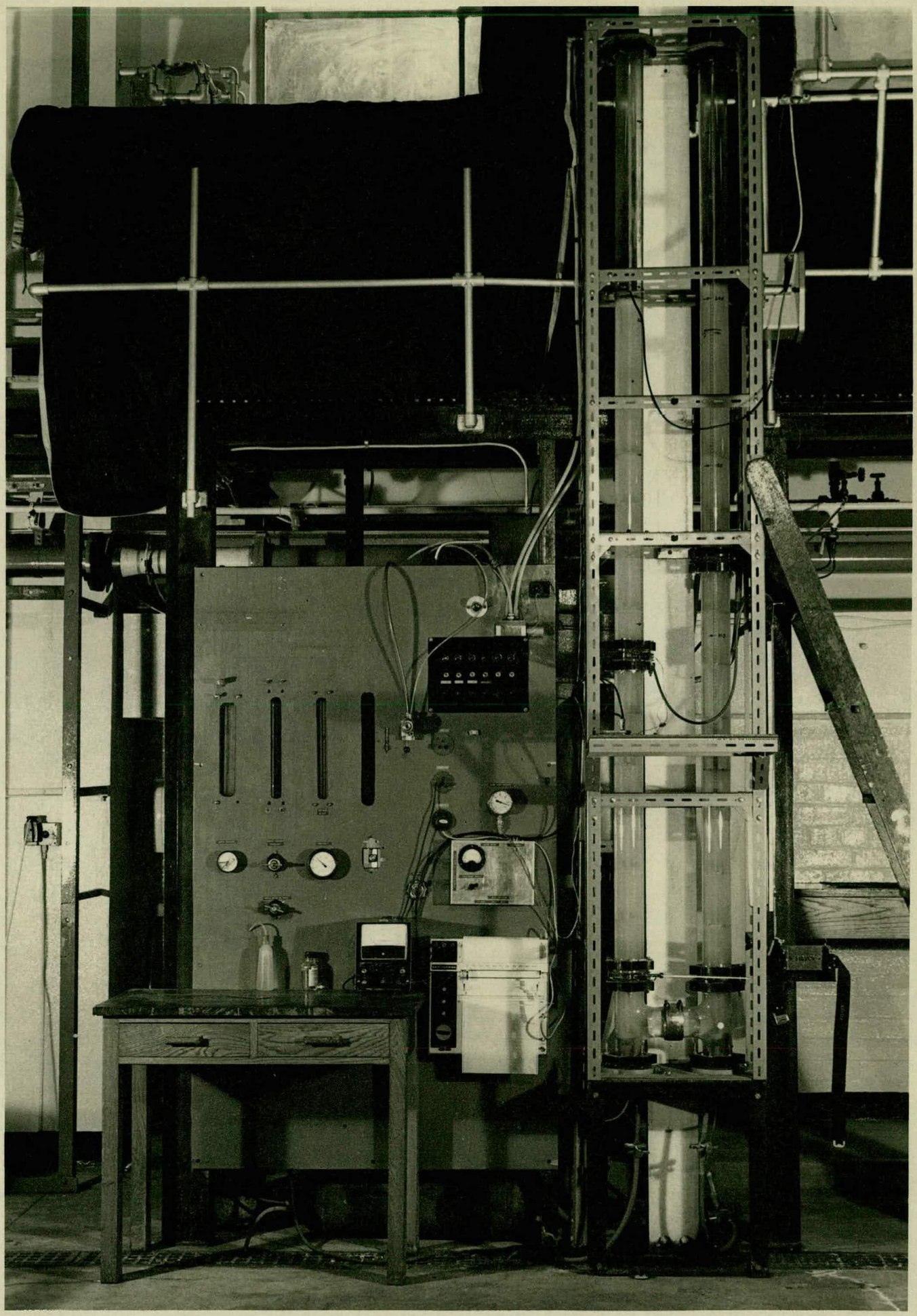

Plate I: General View of Apparatus

straight legs 9 ft. in length and connected at their bases to two T-sections. Connection of the side arms of the T-sections completed the construction of the basic U-form of the absorption column. The vertical axes of the T-sections were 10 in. apart. The horizontal axis of the cross-junction between the two legs was 5 in. above the ends of the legs. The four open ends of the legs were provided with 6 in. dia. end plates turned from $\frac{1}{2}$ in. thick pvc sheet.

The plates closing the lower ends of the legs were each fitted with a sintered polythene compressed air exhaust silencer (Air Automation Ltd.) to act as a gas distributor.(N in Fig. 3.2)

Each leg carried at its vertical axis a 3/8 in. dia. brass rod, fitted at 6 in. intervals with 2 in. dia., $\frac{1}{4}$ in. thick disc-shaped baffles to a total of twelve per leg.

During measurement of absorption rates all metal parts in contact with the absorption system were coated with 'Araldite' in order to preclude any contamination of the system.

3.5.2 The Pulsation Generator

Referring to Fig. 3.2, compressed air from the laboratory supply at 140 psi was filtered and reduced to 30 psi by a pressure controller (D). At this pressure it was metered by a Metric 30 Rotameter, the flow being controlled by a fine disc valve (H) downstream of the Rotameter. The pressure drop across the disc valve was always in excess of the critical pressure drop of about 13 psi, so that the flow was independent of downstream pressure variations. The air entered a five-port solenoid valve (J) by which it could be directed to the top of either leg of the column. The valve allowed air to exhaust from the leg which was not being supplied with air. The principle of operation was

Absorption Column Dimensions

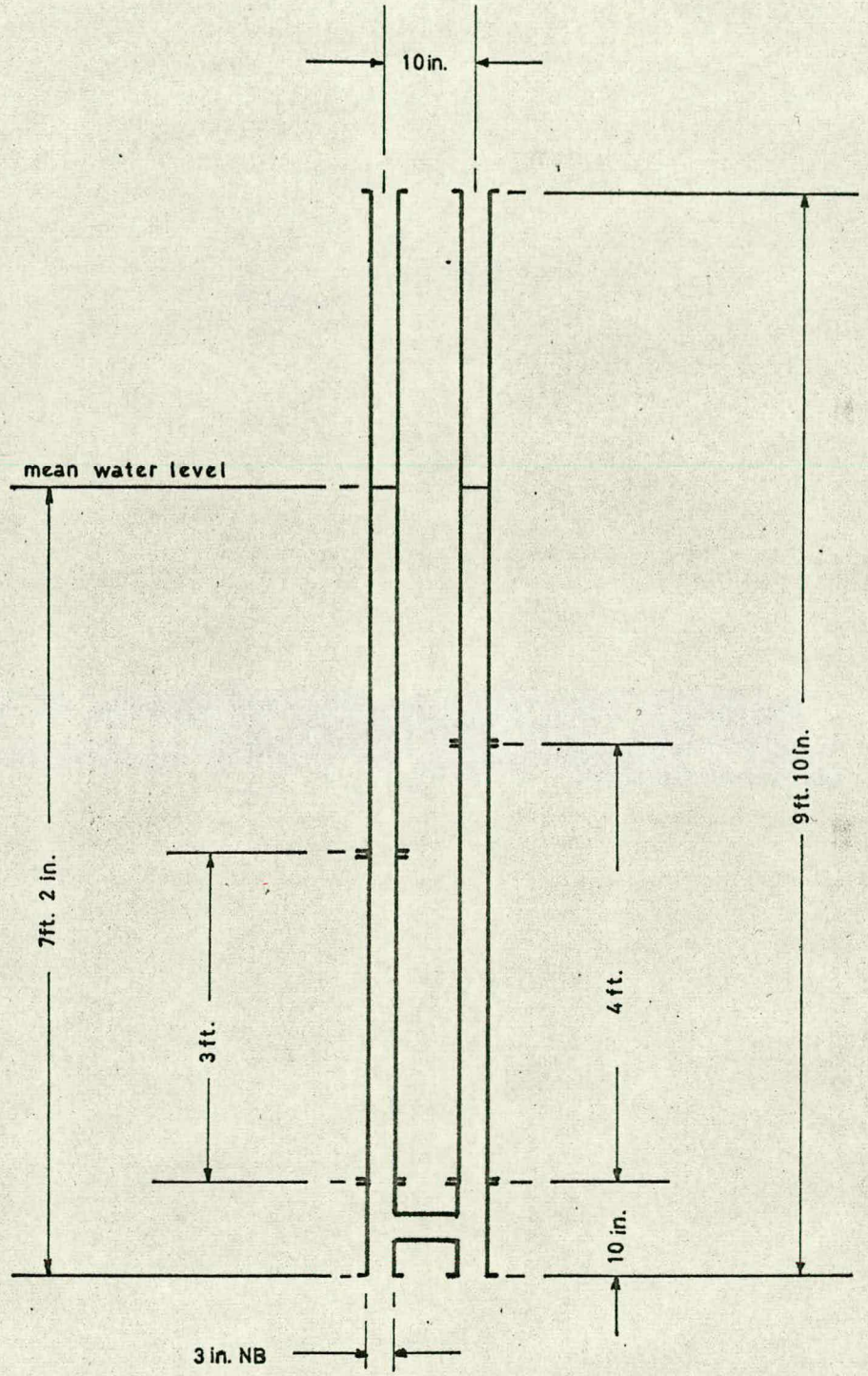

Figure 3.1

Key to Figure 3.2

A	Oscilloscope
B	Stabilised DC power supply
C	DC amplifier
D	Pressure controller
E	Metric 30 Rotameter
F	Needle valve
G	Metric 14 Rotameter
H	Disc valve
I	Pulsation damper chamber
J	Five-port solenoid valve
K	Pressure transducer
M	Proximity switch
N	Sintered polyethylene gas distributor
P	Level meter
Q	Proximity switch probe
R	0 - 30 psi pressure gauge

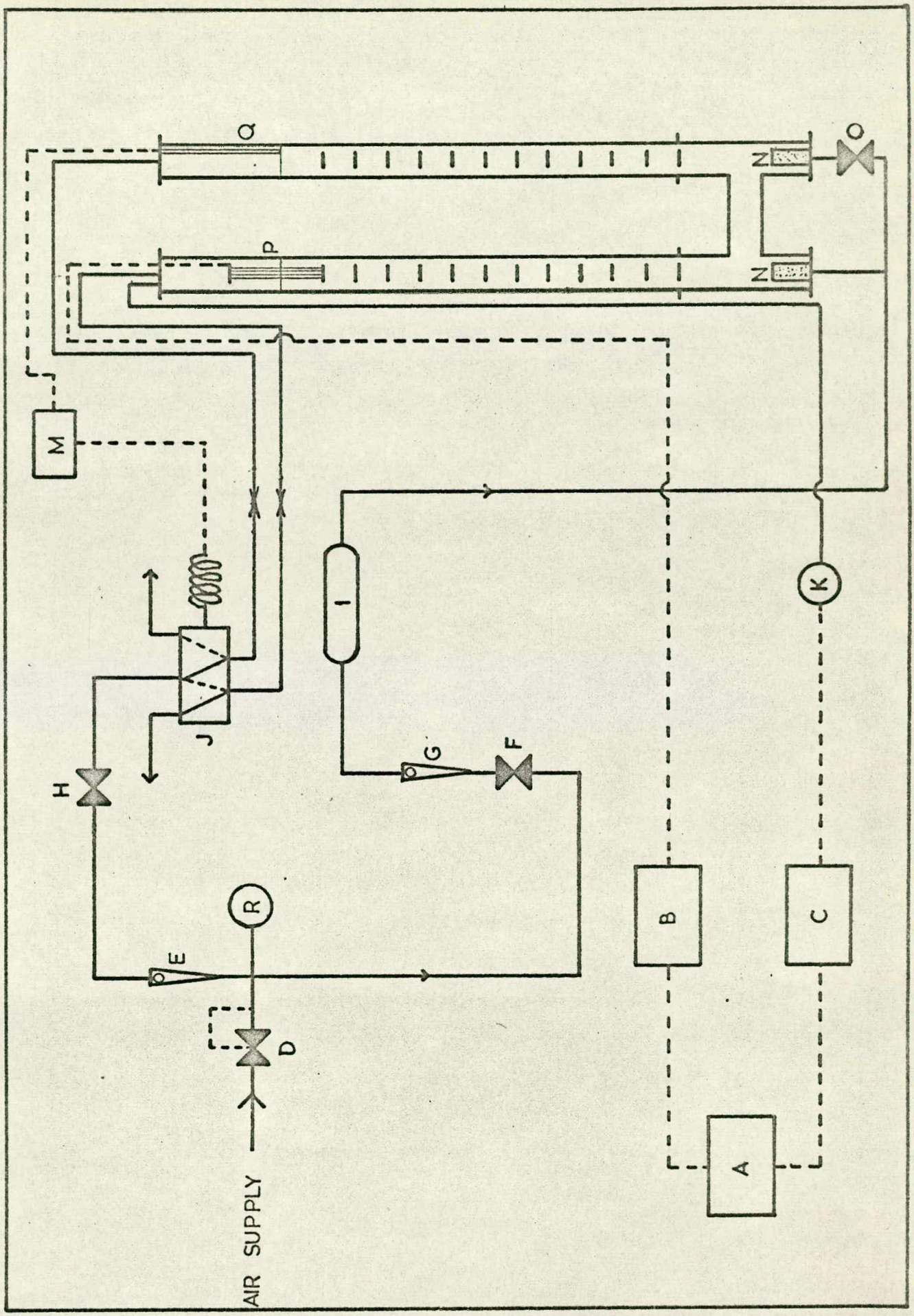

Figure 3.2

similar to that described by Baird (34), except that the system in this case was double-acting. The position of the solenoid valve was controlled by a Lock proximity switch (M). The principle of operation is best described by following a complete cycle.

Assuming that the left-hand leg of the column is at top-dead-centre, and therefore that the right-hand leg is at bottom-dead-centre (in Fig. 3.2), the level of liquid in the LH leg falls and that in the RH leg rises (air being admitted to the top of the LH leg) until the proximity switch probe (Q) is contacted. The proximity switch then switches the solenoid valve so that air is admitted to the RH leg and exhausted from the LH leg. After a lag due to the inertia of the column of liquid the level in the RH leg again begins to fall until the probe of the proximity switch loses contact with the liquid surface, the solenoid valve is again switched to its previous mode, and the cycle starts once again.

The ancillary equipment was set up in two different ways depending upon whether power consumption or absorption rates were being measured.

3.6 Experimental Procedures

3.6.1 Measurement of Power Dissipation

The apparatus as set up for power consumption runs is shown schematically in Fig. 3.2.

As already stated in Section 3.4.1, the method by which the power input was measured was an adaptation of the 'indicator diagram' method used in the testing of heat engines.

It was required that signals representing both the

displacement of the liquid surface and the pressure within the gas space of the column should be obtained, and by some means used to plot the pressure-volume relationship of the gas.

The pressure of the gas was measured by the use of a Solartron pressure transducer, the circuit for which is depicted in Appendix I.

The level of liquid in one leg of the column was measured by a simple conductivity meter consisting of a 3/8 in. dia. brass rod mounted parallel to the axial baffle-carrying rod and partly immersed in the liquid. A constant voltage of 5 V. D.C. was applied between the rods so that the current passed was proportional to the depth of immersion of the rods. The current developed a proportional voltage across a resistor placed in series circuit with the rods (Appendix I).

The signals obtained from the pressure transducer and the level indicator were applied after suitable amplification to the X and Y amplifiers respectively of an oscilloscope. The resulting 'pictures' were photographed and enlarged, in order that their areas could be measured by the use of a planimeter. Some examples of typical pressure-volume diagrams obtained by this method are shown in Plate VII. The measuring system is described in greater detail in Appendix I.

The experimental procedure for the power input measurements was as follows.

The pulsed column (Fig. 3.2) was first filled with tap water to the level of the proximity switch probe (Q). The power supply to the proximity switch (M) was then turned on, and the instrument was

allowed to warm up. Air was then admitted to the solenoid valve (J) by opening the disc valve (H), when the column would begin to pulse. If the run in progress was to be one using the gassed liquid, the needle valve (F) was next opened, admitting air to the gas distributors (N) via the Metric 10 Rotameter (G) and the pulsation damper chamber (I). The distribution of air between the two distributers was balanced visually by adjustment of the valve (O). The mean height of liquid in the column was next balanced by draining water from the column via a drain tube in one of the lower end plates (not shown in the schematic diagram Fig. 3.2).

With the pressure and level measuring instruments described in the previous section in operation, a set of readings could now be taken.

The observations made at each frequency were as follows:-

(i) pulse air pressure (gauge R);

(ii) pulse air flow rate (Rotameter E);

(iii) frequency of pulsation (by timing 60 cycles with a 1/100th sec. stop-watch);

(iv) amplitude (by comparison with a centimetre scale attached to one leg of the column);

(v) bubble air flow rate (Rotameter G, and correction to mean column pressure);

(vi) a photographic record of the oscilloscope trace was taken.

The amplitude of pulsation was then altered by adjustment of the disc valve (H), and another set of observations taken.

In addition to these, at the beginning and end of every run, the pressure transducer was calibrated against a static head of water in the column.

The photographs of the oscilloscope traces were then developed and enlarged, and the areas of the pressure-volume diagrams measured by the use of a planimeter.

3.6.2 Measurement of Gas Holdup

Two methods of measuring the gas holdup in the column were used.

In the first (preliminary) method, the column was set up as for power dissipation runs (Fig. 3.2). The supply of air to the dispersers was turned on and the flow of air to the two legs was balanced by visual inspection. Water was then removed from the bottom of the column to bring the surface of the column of dispersion to a datum. The supply of air was then turned off so that the quantity of water in the column, and hence the holdup at no pulse conditions could be ascertained. The supply of air was then turned on, and the column set pulsing. The amount of water removed from the bottom of the column in order to bring the mean level of dispersion in the column back to the datum was then noted. The rate of pulsation was increased, and the procedure repeated.

The holdup in the column is then simply equal to the total amount of water removed in order to bring the water level to the datum. This method proved to be inaccurate, due to the difficulty of balancing the air flows in the legs visually at high pulse velocities.

In the second, more accurate method the equipment was set up as for absorption rate runs (Fig. 3.3). In this method the air was metered into each leg of the column by a separate Rotameter. When

the column had been balanced for mean water level the following observations were made:

(i) pulse air pressure (gauge K);

(ii) pulse air flow rate (Rotameter C);

(iii) frequency of pulsation;

(iv) amplitude;

(v) bubble air flow (Rotameters G);

(vi) mean level of water in the column;

and after stopping the pulsing of the column and cutting off the bubble air supply:-

(vii) level of residual water in the column.

Subtraction of (vii) from (vi) and multiplication by the column cross-sectional area gives the volume of gas holdup within the bubble bed.

3.6.3 Measurement of Absorption Rates

The apparatus as set up for the measurement of absorption coefficients is shown schematically in Fig. 3.3.

The pulsation generation system was identical to that used in the power consumption and holdup experiments, except that the proximity probe in this case was mounted external to the column, and consisted simply of a coaxial cable split and twisted around the right hand leg of the column. This was found to be as effective as the 3/8th in. dia. rod previously used, and was less sensitive to unevenness of the liquid surface due to bubbling.

Polarographic probes (see Appendix I) for measuring oxygen concentration were mounted at (L) and (M), and the mean pressure at

Key to Figure 3.3

A	Pressure controller
B	Pressure controller
C	Metric 30 Rotameter
D	Plug valves
E	Disc valve
F	Five-port solenoid valve
G	Metric 14 Rotameter
H	0 - 30 psi pressure gauge
I	Proximity switch
J	Mercury manometer mounting point
K	0 - 30 psi pressure gauge
L	Oxygen concentration probe mounting point
M	Oxygen concentration probe mounting point

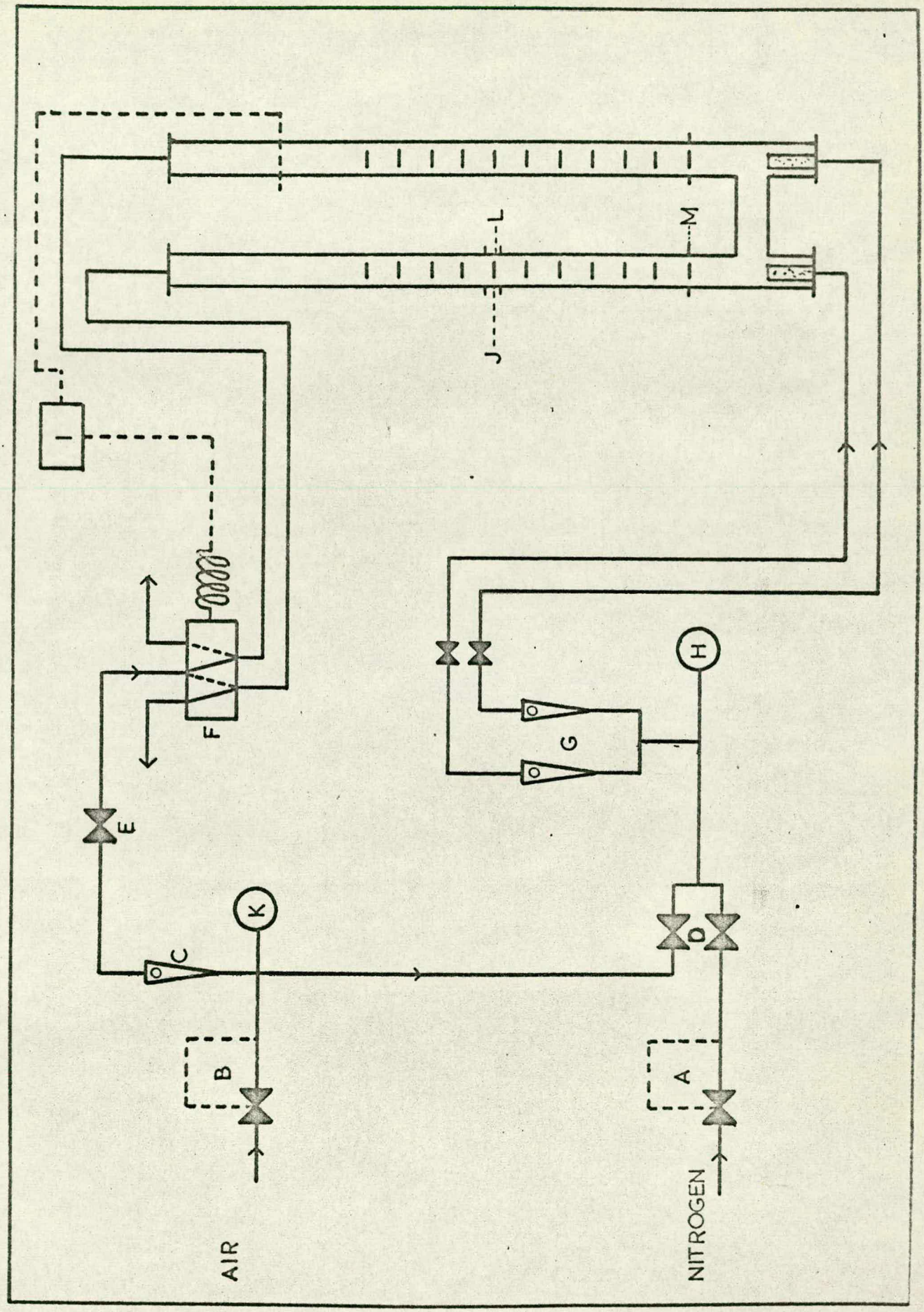

Figure 3.3

the upper probe (L) was measured by a throttled mercury manometer at J. Means of switching the bubble gas between air and oxygen-free nitrogen were provided by two quick-opening valves, D.

Operation of the equipment for the measurement of absorption rates was as follows.

The column was filled with tap water and the pulsation generator was activated as described in Section 3.5.2. The absorption air rate was set to the desired value, and the mean height of liquid in the two legs was balanced by draining water from the bottom of the column. By operation of the valves (D) the gas supply to the bottom of the column was then changed to oxygen-free nitrogen, the flow rate of which was adjusted to be equal to that of the air by operation of the pressure controller (A). The column was purged with nitrogen until the current through the polarographic cells was essentially zero, indicating zero oxygen concentration in the water. This operation required approximately five to fifteen minutes, depending upon the amplitude of pulsation. The gas supply was then quickly switched from nitrogen to air by operation of the valves (D), and the variation of oxygen concentration with time in the water was recorded by a Servocord potentiometric recorder. Observations made were as follows:-

(i) frequency of pulsation;

(ii) amplitude of pulsation;

(iii) mean column pressure at the probe;

(iv) absorption air flow rate;

It was unnecessary to calibrate the oxygen probes for actual oxygen concentration, since the method of dealing with the plots

obtained gave a value of '$k_L a$' direct (Appendix I). After switching from purge nitrogen to air, a short transition period (Fig. I.4) was followed by a true logarithmic rise in the probe output, ξ. The transition period, assumed to be due to the passage of the diffuse boundary between the nitrogen and the air, and was generally of the order of 2 - 5% of the full trace. A plot of $\ln(\xi_* - \xi)$ against time yielded a straight line (after the transition period), the gradient of which was equal to '$k_L a$' (see Appendix I).

Chapter 4

Physical Characteristics and Power Dissipation

4.1 Introduction

Before embarking upon the measurement of power consumption and absorption rates in the column, certain immediately observable characteristics of the equipment were measured. These were:

(i) amplitude as a function of compressed air consumption;

(ii) frequency as a function of compressed air consumption;

(iii) the time-averaged gauge pressure at the level of the probe, i.e. at a height of 3 ft. 10 in. above the base of the column;

and (iv) holdup as a function of the pulse velocity, ωA, at fixed values of V_{sg}.

In the published paper which appears as Appendix VII the superficial gas velocities are erroneously given as twice the actual values used. This error has, however, been corrected in the remainder of this thesis.

4.2 Amplitude and Frequency in the Ungassed Column

Amplitude and frequency were measured for the following ungassed conditions of the column:

(i) undamped;

(ii) with one baffle plate;

(iii) with twenty four baffle plates;

(iv) with 1.5 ft. packing (dumped $\frac{1}{2}$ in. ceramic

(v) with 3.3 ft. of packing.

The results of these observations are shown in Fig. 4.2.

4.2.1 Prediction of Frequency

The equations of motion of U-tube oscillators have been derived by BAIRD (34).

Consider the closed U-tube in Fig. 4.1 below:

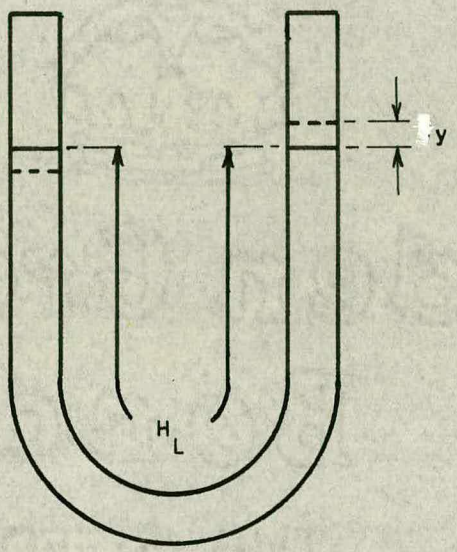

Fig. 4.1

with at equilibrium, gas space volume 'V_G' at pressure 'P_o' and cross sectional area at the interface 'C_o'. If the level of the liquid in one leg of the tube is given a small displacement 'y' from the equilibrium position, a restoring pressure acts upon the liquid column due to the compression and rarefaction of the gas spaces and to the liquid head:

$$p = -2(\gamma p_o C_o / V_G + \rho g) y \qquad (4.1)$$

assuming that $y \ll V_G/C_o$ and that the gas behaves ideally and adiabatically. This restoring pressure causes the column of liquid of length 'H_L' to accelerate towards its equilibrium position. For a column of uniform cross

sectional area the inertial force balance is:

$$\Delta p = \rho H_L \frac{d^2 y}{dt^2} \tag{4.2}$$

If the column is made up of several sections of different cross sectional areas, the force balance becomes:

$$\Delta p = \rho C_o \sum \frac{H_L}{C} \cdot \frac{d^2 y}{dt^2} \tag{4.3}$$

From equations 4.1 and 4.3:

$$\frac{d^2 y}{dt^2} \frac{1}{y} = - \frac{2(\gamma p_o C_o / V_G + \rho g)}{\rho C_o \sum H_L / C} \tag{4.4}$$

Equation (4.4) describes a simple harmonic oscillation of the liquid column at a resonance frequency 'f_r', where

$$f_r = \frac{1}{2\pi} \left(\frac{2\gamma p_o}{\rho V_G \sum H_L / C} + \frac{2g}{C_o \sum H_L / C} \right)^{\frac{1}{2}} \tag{4.5}$$

If one leg of the U-tube is open to atmosphere, the gas compressibility term in (4.5) is halved giving:

$$f_r = \frac{1}{2\pi} \left(\frac{p_o}{\rho V_G \sum H_L / C} + \frac{2g}{C_o \sum H_L / C} \right)^{\frac{1}{2}} \tag{4.6}$$

These predictions of frequency do not consider the effects of damping, but BAIRD (34) and VERMIJS (42) used similar approaches with reasonable accuracy in the prediction of the frequencies of single-leg air pulsed columns.

4.2.2 Frequency of Undamped Column

The resonant frequency of the undamped column was calculated taking $C = C_o = 0.0491$ ft^2, $H_L = 14.17$ ft., $V_G = 0.135$ ft^3, and $p_o = 1$ atm.

The frequencies as predicted by equations (4.5) and (4.6) are shown in the Table 4.I below.

4.2.3 Frequency of Baffled Column

The cross sectional area of the column is reduced by a factor of 0.555 in the region of the 2 in. dia. disc baffles. The equivalent length of the constriction was estimated by RAYLEIGH's (43) expression for circular apertures to be 2.01 in. per baffle. Therefore with twenty four baffle plates the liquid column consists of an equivalent 4.02 ft. with cross sectional area of 0.0273 ft^2, and 10.15 ft. with cross sectional area of 0.0491 ft^2. The frequencies predicted on this basis are shown in Table 4.I below.

4.2.4 Frequency of Packed Column

VERMIJS (42) has proposed that the acoustic impedance of a packed section is approximately 2.85 times that of the same length of unobstructed column. Therefore the total equivalent length of the column, using 3.3 ft. of packing, and with $C = C_o = 0.0491$ ft^2 is:

$$H_L = (14.17 - 3.3) + 3.3 \times 2.85$$

$$= 20.27 \text{ ft.}$$

This value for H_L was used to calculate the frequencies shown in Table 4.I below.

Table 4.I: Predicted Resonant Frequencies (Hz)

	Both ends closed Equ. (4.5)	One end open Equ. (4.6)
Undamped column	1.45	1.05
Column with 24 baffles	1.31	0.95
Column with 3.3 ft. packing	1.19	0.86

4.2.5 Observed Behaviour of Column

Observed frequencies and amplitudes for the ungassed column are shown in Fig. 4.2. In general the observed frequencies are bracketted by the two extreme values computed by equations (4.5) and (4.6). At low air flow rates the resistance of the exhaust system to flow is minimal, so that in effect the column is behaving as a U-tube oscillator with one leg open to atmosphere, and equation (4.6) should apply. At high air flow rates, the flow of air from the gas spaces is throttled, and the behaviour of the column tends towards the 'both ends closed' model, described by equation (4.5). The increase in frequency with increasing air rate is partly attributable to this, and partly to the increasing total pressure in the column due to choking of the exhaust. The packed column demonstrated a tendency to fall in frequency at high air flow rates. BAIRD (44) has suggested that this is probably due to the heavy damping of this system.

The rapid fall-off in frequency at the low air flow rate end of the range of observed frequencies is probably due to a control system lag caused by surface tension effects between the slowly moving liquid surface under these conditions and the tip of the proximity switch

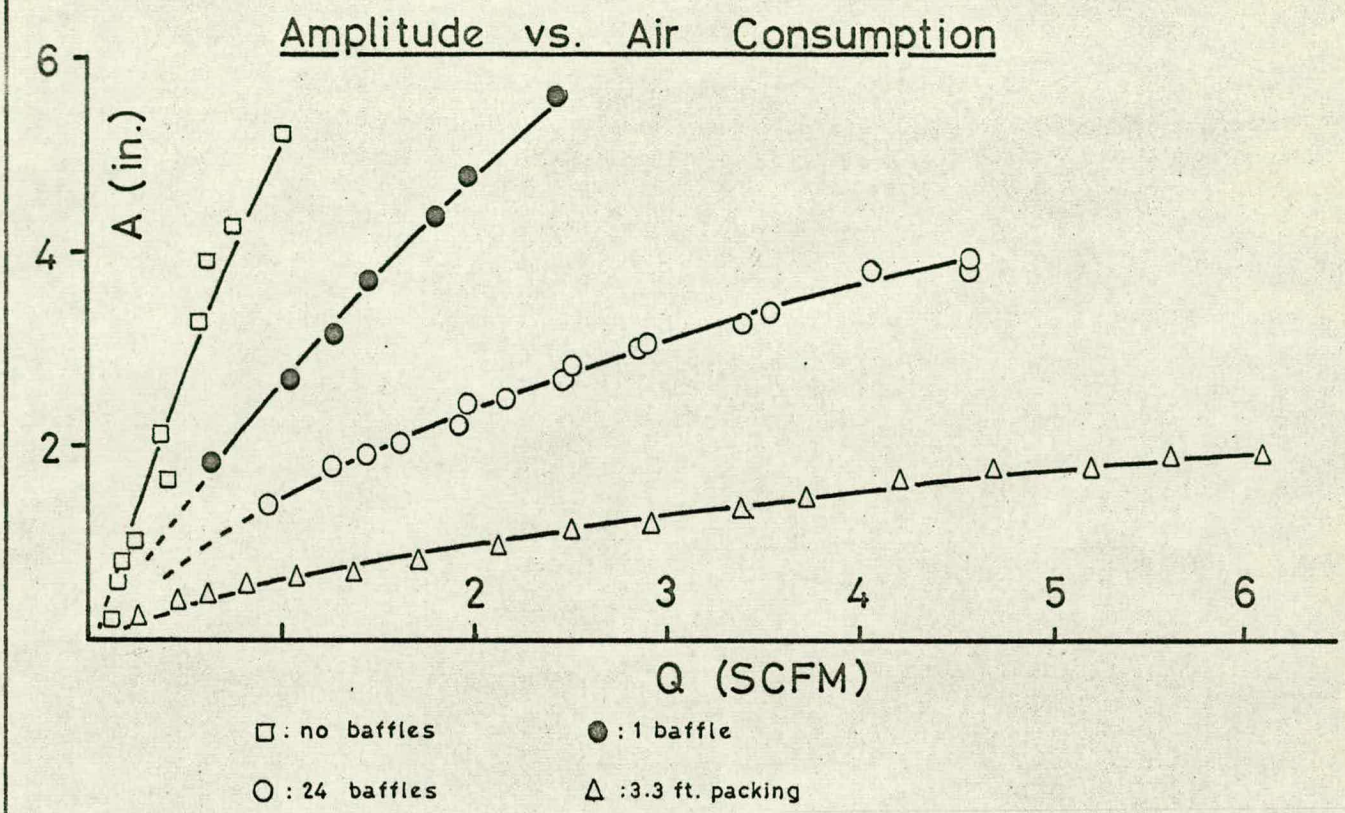
Amplitude vs. Air Consumption
A (in.)
6
4
2
2
3
4
5
6
Q (SCFM)
□ : no baffles
● : 1 baffle
○ : 24 baffles
△ : 3.3 ft. packing

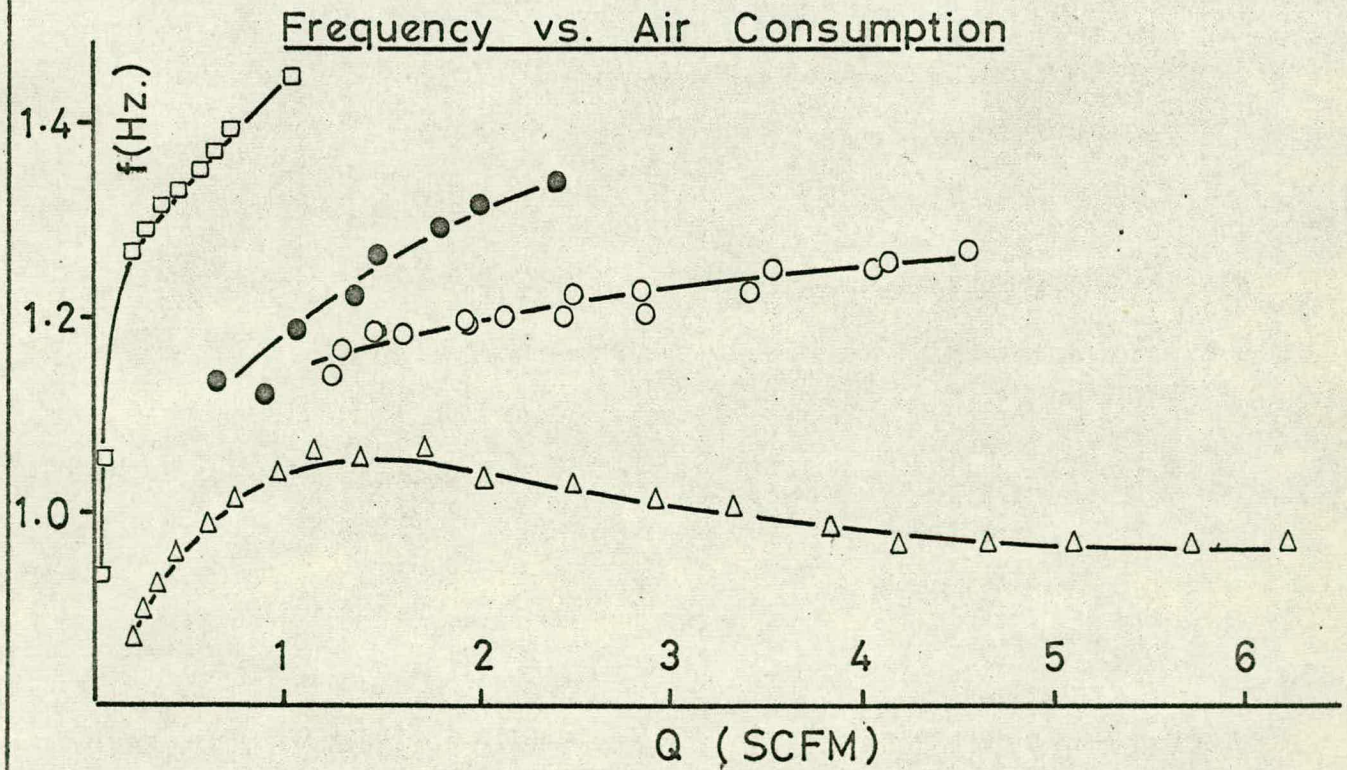
Frequency vs. Air Consumption
f(Hz.)
1.4
1.2
1.0
1
2
3
4
5
6
Q (SCFM)

Figure 4.2

probe.

4.3 Amplitude and Frequency in the Gassed Column

For subsequent experiments with gas-liquid dispersions, the 24-baffle configuration was chosen as representing a moderately damped case. Preliminary experiments with both the undamped column and the packed column showed that in the first case there were no observable effects of the pulsation upon the dispersion, other than a very slight reduction of the frequency according to Baird's (34,44) prediction, while in the case of the packed column, damping was found to be too great to allow sufficient variation of frequency and amplitude within the range of interest.

Frequencies and amplitudes for the 24-baffle column with dispersed air are shown in Fig. 4.3.

Frequency of operation at a given pulse-air flow rate tends to increase slightly with dispersed air flow rate. Consideration of Fig. 4.2 and Fig. 4.3 indicates that the frequency rises by about 5% as the superficial gas velocity is increased from zero to 0.043 ft./sec. This result contradicts BAIRD (34), whose theory and observations showed that dispersed gas reduces the resonant frequency of a liquid column. The latter work however concerned a uniform gas-liquid dispersion, whereas in the present investigation the bubble bed was seen to consist of clusters of bubbles oscillating around each baffle. Examples of the cluster forms encountered for varying conditions are presented in Plates II-VI. A possible explanation for the increase in frequency is suggested by BAIRD (45):

(a) The restriction due to each baffle contributes

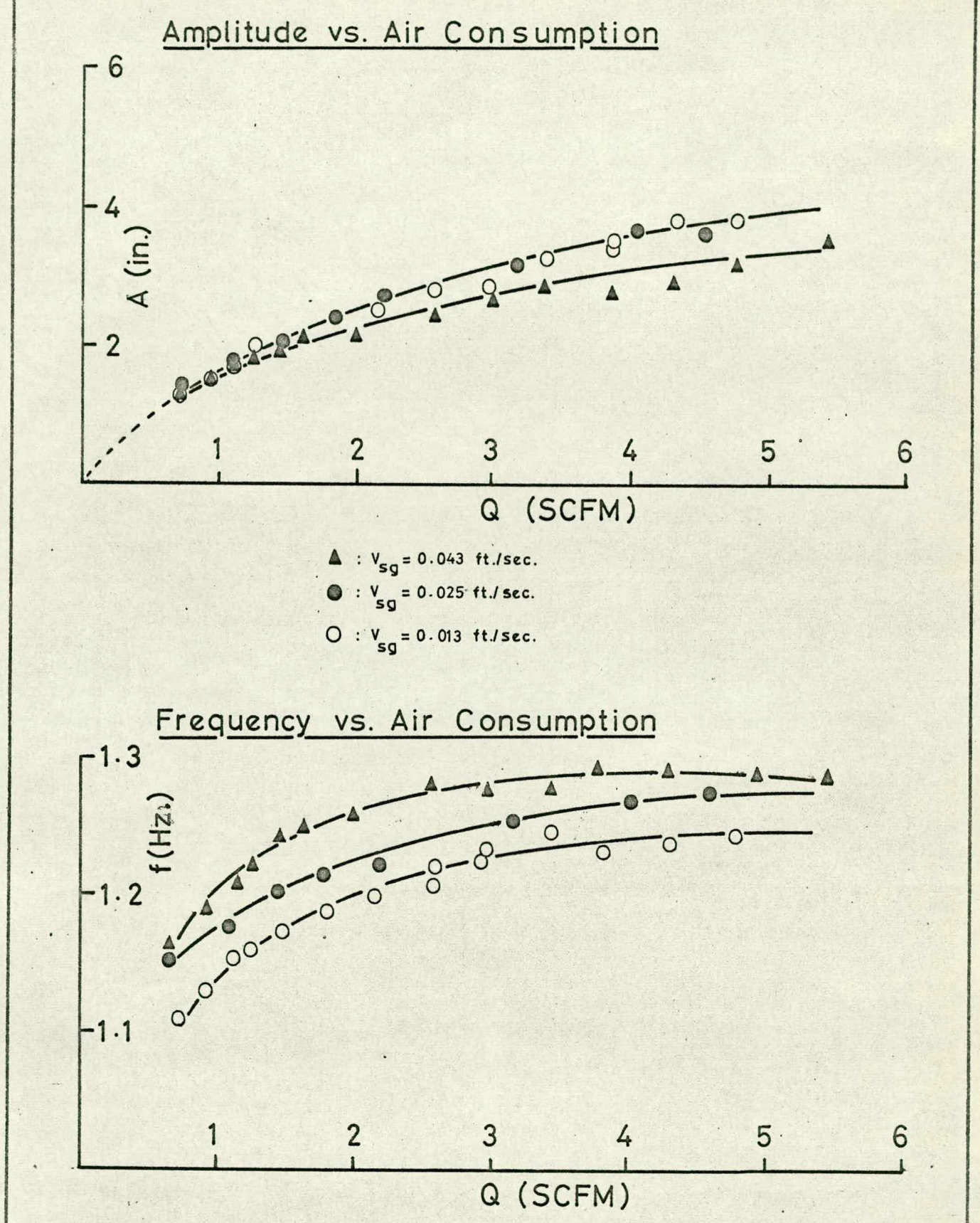
Amplitude vs. Air Consumption
6
4
2
A (in.)
1
2
3
4
5
6
Q (SCFM)
▲ : V_{sg} = 0.043 ft./sec.
● : V_{sg} = 0.025 ft./sec.
○ : V_{sg} = 0.013 ft./sec.
Frequency vs. Air Consumption
1.3
1.2
1.1
f(Hz)
1
2
3
4
5
6
Q (SCFM)

Figure 4.3

significantly to the total impedance of the system;

(b) The bubble density is greatest around the baffle plates;

(c) Hence the dispersed gas reduces the total impedance by more than it would in a uniformly dispersed system, causing an overall increase in the resonant frequency.

An effect of dispersed gas upon the amplitude of the column was observable only at the highest superficial gas velocity (0.043 ft.sec.$^{-1}$) at which it is reduced by 15%.

4.4 Mean Static Pressure in the Gassed Column

The mean static pressure as measured in the gassed column (24 baffles) at the height of the oxygen concentration probe is depicted in Fig. 4.4 as a function of ωA, the pulse velocity. It can be seen that the pressure in the column increases slowly with pulse velocity up to about $\omega A = 1.8$ ft./sec., when the curve makes a distinct break, the column pressure begins to increase rapidly with ωA, and the scatter of the observed pressures becomes more pronounced.

It is believed that the discontinuity in the curve at $\omega A = 1.8$ ft./sec. is due to the air-exhaust system of the column becoming 'choked', that is sonic velocity is approached in the exhaust system.

4.5 Holdup in the Gassed Column

The fractional holdup in the 24-baffle column was measured in two separate sets of runs by the two methods detailed in Section 3.6.2. In the paper which was published on the power dissipation work in this thesis, (Appendix VII), the superficial gas velocities were

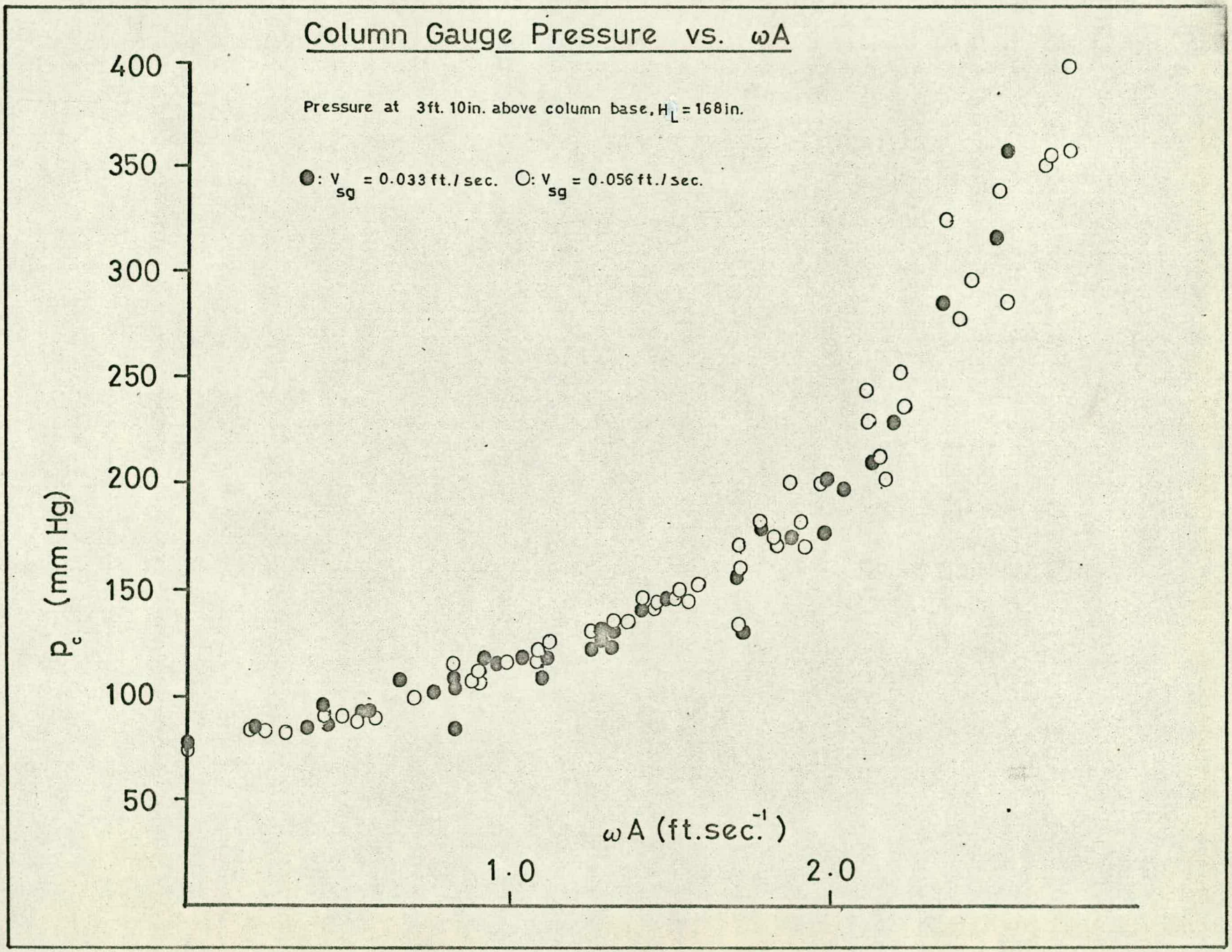
Column Gauge Pressure vs. ωA
Pressure at 3ft. 10in. above column base, H_L = 168in.
●: V_{sg} = 0.033 ft./sec. ○: V_{sg} = 0.056 ft./sec.
p_c (mm Hg)
400
350
300
250
200
150
100
50
ωA (ft.sec.$^{-1}$)
1·0
2·0

Figure 4.4

erroneously quoted as twice their actual value, and were in fact 0.043, 0.025 and 0.013 ft./sec. However, the holdup figures given in the paper were obtained by the first method (Section 3.6.2) in preliminary experiments. Some doubt was cast on the accuracy of higher pulsation rate holdups obtained by this method when the two-Rotameter arrangement was used.

The holdup was measured as function of the pulse velocity by the first method at superficial gas velocities of 0.043, 0.025 and 0.013 ft./sec., and by the second method at superficial gas velocities of 0.081, 0.051 and 0.027 ft./sec. The results of the two sets of runs are shown in Fig. 4.5 and Fig. 4.6 respectively, and tabulated in Appendix II.

It will be seen that the points for V_{sg} = 0.025 ft./sec. (first method) and V_{sg} = 0.027 ft./sec. (second method) are coincident at low power inputs, but that holdups obtained by the first method tend to fall off at higher power inputs. This is thought to be due to imperfect balancing of the gas flow to the column legs in the first method of measurement.

Further discussion of holdups will be concerned with the more accurate results obtained by the later method.

A significant increase in gas hold-up with pulsation is observed (Fig. 4.6), but only at pulse velocities higher than about 1.0 ft./sec. An explanation for the lack of hold-up increase at low values of ωA is suggested by the series of photographs (Plates II-VI) depicting the appearance of the dispersion in the region of a baffle for different conditions.

All photographs of the pulsed column were taken at

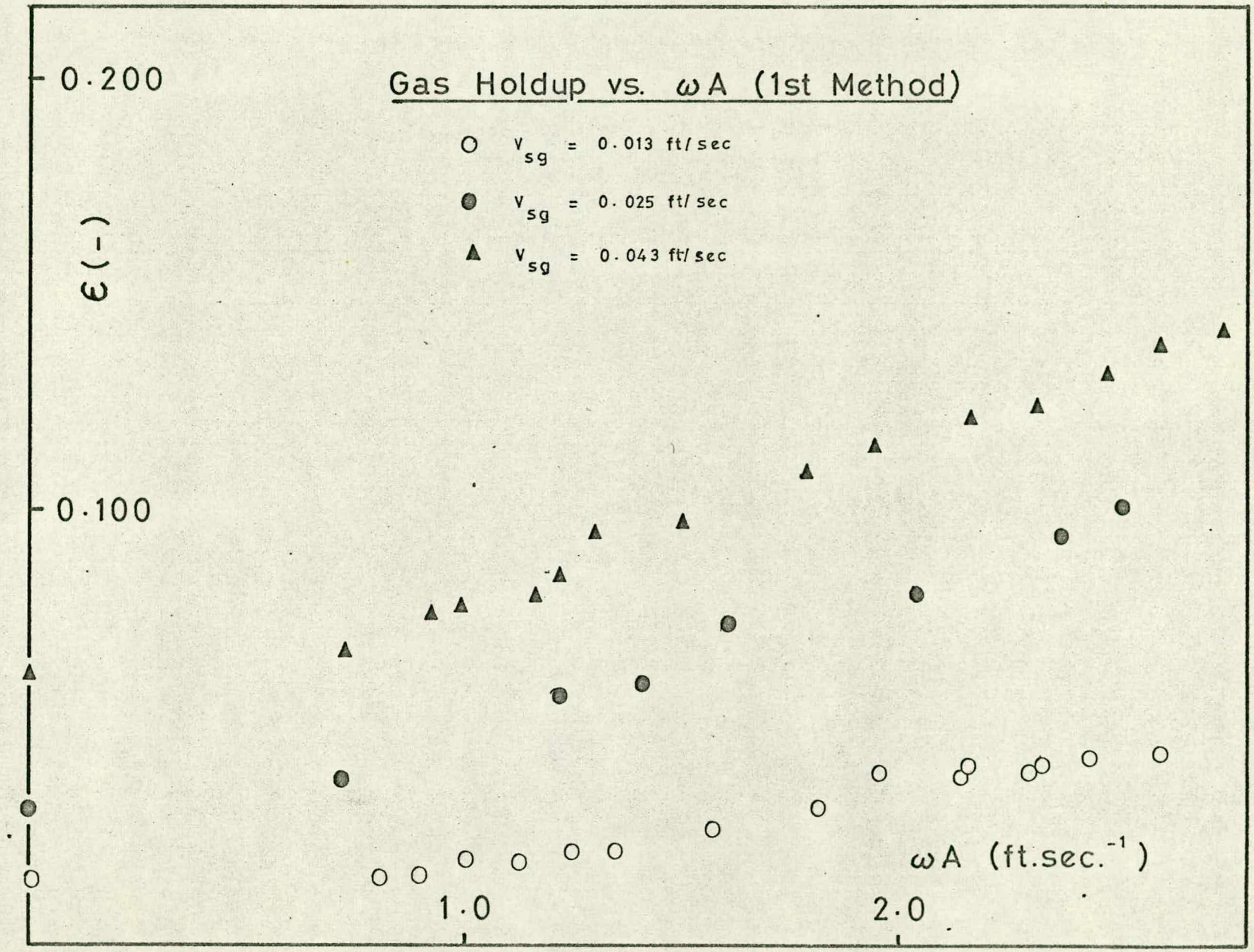
Gas Holdup vs. ωA (1st Method)
○ V_{sg} = 0.013 ft/sec
● V_{sg} = 0.025 ft/sec
▲ V_{sg} = 0.043 ft/sec
ε (-)
0.200
0.100
ωA (ft.sec.$^{-1}$)
1.0
2.0

Figure 4.5

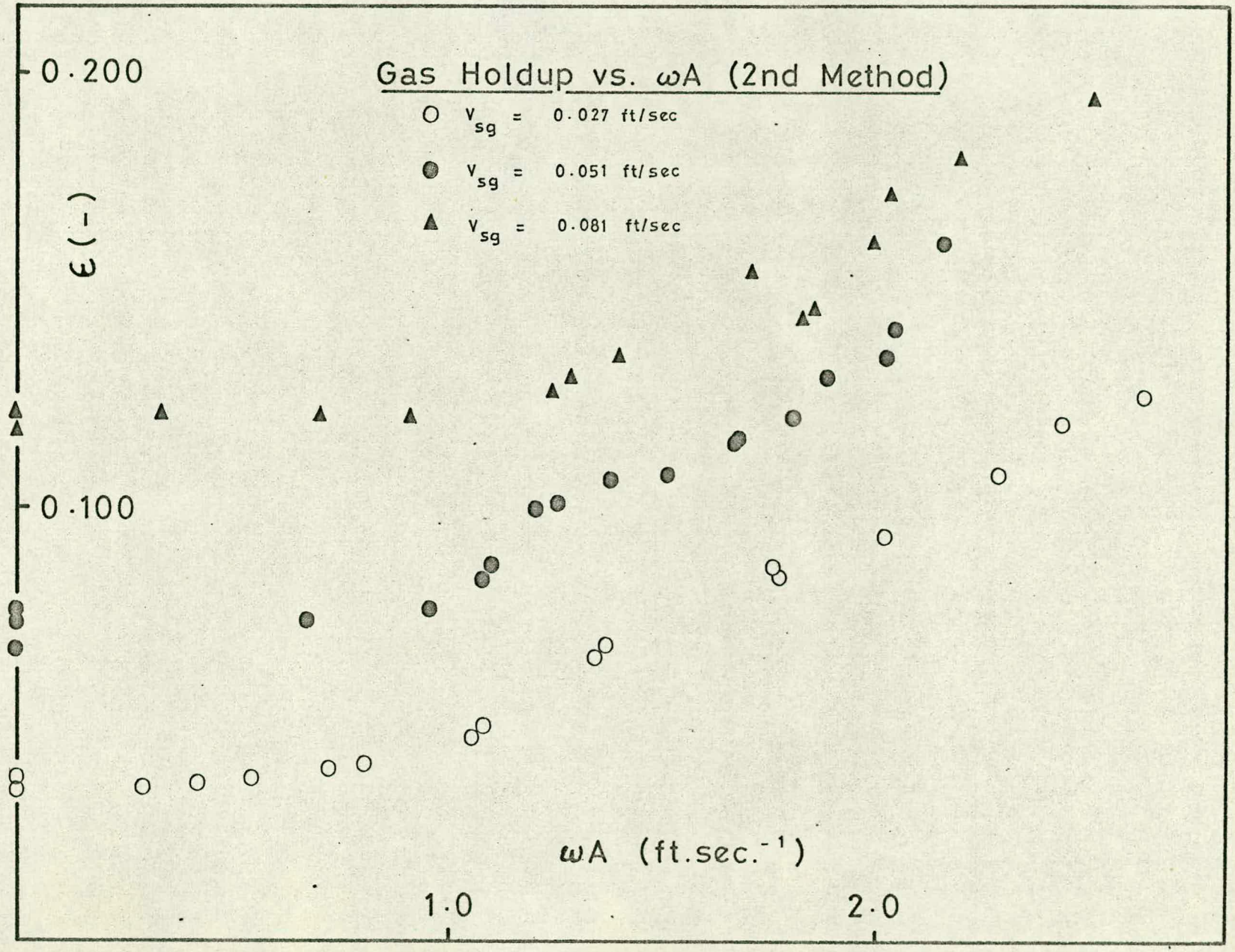
Gas Holdup vs. ωA (2nd Method)
O V_{sg} = 0.027 ft/sec
● V_{sg} = 0.051 ft/sec
▲ V_{sg} = 0.081 ft/sec
0.200
0.100
ε (-)
ωA (ft.sec.$^{-1}$)
1.0
2.0

Figure 4.6

maximum velocity of the dispersion (in an upward and downward direction as indicated by the arrow accompanying each photograph).

Plate II (a1,2,3) shows the appearance of the dispersion in its unpulsed state, while Plate II (b1,2,3) and Plate III (c1,2,3) show that of the dispersion under conditions of low pulse velocity. It will be observed that pulsations of this magnitude have no effect upon the size of the bubbles in the dispersion. Furthermore, it was observed that there was no trapping of bubbles in the region of the baffles, and the swarm of bubbles to be seen below the baffle on the downward stroke in (b1,2,3) is shed in its entirety to the baffle above on the upward stroke - this is more clearly seen in (c1).

A change in the visible behaviour of the dispersion occurs at about $\omega A = 0.8$ ft./sec., when the bubbles begin to be entrained in a 'permanent' cluster which oscillates about each baffle. The appearance of the dispersion in this case is shown in Plate III (d1,2,3) and Plate IV (e1,2,3). The entrainment of the bubbles in the region of the baffles is thought to be due to the existence of an oscillating annular vortex similar to that demonstrated by BAIRD (46) (Appendix VII) in a two-dimensional simulation of this equipment.

A further change in the behaviour of the dispersion takes place at around $\omega A = 1.3$ ft./sec. when a shearing of the bubbles is observed at the edges of the baffles, giving an appearance in this region similar to that encountered in the case of cavitation. This condition of the dispersion is shown in Plate IV (f1,2,3) and Plate V (g1,2,3). The size of the individual bubble begins to be affected at this stage, decreasing with increasing ωA.

Key to Plates II-VI

Appearance of the Dispersion in the Region of a Baffle

Photograph nos.	ωA ft./sec.	f^{-1} sec.$^{-1}$	A in.	Direction
II (a1,2,3)	0	0	0	-
II (b1,2,3)	0.44	1.07	0.8	down
III (c1,2,3)	0.44	1.07	0.8	up
III (d1,2,3)	0.85	1.18	1.4	down
IV (e1,2,3)	0.85	1.18	1.4	up
IV (f1,2,3)	1.51	1.24	2.3	down
V (g1,2,3)	1.51	1.24	2.3	up
V (h1,2,3)	2.87	1.35	4.1	down
VI (i1,2,3)	2.87	1.35	4.1	up

(a-i1) : V_{sg} = 0.026 ft./sec.

(a-i2) : V_{sg} = 0.051 ft./sec.

(a-i3) : V_{sg} = 0.085 ft./sec.

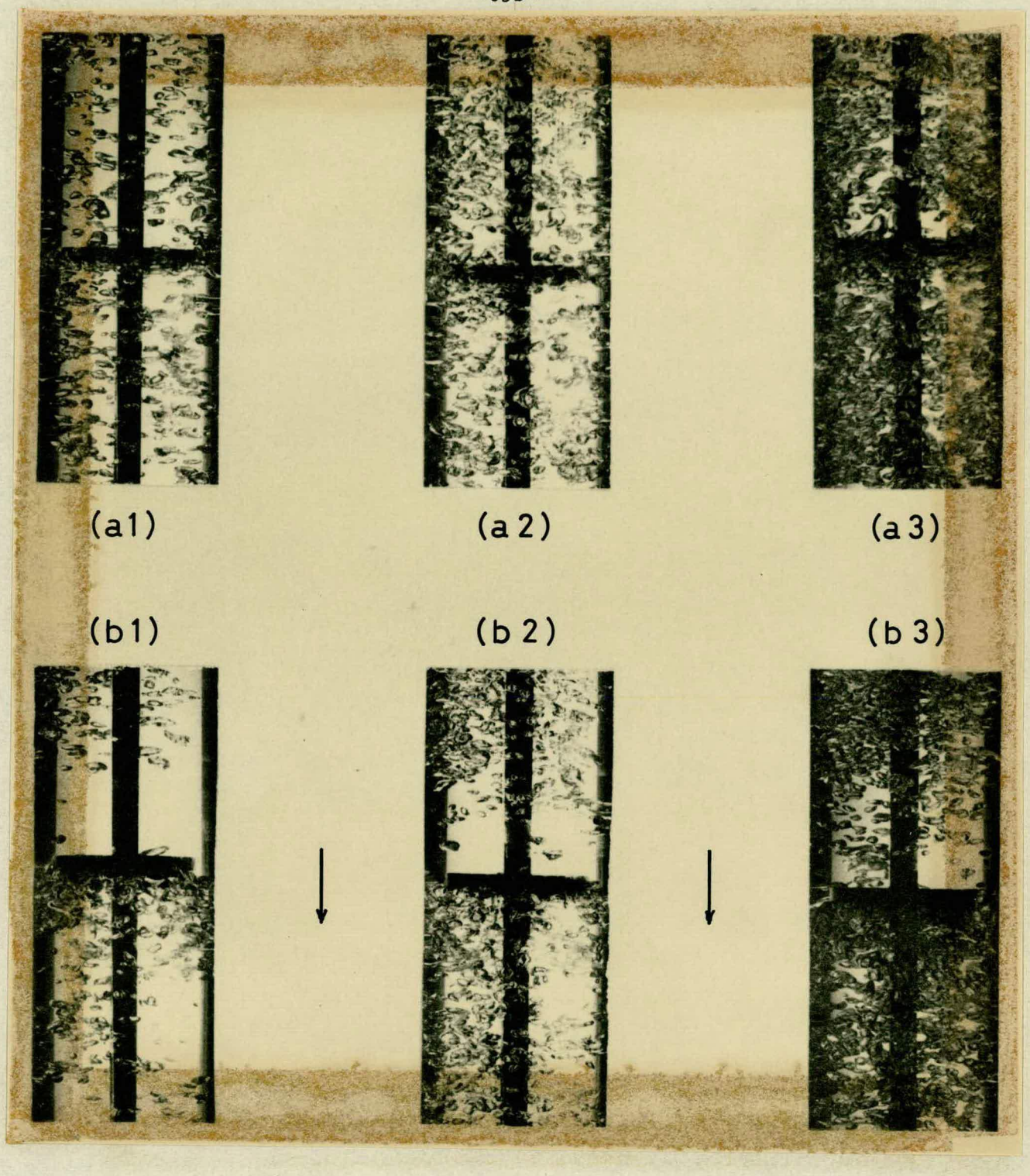

Plate II

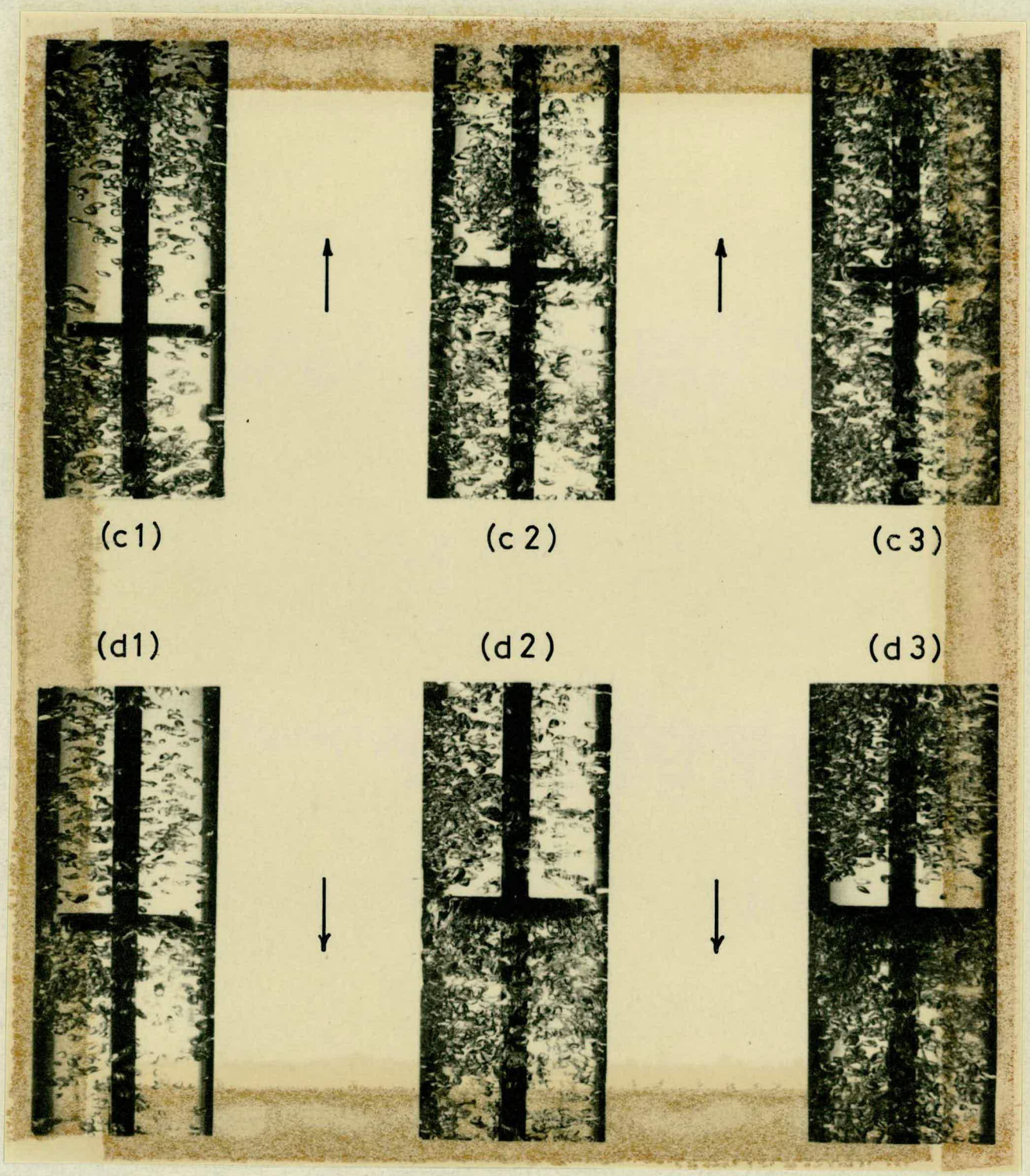

Plate III

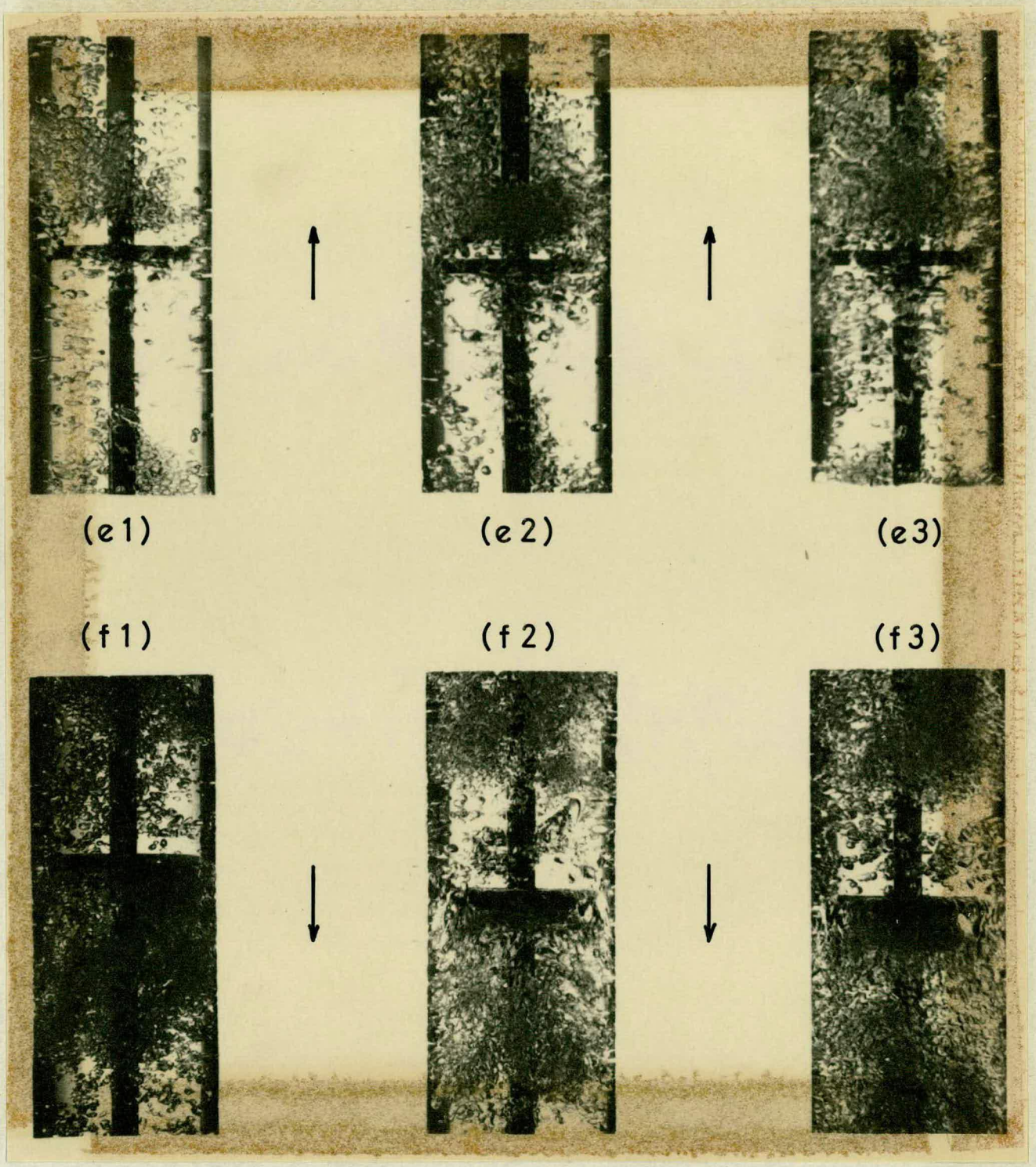

Plate IV

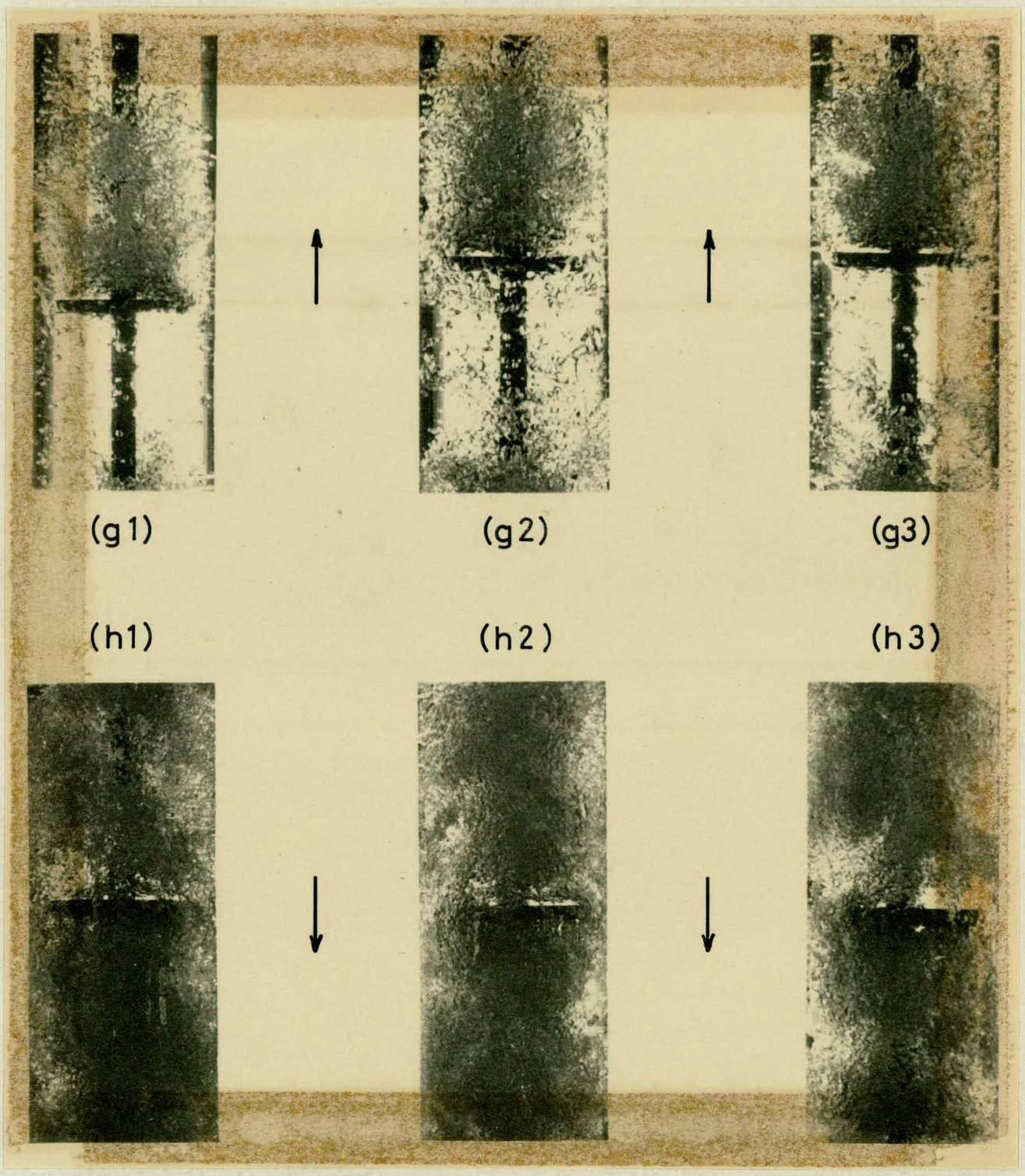

Plate V

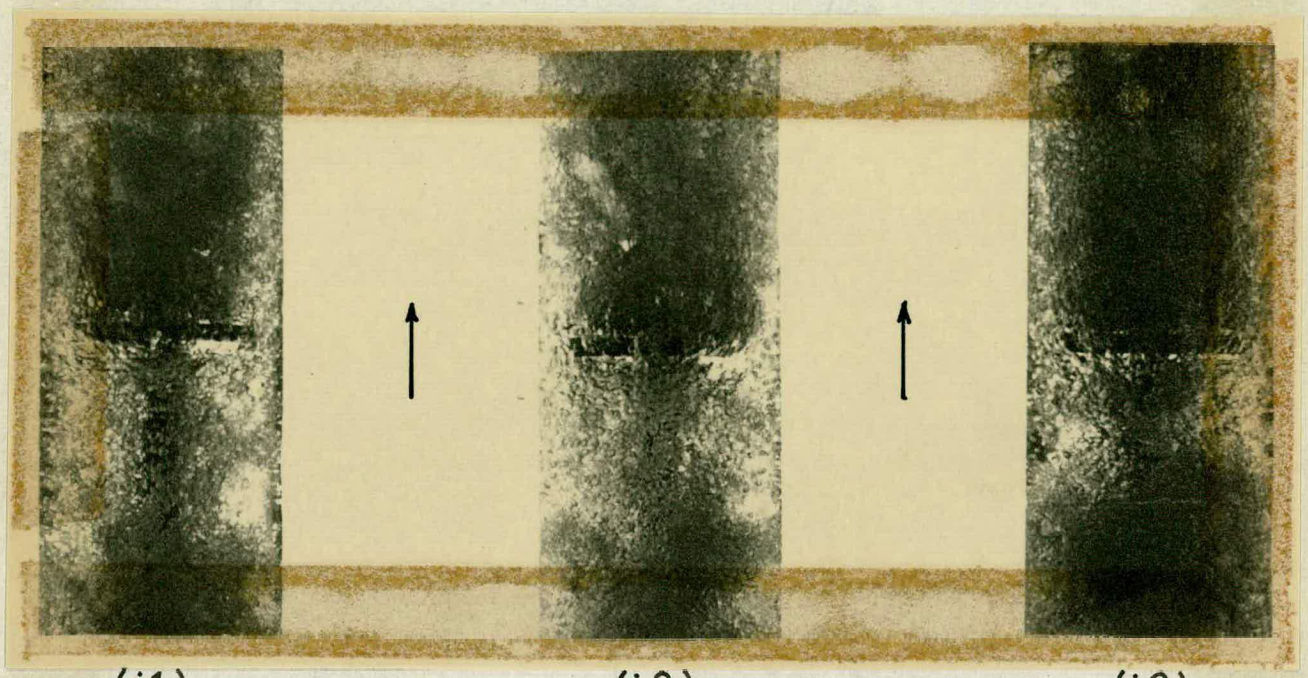

(i1) (i2) (i3)

Plate VI

The range of ωA from 0.8 to 1.3 ft./sec. is significantly coincident with the discontinuities in the holdup/pulse velocity relationship (Fig. 4.6), and would seem to be analogous to the 'critical impeller speed' reported by Westerterp et al (54). No direct comparison is possible between Westerterp's critical impeller tip speed of 7.9 ft./sec. and the critical pulse velocity of about 1.0 ft./sec.

Plate V (h1,2,3) and Plate VI (i1,2,3) demonstrate the highly dispersed nature of the bubble cluster at the (for the present apparatus) very high pulse velocity of 2.87 ft./sec.

The holdup results are further discussed in Chapter 6.

4.6 Power Dissipation

4.6.1 Indicator Diagrams

Examples of indicator diagrams obtained for various column conditions are presented in Plate VII. Pressure and volume waveforms varied from almost purely sinusoidal forms in the case of the unbaffled column to the most heavily damped case (the packed column) shown in diagrams (a) and (b). The switching points in the pressure waveform are indicated by the discontinuities.

In the diagram for the unbaffled (Plate VIIc) an area of negative work may be seen at the high volume, low pressure end of the diagram. This is due to the practically undamped condition of the column causing an amount of work to be done by the column of liquid on the gas space at the end of the downstroke. The net area and hence the net power dissipated in the column is relatively small. In this condition the pressure and volume waveforms are almost 180° out of phase (cf. Lissajou's

figures).

The baffled column diagram (Plate VIId) represents a degree of damping intermediate between the unbaffled column and the packed column. Starting at the lower left hand corner of the figure (low pressure and volume), the sudden rise in pressure is due to the opening of the inlet port, combined with a decreasing volume on the upstroke. As the surface passes through its maximum height, the pressure begins to fall, in spite of the continued inflow of air. When the exhaust port opens, the pressure falls more rapidly. After the liquid level has reached its minimum the pressure begins to rise slowly once more, until the inlet port opens, and the cycle is repeated. The pressure and volume waveforms are still almost 180° out of phase.

In the case of the packed column diagram (Plate VIIe), the form of the diagram has been modified considerably. In this case, the pressure is leading the volume by about 90°. The exhaust and inlet opening points are very marked. The inlet port opens at the lower left-hand corner of the diagram and the pressure rises steeply until minimum volume, after which the rate of inflow of air is almost balanced by the rate of fall of the surface, until the exhaust port opens and the pressure falls quite rapidly. After the maximum volume, the rate of exhaust is almost balanced by the rate of rise of the surface, until the inlet port opens and the cycle is repeated.

An example of the diagrams obtained from the gassed baffled column is shown in Plate VIIf. As can be seen, the diagram is basically the same as Plate VIId, except for the small loop at the top left-hand corner. This is due not to negative work, but to bubbling around

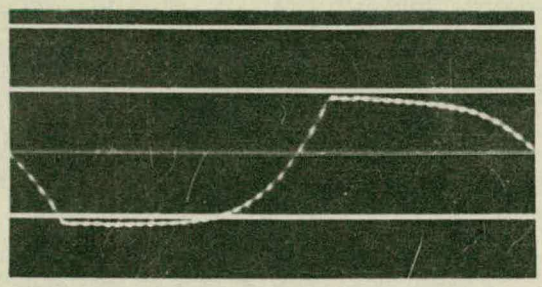

(a)

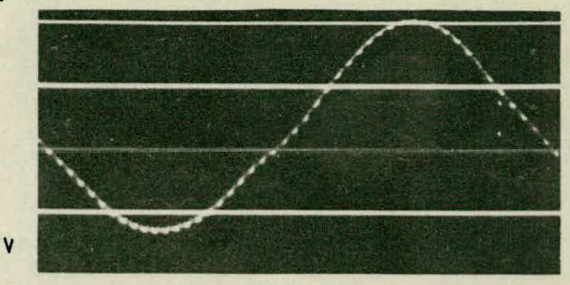

(b)

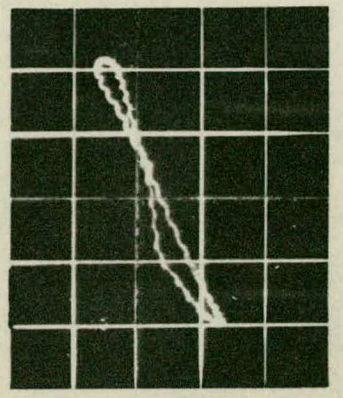

(c)

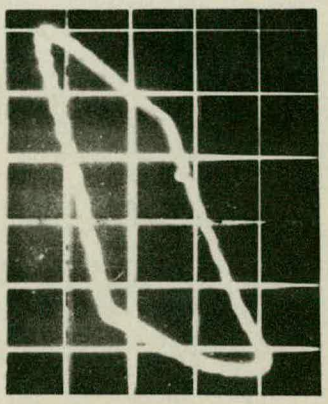

(d)

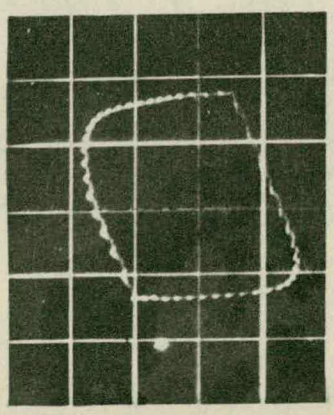

(e)

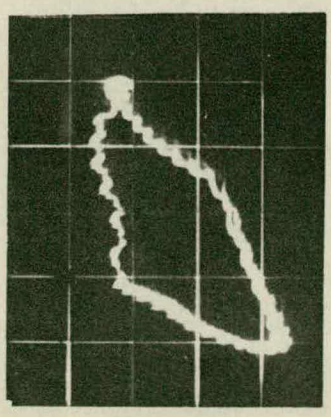

(f)

Plate VII

p-V Diagrams

the electrodes of the level meter, and was not a reproducible feature of the diagram for any set of conditions in the gassed column. The bubbling effect reduced the accuracy of the power dissipation measurement.

4.6.2 Prediction of Power Dissipation

JEALOUS & JOHNSON (40) calculated the theoretical power dissipation in a sinusoidally pulsed column. They showed that the power required to pulse a liquid-liquid extraction column is determined by the static head of the liquid system, the acceleration and deceleration forces on the system and the frictional losses.

The theoretical power dissipation in the present column is now derived after the method of Jealous and Johnson.

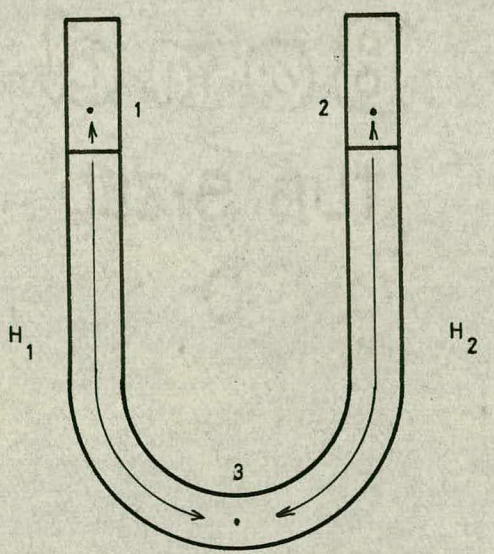

Fig. 4.7

Assuming that the column is in balanced operation, there is no pressure drop between points 1 and 2 in Fig. 4.7 due to static head.

There is an instantaneous pressure drop due to the inertia of the liquid column (subscripts refer to points marked in Fig. 4.7):

$$(p_3 - p_1)_{inertia} = \frac{\rho H_1}{g_c} \cdot \frac{d^2y}{dt^2} \qquad (4.7)$$

$$(p_2 - p_3)_{inertia} = \frac{\rho H_2}{g_c} \cdot \frac{d^2y}{dt^2} \qquad (4.8)$$

so that the total pressure drop due to inertia is

$$\Delta p_{inertia} = \frac{\rho}{g_c}(H_1 + H_2)\frac{d^2y}{dt^2} \qquad (4.9)$$

where y = instantaneous displacement from the mean position.

Hence the instantaneous power required to overcome the inertia of the column is

$$P_{inertia} = \Delta p_{inertia}\, C\, \frac{dy}{dt} \qquad (4.10)$$

There is an instantaneous pressure drop due to frictional losses at the baffles (or in the packing) given by

$$\Delta p_{friction} = \frac{\rho}{g_c} R\left[\frac{dy}{dt}\right]\left|\frac{dy}{dt}\right| \qquad (4.11)$$

where R, the frictional resistance of the dispersers is given by

$$R = \left[\frac{N(1 - \psi^2)}{2C_D^2\psi^2}\right] \text{ for an assembly of N baffles} \qquad (4.12)$$

(from the usual expression for flow through an orifice)

or

$$R = \left[\frac{2F_m(1 - \varepsilon_b)^{3-n}}{\Phi_s^{3-n}\,\varepsilon_b^3}\right]\left[\frac{L_p}{D_p}\right] \text{ for packing} \qquad (4.13)$$

(Ref. PERRY (41))

Hence the total instantaneous power dissipation is

given by

$$P_{inst} = C(\Delta p_{inertia} + \Delta p_{friction}) \frac{dy}{dt} \tag{4.14}$$

or substituting Equ. 4.9 and Equ. 4.11

$$P_{inst} = \frac{C\rho}{g_c} \frac{dy}{dt} \left\{ (H_1 + H_2) \frac{d^2y}{dt^2} + R \left[\frac{dy}{dt}\right] \left| \frac{dy}{dt} \right| \right\} \tag{4.15}$$

Now the displacement from the mean position, y, is given by

$$y = A \sin \omega t \tag{4.16}$$

so that

$$\frac{dy}{dt} = A\omega \cos \omega t \tag{4.17}$$

and

$$\frac{d^2y}{dt^2} = -A\omega^2 \sin \omega t \tag{4.18}$$

so that the total instantaneous power dissipation in the column is given by substitution in Equ. 4.15

$$P_{inst} = \frac{C\rho}{g_c} A\omega \cos \omega t \left[(H_1 + H_2)(-A\omega^2 \sin \omega t) + R(A\omega)^2 \cos \omega t \left| \cos \omega t \right| \right] \tag{4.19}$$

Integrating over one cycle, the inertial term vanishes, so that

energy dissipation/cycle =

$$\frac{4C\rho}{g_c} (A\omega)^3 R \int_0^{\pi/2\omega} \cos^2 \omega t \left| \cos \omega t \right| dt \tag{4.20}$$

Integrating Equ. 4.20

$$\text{energy dissipation/cycle} = \frac{4C\rho}{g_c} (A\omega)^3 R \frac{2}{3\omega} \tag{4.21}$$

Since the period of pulsation $T = \frac{2\pi}{\omega}$ (4.22)

the theoretical average energy dissipation/unit time (the power dissipation is given by

$$P_{th} = \frac{4}{3\pi} \cdot \frac{C\rho}{g_c} \cdot R (A\omega)^3 \tag{4.23}$$

Substituting for R from Equ. 4.12 and Equ. 4.13 in Equ. 4.23 we obtain for the baffled column

$$P_{th} = \frac{4}{3\pi} \frac{C\rho}{g_c} \left[\frac{N(1 - \psi^2)}{2C_D^2 \psi^3} \right] (A\omega)^3 \qquad (4.24)$$

and for the packed column

$$P_{th} = \frac{4}{3\pi} \frac{C\rho}{g_c} \left[\frac{2F_m(1 - \varepsilon_b)^{3-n}}{\phi_s^{3-n} \varepsilon_b^3} \right] \left[\frac{L_p}{D_p} \right] (A\omega)^3 \qquad (4.25)$$

4.6.3 Power Dissipation - Results

Data and results obtained for the power dissipation experiments are tabulated in Appendix III, and compared with the predicted power dissipations in Figs. 4.8, 4.9 and 4.10. It is seen that although the data for the packed column (Fig. 4.8) are mostly within 10% of the prediction, the observed power dissipations with 24 baffles (Fig. 4.9) are about 30% too low. The results with the single baffle appear to agree with the prediction, but this may not be significant because of the relatively large effect of wall friction and dissipation at bends. It was suggested by BAIRD (46) that the unexpectedly low power dissipations obtained with the baffle column were perhaps due in some measure to energy recovery by winding and unwinding vortices through the annular orifice around the baffle plate, such an effect being less likely in the randomly-shaped interstices of the packed column.

Results obtained for the gassed column (Fig. 4.10) at superficial gas velocities of 0.025 ft./sec. and 0.043 ft./sec. do not appear to differ significantly from those obtained in the absence of dispersed gas.

A working equation for the power input to the baffle

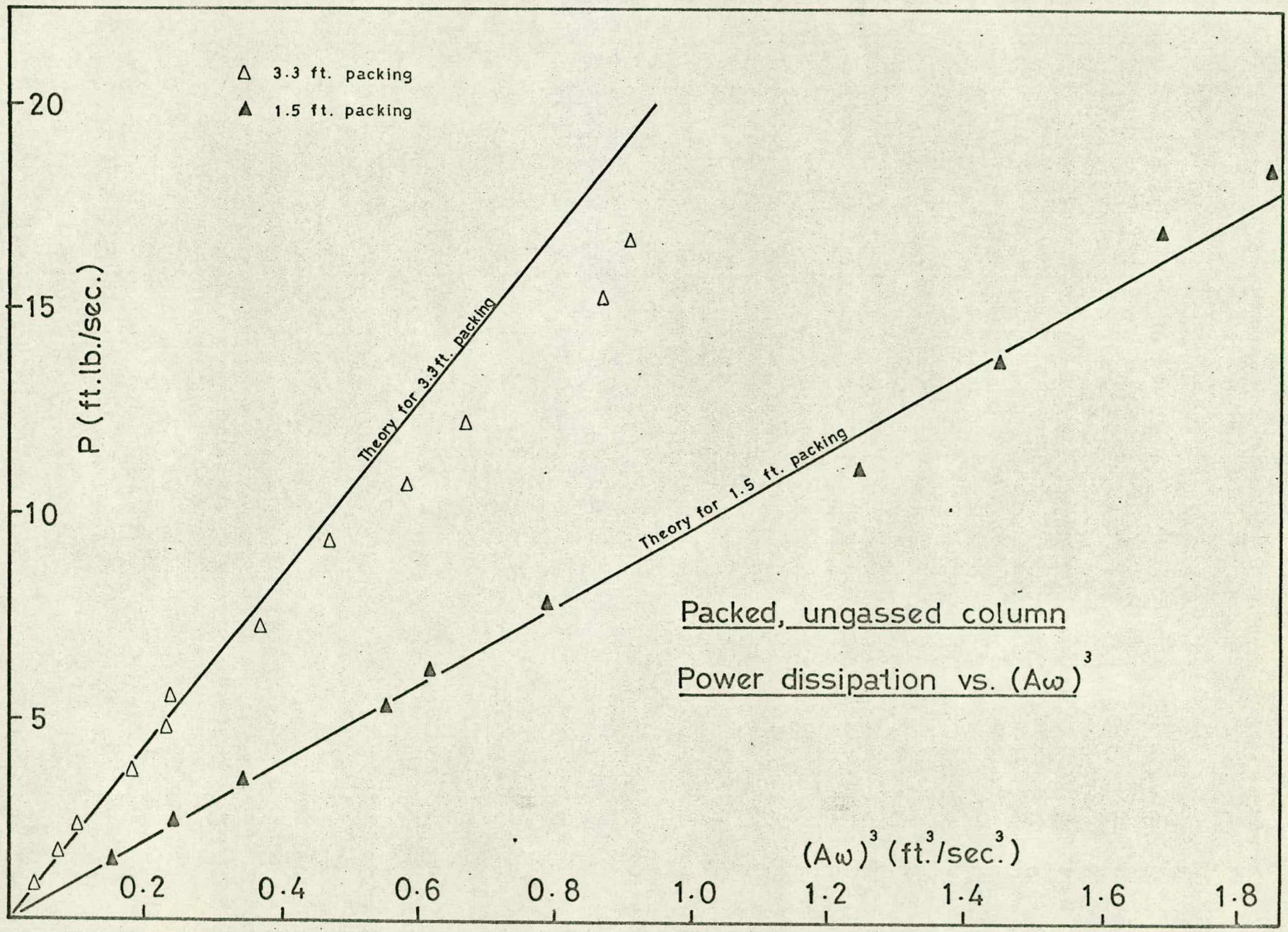
△ 3.3 ft. packing
▲ 1.5 ft. packing
20
15
10
5
P (ft.lb./sec.)
Theory for 3.3 ft. packing
Theory for 1.5 ft. packing
Packed, ungassed column
Power dissipation vs. (Aω)³
(Aω)³ (ft.³/sec.³)
0.2
0.4
0.6
0.8
1.0
1.2
1.4
1.6
1.8

Figure 4.8

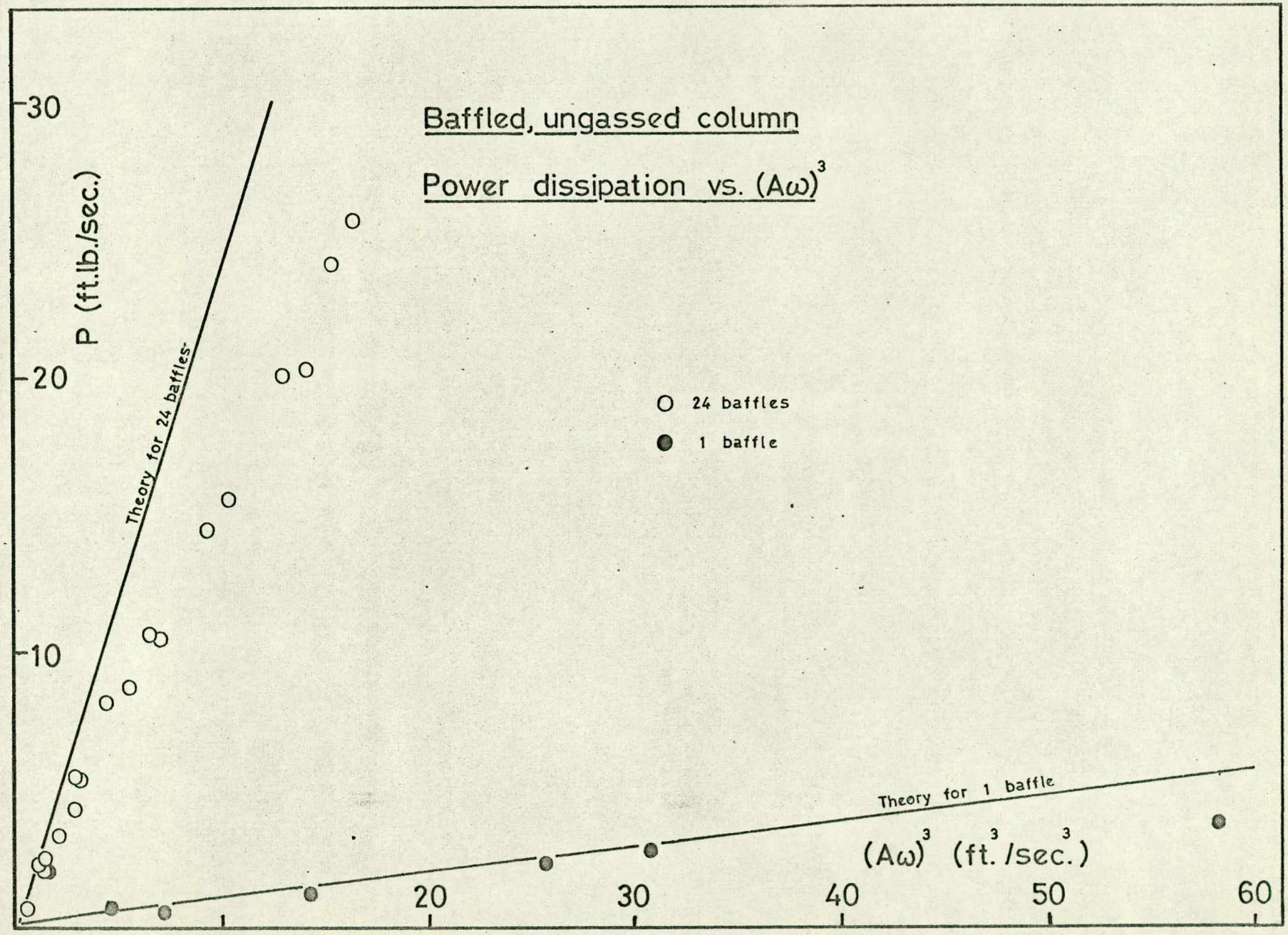
Baffled, ungassed column
Power dissipation vs. (Aω)³
P (ft.lb./sec.)
30
20
10
Theory for 24 baffles
24 baffles
1 baffle
Theory for 1 baffle
(Aω)³ (ft.³/sec.³)
20
30
40
50
60

Figure 4.8

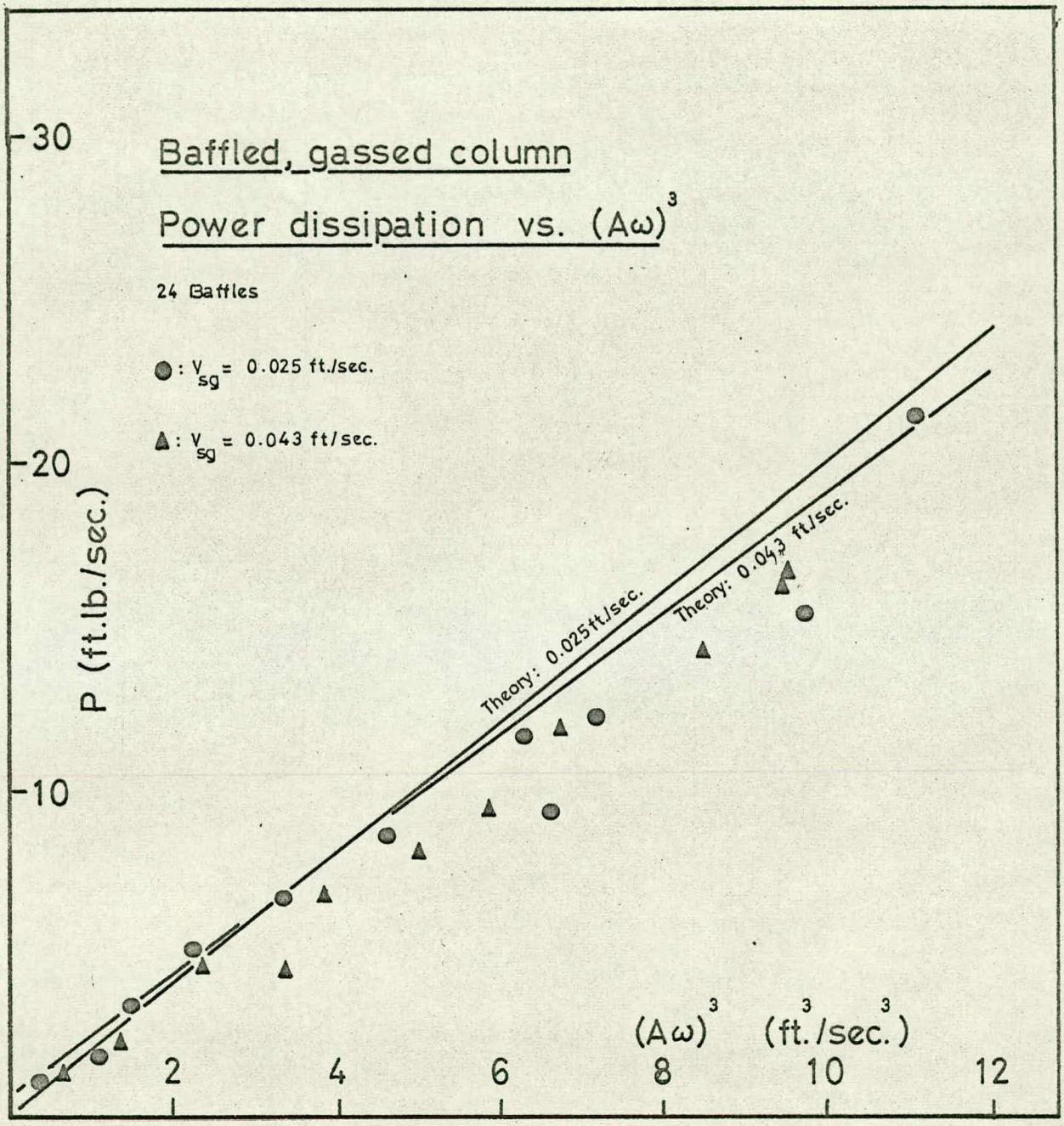
Baffled, gassed column
Power dissipation vs. $(A\omega)^3$
24 Baffles
● : V_{sg} = 0.025 ft./sec.
▲ : V_{sg} = 0.043 ft/sec.
Theory: 0.025ft/sec.
Theory: 0.043 ft/sec.
P (ft.lb./sec.)
30
20
10
2
4
6
8
10
12
$(A\omega)^3$ $(ft./sec.)^3$

Figure 4.10

column may be developed.

The theoretical power input to the column is given by Equ. 4.24 and from observations above, the actual power dissipated in the column is about 90% of that predicted by Equ. 4.24. Hence the power input to the column should be reasonably accurately predicted by

$$P'_{th} = 0.90 \cdot \frac{4}{3\pi} \cdot \frac{C \rho A^3 \omega^3 N(1 - \psi^2)}{2 g_c C_D^2 \psi^2} \qquad (4.26)$$

where $\rho = \rho_L(1 - \varepsilon)$. Substituting the values given for the constants in Appendix III.4, this reduces to

$$P'_{th} = 1.98(1 - \varepsilon)(\omega A)^3 \text{ ft.lb./sec.} \qquad (4.27)$$

A plot of the observed values of the power input against those predicted by Equ. 4.27 (Fig. 4.11) shows that a satisfactory prediction is obtained. The specific power input is therefore given by

$$P_s = P_{th}/(\text{volume of dispersion in the column})$$

$$= P_{th}/(0.67 \text{ ft}^3)$$

$$= 2.96(1 - \varepsilon)(\omega A)^3 \text{ ft.lb./ft}^3\text{sec.} \qquad (4.28)$$

4.7 Compressed Air Consumption

4.7.1 Prediction of Compressed Air Consumption

The rate of consumption of compressed air in maintaining pulsation of the column may be predicted in a similar manner to that of VERMIJS (42). The derivation is subject to certain simplifying assumptions, i.e.:

(a) The gas in the spaces at the top of the column behaves isothermally;

(b) The injection-exhaust valve has a sinusoidal

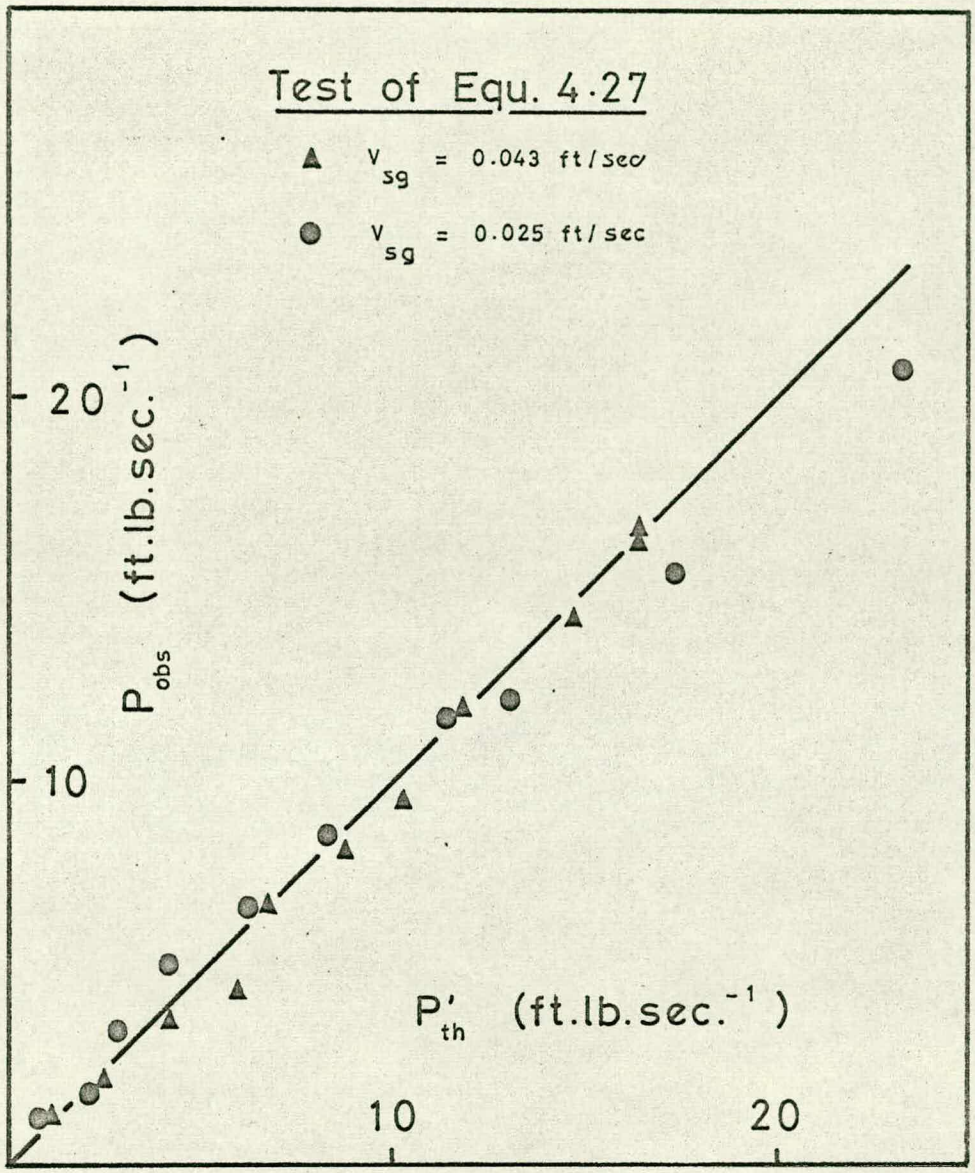
Test of Equ. 4·27
▲ V_{sg} = 0.043 ft/sec
● V_{sg} = 0.025 ft/sec
P_{obs} (ft.lb.sec.$^{-1}$)
20
10
P'_{th} (ft.lb.sec.$^{-1}$)
10
20

Figure 4.11

flow characteristic;

(c) The frictional force is proportional to the square of the velocity;

and (d) The assumptions that changes in pressure and displacements are relatively small.

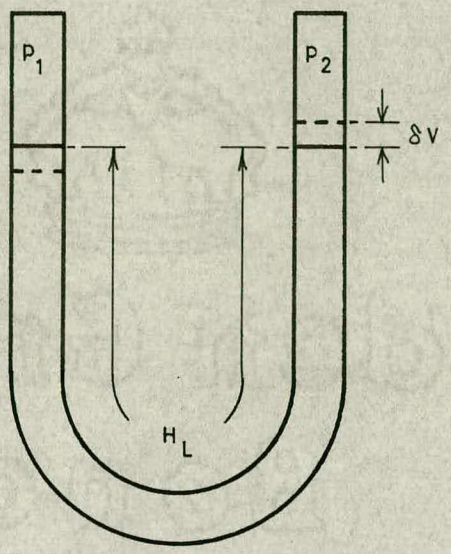

Fig. 4.12

Referring to Fig. 4.12:

Let V_G = volume of each gas space at equilibrium.

Let volume $V_1 = V_G + V_o.\cos \omega t$ (4.29)

and $V_2 = V_G - V_o.\cos \omega t$ (4.30)

where $V_o = A.C$

Let $p_2 > p_1$ as shown in Fig. 4.12.

There will be a restoring pressure balanced by inertia and friction, and augmented by gravity

$$p_1 - p_2 = \frac{\rho}{g_c}\left[\frac{H_L}{C}\frac{d^2V}{dt^2} + \frac{R}{C^2}\frac{dV}{dt}\left|\frac{dV}{dt}\right| - \frac{2g}{C}V\right] \qquad (4.31)$$

The difference between amounts of gas in each arm is

$$p_2V_2 - p_1V_1 = p_2(V_G - V_o\cos\omega t) - p_1(V_G + V_o\cos\omega t)$$

$$= (p_2 - p_1)V_G - (p_1 + p_2)V_o\cos\omega t \qquad (4.32)$$

Now $(p_1 + p_2) \simeq 2p_o$, where p_o = average gas pressure

Therefore

$$p_2V_2 - p_1V_1 = (p_2 - p_1)V_G - 2p_oV_o\cos\omega t \qquad (4.33)$$

Differentiating Equ. 4.33 with respect to time gives the difference between the flow of gas entering arm 1 and that entering arm 2, i.e.

$$\frac{d}{dt}(p_2V_2 - p_1V_1) = p_o(Q_2 - Q_1) \qquad (4.34)$$

where Q_1, Q_2 are gas flows referred to p_o.

$(Q_2 - Q_1)$ is evaluated by differentiating the RHS of Equ. 4.34

$$\frac{d}{dt}(RHS) = V_G\frac{d}{dt}(p_2 - p_1) + 2\omega p_oV_o\sin\omega t \qquad (4.35)$$

Now the volume of the gas space at any time is given by

$$V = V_o\cos\omega t \qquad (4.36)$$

so that

$$\frac{dV}{dt} = -V_o\omega\sin\omega t \qquad (4.37)$$

$$\frac{d^2V}{dt^2} = -V_o\omega^2\cos\omega t \qquad (4.38)$$

and substituting for $(p_2 - p_1)$ from Equ. 4.31 in Equ. 4.35 gives

$$\frac{d}{dt}(RHS) = \frac{V_G\rho}{g_o}\left[\frac{H_L}{C}V_o\omega^3\sin\omega t - 2\frac{R}{C^2}V_o^2\omega^3|\sin\omega t|\cos\omega t + 2\frac{g}{C}V_o\omega\sin\omega t\right] + 2\omega p_oV_o\sin\omega t \qquad (4.39)$$

Now if $-\pi/2\omega < t < \pi/2\omega$, the volume of chamber 1 will always be greater than that of chamber 2; that is air will be supplied to 2 and exhausted from 1. The difference between the amounts of air during this half-cycle will be equal to the total amount of air injected during a complete cycle.

Integrating Equ. 4.39 over the half-cycle from $-\pi/2\omega$ to $\pi/2\omega$, the sin t terms vanish, leaving the frictional term

$$\int_{-\pi/2\omega}^{\pi/2\omega} p_o(Q_2 - Q_1)dt = p_o Q_{th} = -\frac{}{g_c}\ \frac{R}{C^2}\ 2V_G\ V_o^2\ \omega^3 \int_{-\pi/2\omega}^{\pi/2\omega} |\sin \omega t| \cos \omega t.dt \qquad (4.40)$$

$$= 2\ \frac{R}{C^2}\ \frac{\rho}{g_c}\ V_G\ (V_o\ \omega)^2 \qquad (4.41)$$

Hence the average air flow is

$$Q_{th}{}^f = \frac{Q\omega}{2\pi} = \frac{\rho}{g_c}\left[\frac{RV\ V_o^2\ \omega^3}{\pi p_o C^2}\right] \qquad (4.42)$$

Now substituting for R from Equ. 4.12 and Equ. 4.13, and for $V_o = C.A$, the theoretical air consumption for the baffled column is given by

$$Q_{th} = \frac{\rho}{g_c}\ \frac{V_G}{\pi p_o}\left[\frac{N(1 - \psi^2)}{2C_D^2\ \psi^2}\right] A^2\ \omega^3 \qquad (4.43)$$

and for the packed column by

$$Q_{th} = \frac{\rho}{g_c} \cdot \frac{V_G}{p_o}\left[\frac{2F_m(1 - \varepsilon_b)^{3-n}}{\phi_s^{3-n}\ \varepsilon_b^3}\right]\left[\frac{L_p}{D_p}\right] \qquad (4.44)$$

4.7.2 Compressed Air Consumption - Results

Measured compressed air consumptions are tabulated in Appendix III, and are compared with the predicted air consumptions in Figs. 4.13 and 4.14.

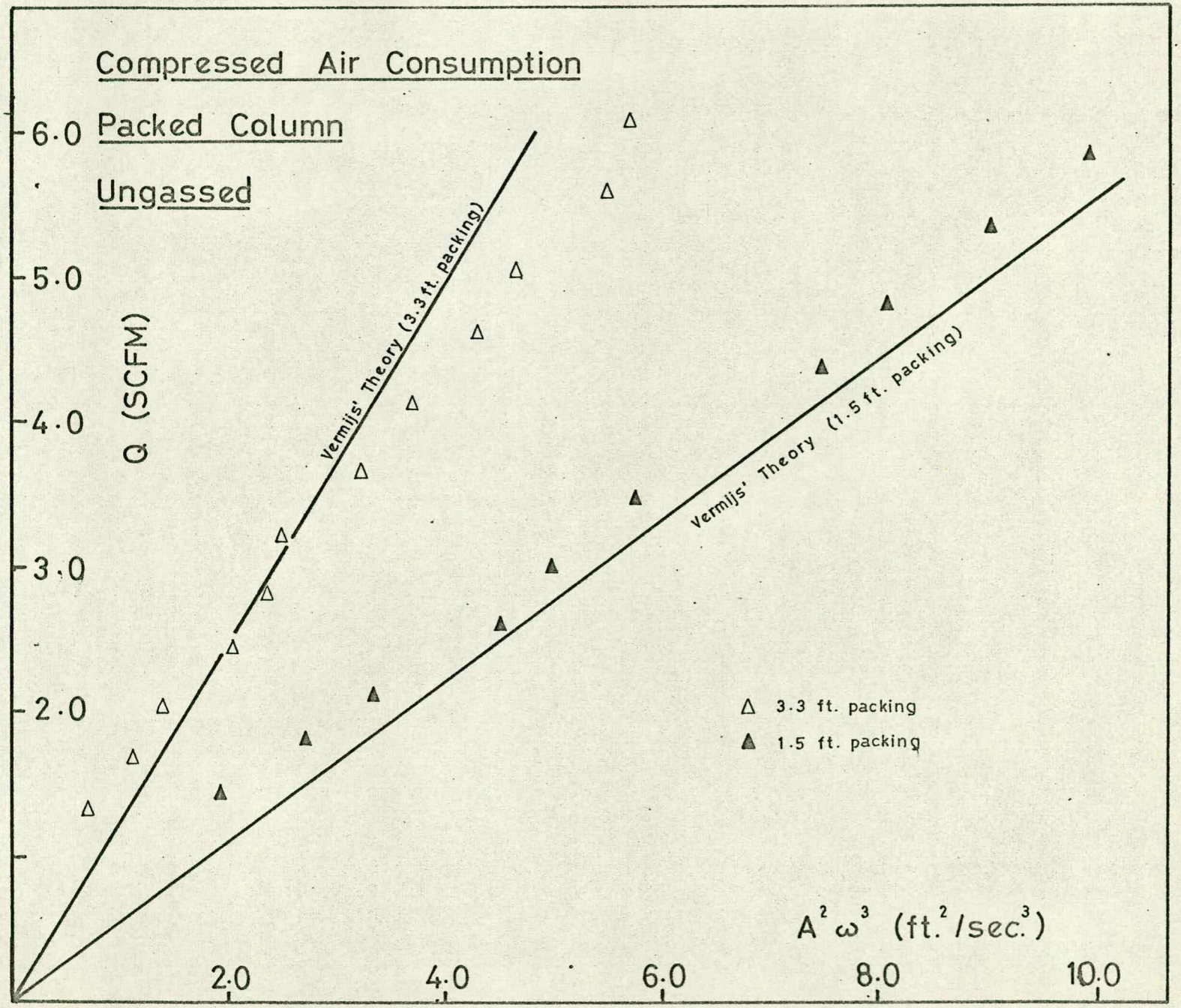
Compressed Air Consumption
Packed Column
Ungassed
Q (SCFM)
6.0
5.0
4.0
3.0
2.0
Vermijs' Theory (3.3 ft. packing)
Vermijs' Theory (1.5 ft. packing)
3.3 ft. packing
1.5 ft. packing
A² ω³ (ft.²/sec.³)
2.0
4.0
6.0
8.0
10.0

Figure 4.13

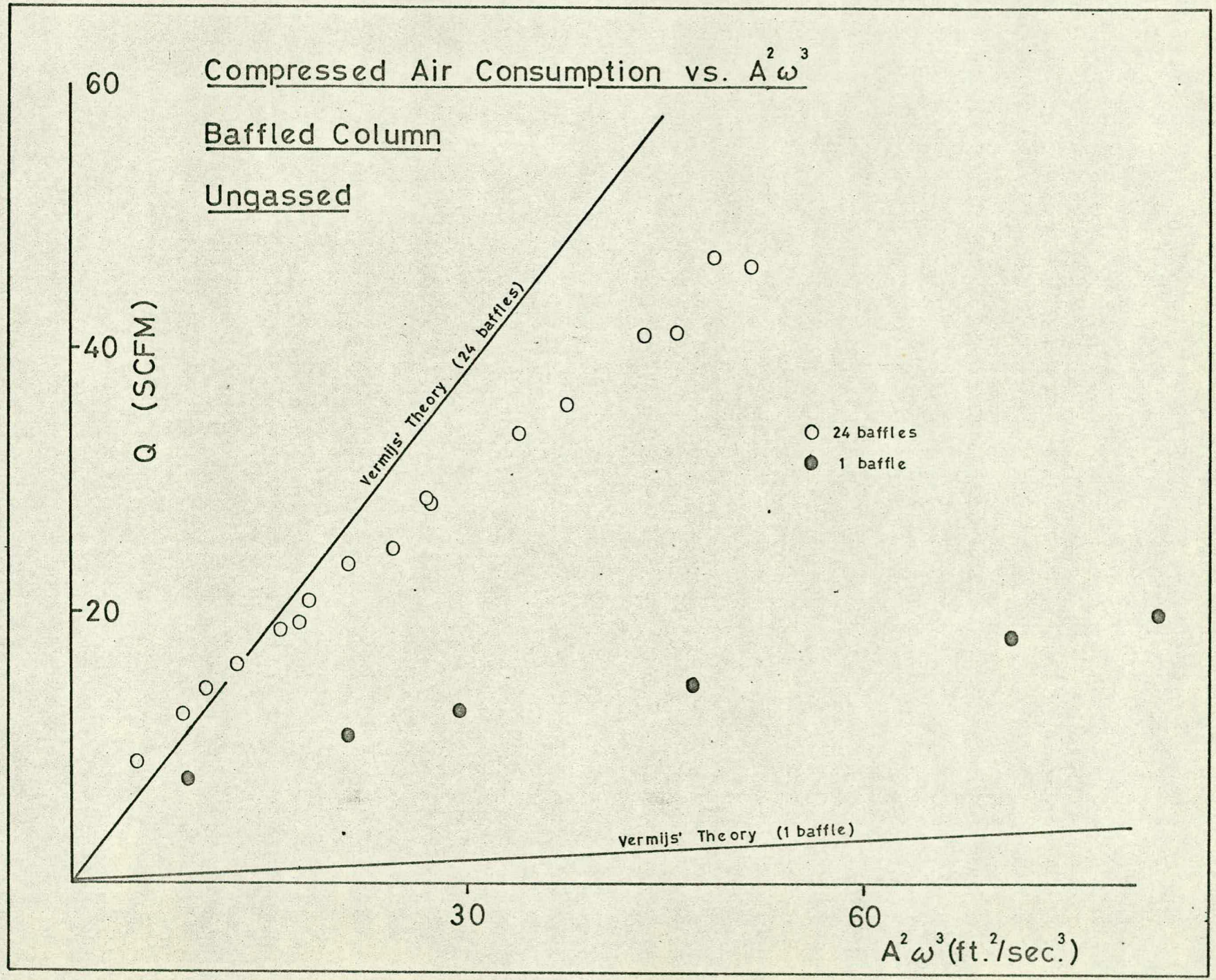
Compressed Air Consumption vs. $A^2\omega^3$
Baffled Column
Ungassed
60
40
20
Q (SCFM)
Vermijs' Theory (24 baffles)
24 baffles
1 baffle
Vermijs' Theory (1 baffle)
30
60
$A^2\omega^3$ (ft.^{2}/sec.^{3})

Figure 4.14

The observed air consumptions were within ± 20% of the theory in the case of the 24 baffle column and the packed column. Considering the ideal conditions assumed in the prediction of the air consumptions, this is a reasonable agreement.

By Equ. 4.37, the air consumption of the single baffle column should be 1/24 of that for the 24 baffle column. In Fig. 4.14 it can be seen that the measured air consumption of the single baffle column is much higher than the prediction. The discrepancy may be explained by the relatively large additional drag due to wall effects and bends. These effects are less significant in heavily damped columns.

Chapter 5

Absorption Rates in the Pulsed Column

5.1 Introduction

In the process of absorption of a gas into a liquid the rate of absorption may be controlled by either the rate of diffusion of the gas species across the gas-liquid interface, or the rate of any chemical reaction which may occur within the body of the liquid. In gauging the performance of a gas-liquid contactor, therefore, it is necessary that the physical absorption be the rate determining step for the process. In the present work the possibility of any rate-limiting chemical reaction is avoided by the use of an unsteady state absorption of oxygen from air into water. The method has been successfully applied by PROCTOR (38) to measure aeration rates in model rivers and by GAL-OR et al (39) to measure mass transfer rates in stirred tanks.

A serious problem in the measurement of mass transfer rates by any method is the effect of surfactants (39), (40), (48), which may inhibit coalescence and hence lead to the formation of smaller bubbles, and which may reduce the mass transfer coefficient, 'k_L', by 150-220% (39). CALDERBANK (47) in using distilled water found that results were not reproducible, whereas allowing a degree of contamination by surfactants, achieved by using tap-water, greatly improved the reproducibility of results. For this reason tap water has been used in the present work.

5.2 Dependence of Absorption Rate upon Pulse Velocity

The variation of the absorption rate in the column, expressed as 'k_La', with pulse velocity, 'ωA', was measured at three

constant values of the superficial gas velocity 0.026, 0.051 and 0.085 ft./sec. These values were chosen visually (Plates II-VI) as low, medium and high gassing rates for the column. The results obtained are tabulated in Appendix IV.1 and presented graphically in Fig. 5.1. As in the case of the gas holdup (Fig. 4.6), within the limits of experimental error the absorption rate exhibits a linear dependence upon the pulse velocity. The results are further discussed in Chapter 6.

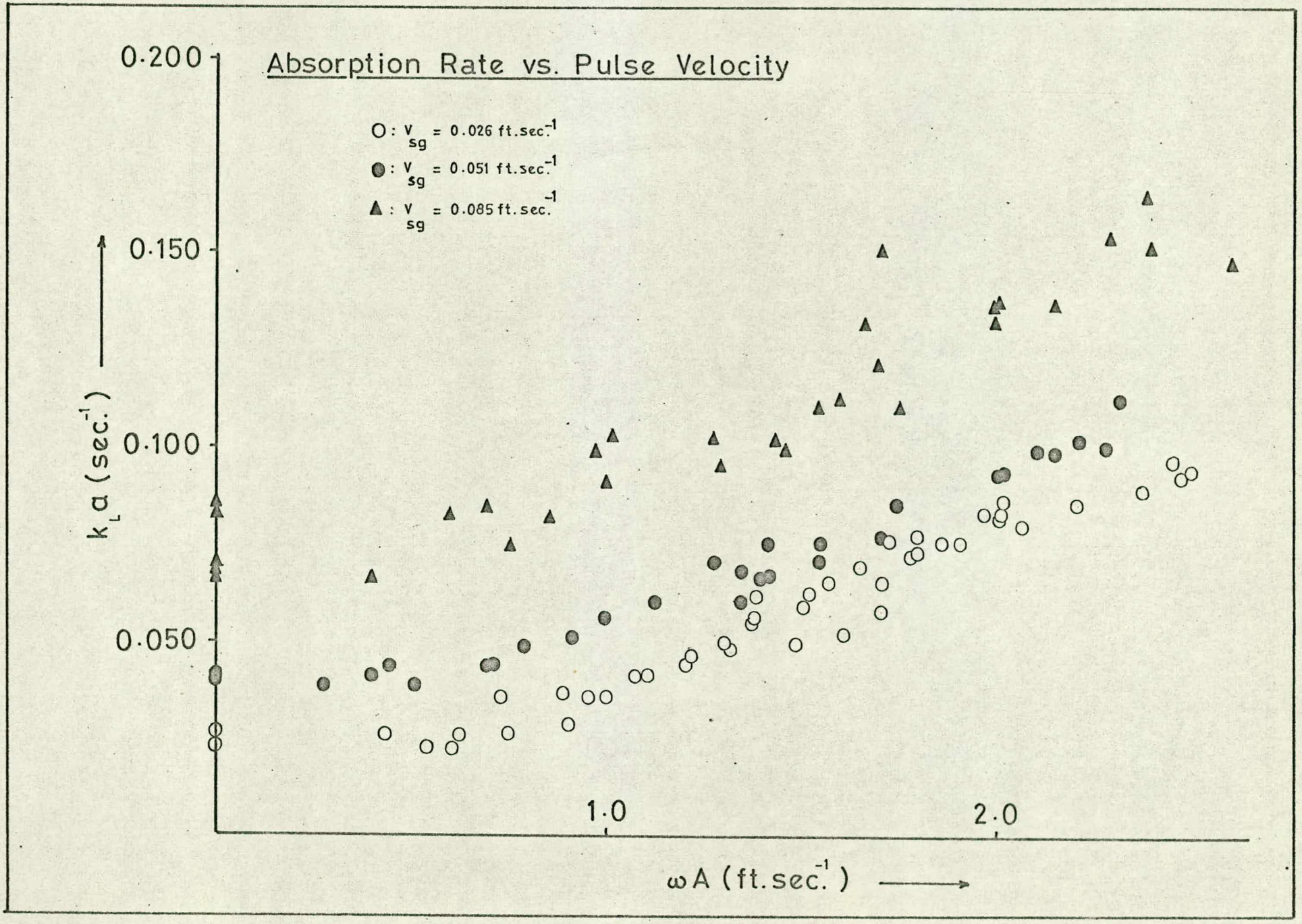
Absorption Rate vs. Pulse Velocity
O : V_sg = 0.026 ft.sec.^-1
● : V_sg = 0.051 ft.sec.^-1
▲ : V_sg = 0.085 ft.sec.^-1
0.200
0.150
0.100
0.050
k_l a (sec.^-1)
1.0
2.0
ωA (ft.sec.^-1)

Figure 5.1

Chapter 6

Discussion of Results and Conclusions

6.1 Treatment of Observed Data

No satisfactory means of predicting gas holdup and mass transfer rates in gas-liquid systems has yet been developed, (see Section 6.2), although in general it is possible to correlate the data in terms of a relatively few 'independent' variables. It is usual to evaluate the performance of a given stirred tank contacter in terms of the superficial gas velocity 'V_{sg}', the specific power input 'P_s' and the impeller speed 'N_i'. In the present work the pulse velocity 'ωA', the maximum velocity of the column of liquid during a pulsation cycle, may be regarded as analogous to the impeller speed in the conventional stirred tank contacter. Correlation in terms of this small number of variables assumes of course that the geometry and physical properties of the system remain constant.

Since both 'k_La' and 'ε' exhibit a linear dependence upon the pulse velocity 'ωA', and it has been shown that in effect 'P_s' varies as the cube of 'ωA' (Equ. 4.27), then both 'ε' and 'k_La' should correlate linearly with $P_s^{0.33}$, where 'P_s' is given by Equ. 4.28.

Most of the observed data above the critical pulse velocity are represented (Figs. 6.1 and 6.2) by

$$\varepsilon = 0.240\ P_s^{0.33}\ V_{sg}^{0.53} \qquad (6.1)$$

and

$$k_La = 0.180\ P_s^{0.33}\ V_{sg}^{0.53} \qquad (6.2)$$

(fps units)

A better correlation of the data is obtained if the specific power input, 'P_s', is replaced by the total specific power dissipation

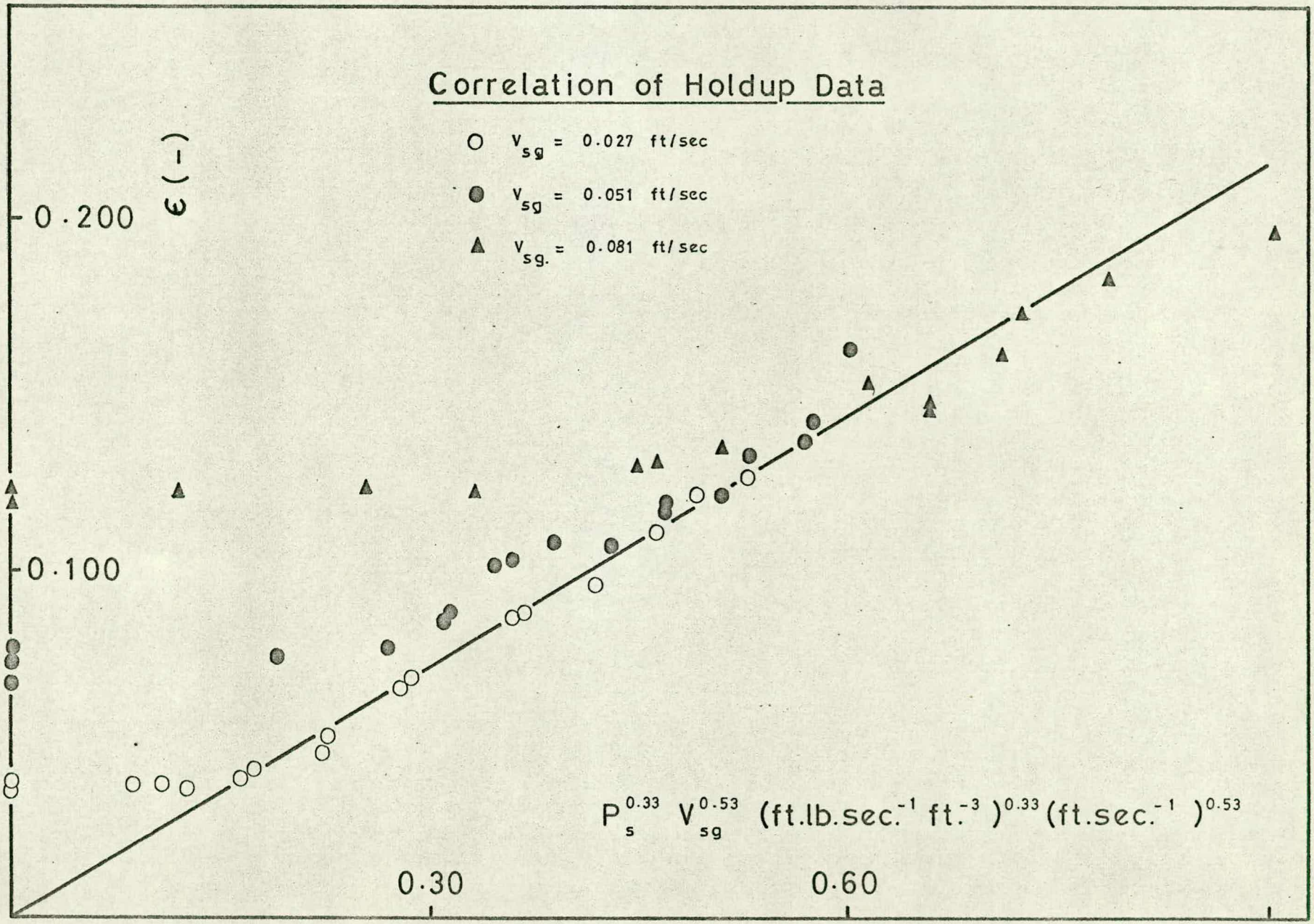
Correlation of Holdup Data
O V_{sg} = 0.027 ft/sec
● V_{sg} = 0.051 ft/sec
▲ V_{sg} = 0.081 ft/sec
ε (-)
0.200
0.100
0.30
0.60
$P_s^{0.33}$ $V_{sg}^{0.53}$ (ft.lb.sec.$^{-1}$ ft.$^{-3}$)$^{0.33}$ (ft.sec.$^{-1}$)$^{0.53}$

Figure 6.1

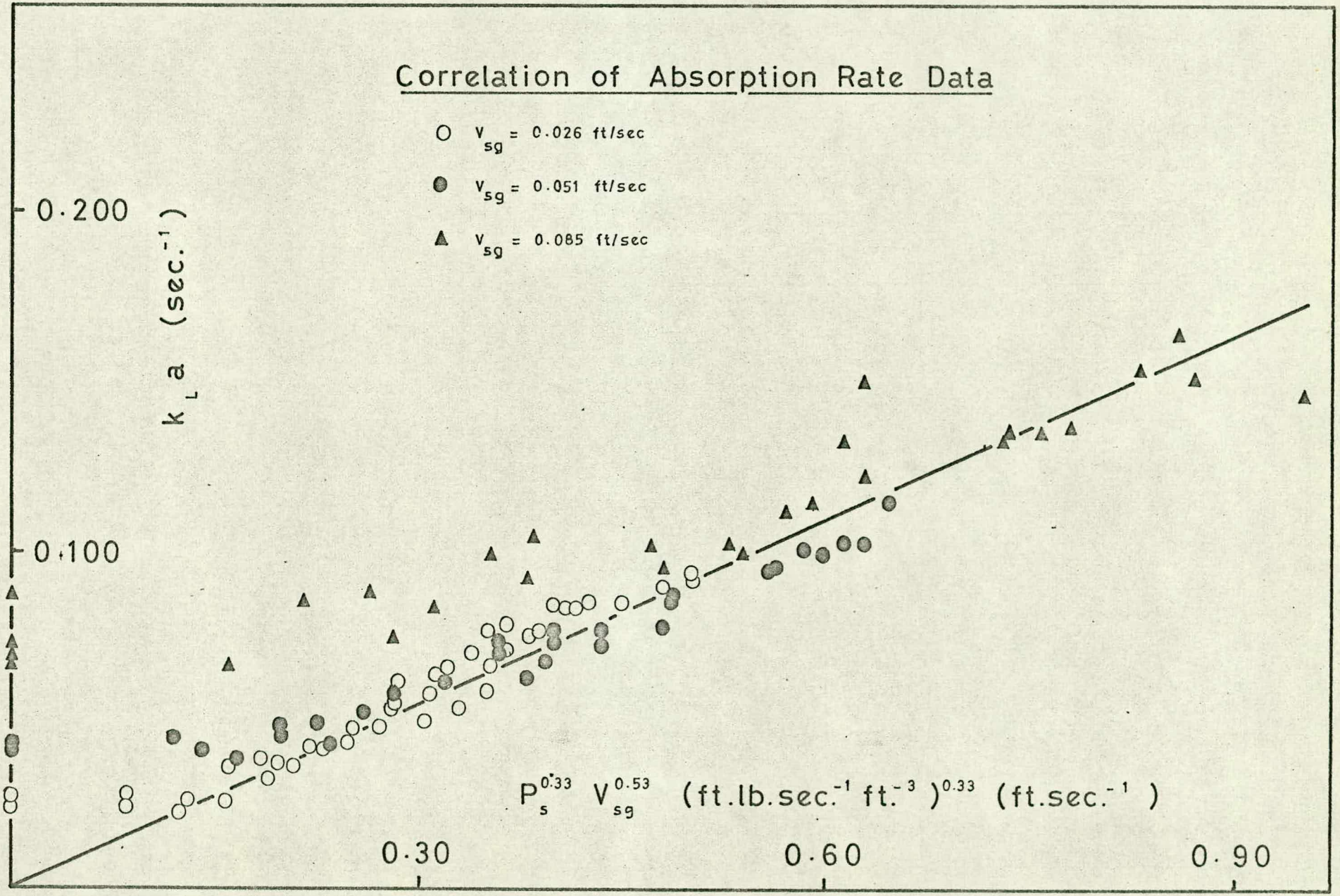
Correlation of Absorption Rate Data
O V_{sg} = 0.026 ft/sec
V_{sg} = 0.051 ft/sec
V_{sg} = 0.085 ft/sec
0.200
0.100
$k_L a$ (sec.$^{-1}$)
$P_s^{0.33}$ $V_{sg}^{0.53}$ (ft.lb.sec.$^{-1}$ ft.$^{-3}$)$^{0.33}$ (ft.sec.$^{-1}$)
0.30
0.60
0.90

Figure 6.2

'P_{st}', where

$$P_{st} = P_s + P_b \tag{6.3}$$

and 'P_b', the power input in the non-agitated system due to the rising bubbles is defined (49) as

$$P_b = \frac{V_{sg} \rho_L g}{g_c} \tag{6.4}$$

so that the total power dissipation by substituting Equ. 4.28 and Equ. 6.4 in Equ. 6.3 is given by

$$P_{st} = 2.96(1 - \varepsilon)(\omega A)^3 + \frac{V_{sg} \rho_L g}{g_c} \tag{6.5}$$

The data are then correlated (Figs. 6.3 and 6.4) by

$$\varepsilon = 0.155\, P_{st}^{0.42}\, V_{sg}^{0.50} \tag{6.6}$$

$$k_L a = 0.116\, P_{st}^{0.42}\, V_{sg}^{0.50} \tag{6.7}$$

(fps units)

The observed data are also correlated in terms of ωA and V_{sg} by

$$\varepsilon = 0.322\, \omega A\, V_{sg}^{0.53} \tag{6.8}$$

$$k_L a = 0.241\, \omega A\, V_{sg}^{0.53} \tag{6.9}$$

(fps units)

Comparison of Equ. 6.1 and Equ. 6.2, and Equ. 6.6 and 6.7 indicates that in the pulsed column $k_L a$ is directly dependent upon the gas holdup.

$$k_L a = 0.75\, \varepsilon \tag{6.10}$$

The ranges of the parameters investigated were as

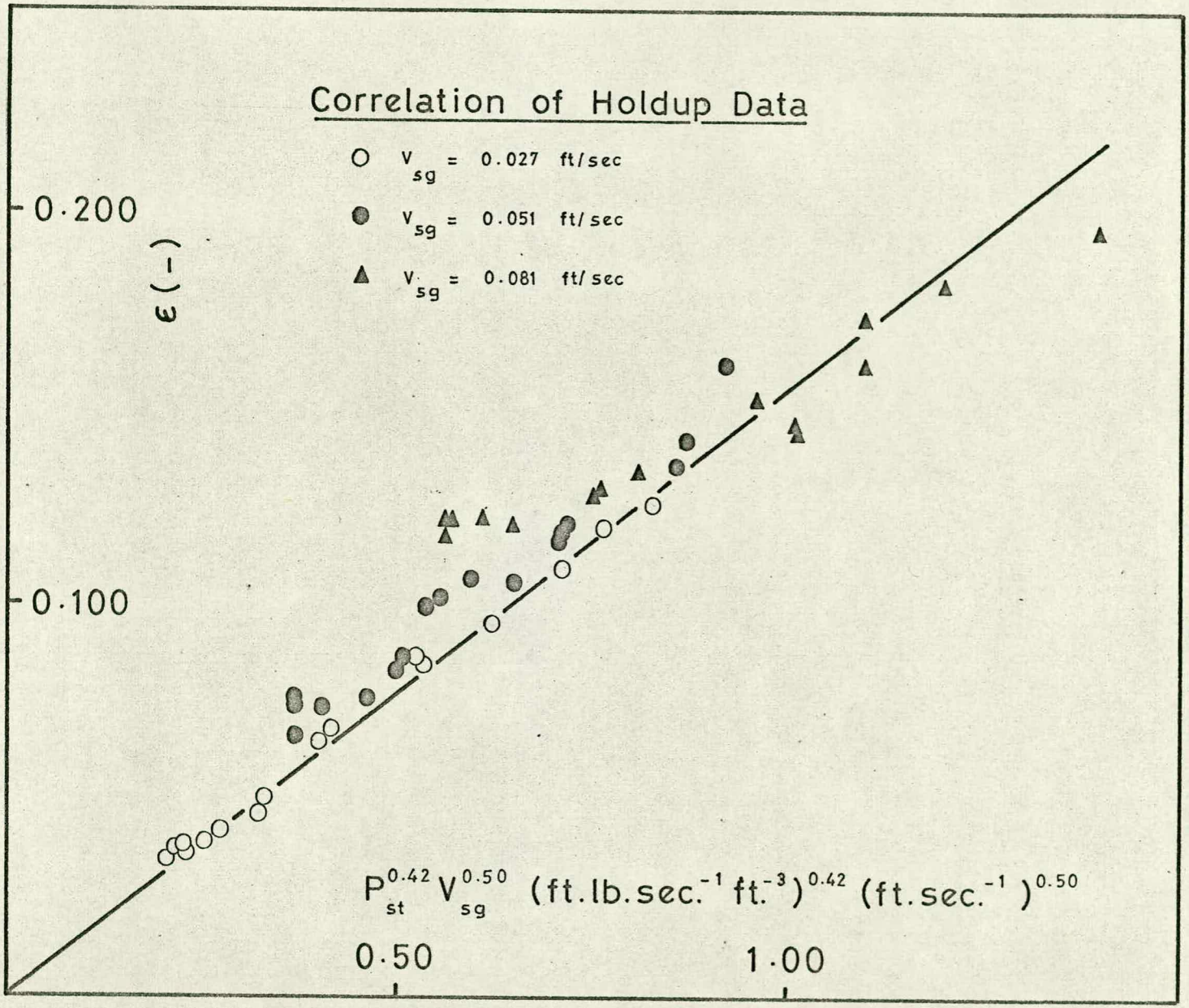
Correlation of Holdup Data
○ V_{sg} = 0.027 ft/sec
● V_{sg} = 0.051 ft/sec
▲ V_{sg} = 0.081 ft/sec
0·200
0·100
ε (-)
$P_{st}^{0.42} V_{sg}^{0.50}$ (ft.lb.sec.$^{-1}$ ft.$^{-3}$)$^{0.42}$ (ft.sec.$^{-1}$)$^{0.50}$
0·50
1·00

Figure 6.3

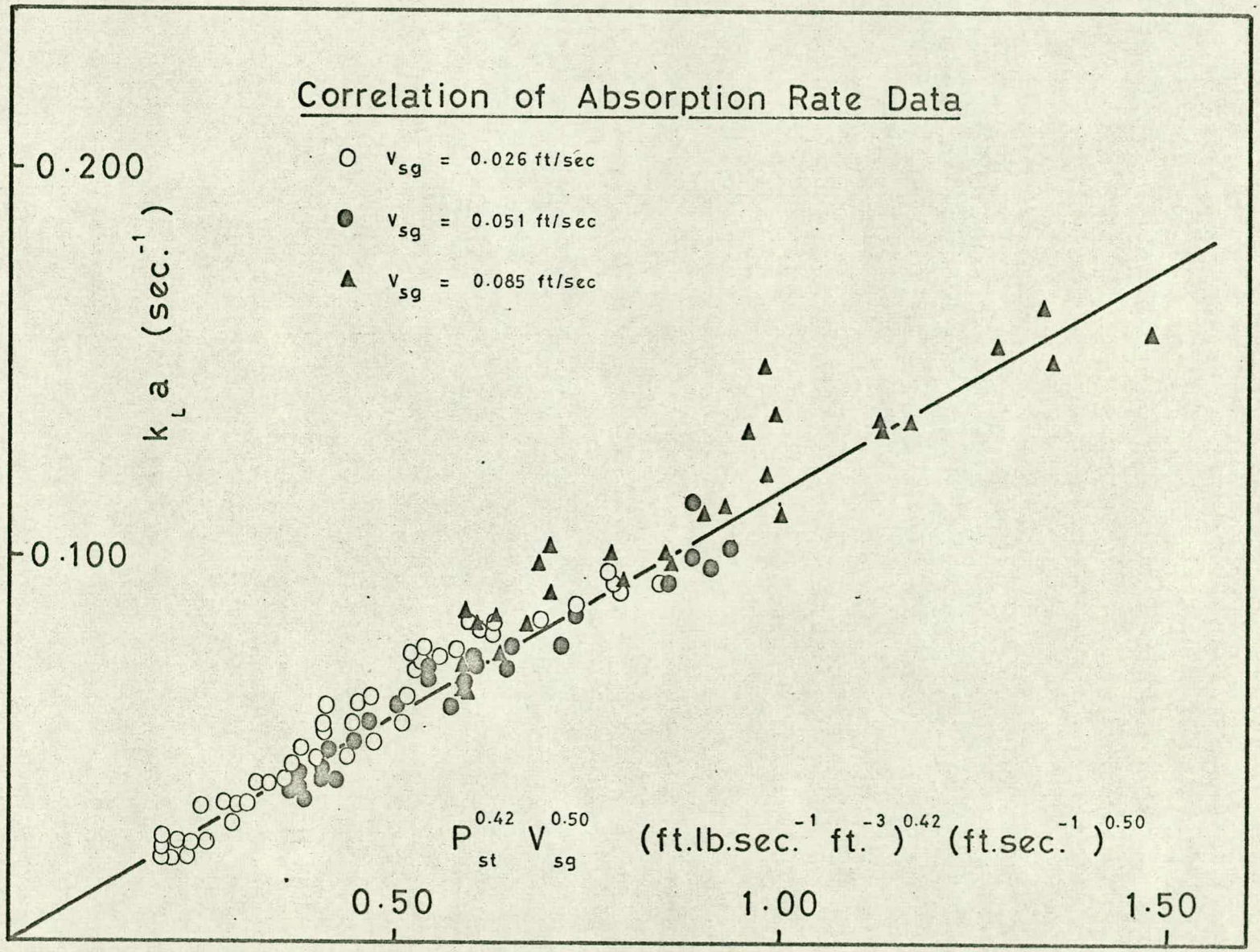
Correlation of Absorption Rate Data
O V_{sg} = 0.026 ft/sec
V_{sg} = 0.051 ft/sec
V_{sg} = 0.085 ft/sec
0·200
0·100
$k_L a$ (sec.$^{-1}$)
0·50
1·00
1·50
$P_{st}^{0.42} V_{sg}^{0.50}$ (ft.lb.sec.$^{-1}$ ft.$^{-3}$)$^{0.42}$ (ft.sec.$^{-1}$)$^{0.50}$

Figure 6.4

follows:

$$0.03 < \varepsilon < 0.20$$

$$0.02 < k_L a < 0.17 \qquad \text{sec.}^{-1}$$

$$0 < P_s < 35 \qquad \text{ft.lb./ft.}^3\text{sec.}$$

$$0 < \omega A < 2.6 \qquad \text{ft./sec.}$$

$$0.026 < V_{sg} < 0.085 \qquad \text{ft./sec.}$$

6.2 Discussion of Results

In general rigorous mathematical analysis of gas-liquid systems is not feasible, except in the case of certain well-defined systems such as wetted wall columns. SIDEMAN et al (49) have enumerated some of the factors affecting mass transfer in gas-liquid contacting systems. They include:

(a) physical properties of the gas and liquid;

(b) type of distributor, orifice diameter, spacing and position;

(c) dimensions of column or tank, baffles (number, position, size);

(d) type of mechanical agitator, size and relative dimensions;

(e) velocity of rotating impeller and energy input;

(f) gas flow rate;

(g) continuous phase flow rate in countercurrent flow systems;

(h) presence of chemical reaction, concentration of electrolytes;

(i) position of downcomers in multiplate counter-current systems;

and (j) presence of solid catalysts.

Mass transfer rates have been predicted successfully only in wetted wall absorption equipment (32,36), being a physically simple system and therefore amenable to mathematical analysis.

Prediction of transfer rates in a stirred tank absorber has been attempted by GAL-OR et al (39) using very much simplified models for the mass transfer rate in the dispersion with limited success, the observed data being bracketted within a few orders of magnitude by two simplified models.

To attempt to compare absolute magnitudes of the holdup and mass transfer rate in different equipment reported by various investigators using differing gas-liquid systems is not therefore meaningful. More significance may be attached to the exponents of 'P_s' and 'V_{sg}' than to the proportionality constants (49) in the general correlations:

$$\varepsilon = b \; P_s^k \; V_{sg}^l \tag{6.11}$$

$$k_L a = c \; P_s^m \; V_{sg}^n \tag{6.12}$$

6.2.1 Gas Holdup

The fractional gas holdup in agitated gas-liquid dispersions has been correlated with the power input and superficial gas velocity by several workers, and the published correlations are reviewed by SIDEMAN, HORTACSU & FULTON (49). CALDERBANK (47) found that for air and several liquids in a stirred tank using a flat-bladed impeller

$$\varepsilon \propto P_s^{0.4} V_{sg}^{0.5} \tag{6.13}$$

for $5.5 < P_s < 110$ ft.lb./ft^3 and $0.01 < V_{sg} < 0.06$ ft./sec., while FOUST, MACK

and RUSHTON (51) found that for high-efficiency turbine dispersers in the air-water system

$$\varepsilon \propto P_s^{0.47} V_{sg}^{0.53} \qquad (6.14)$$

for $3.9 < P_s < 11$ ft.lb./ft.^{3} and $0.02 < V_{sg} < 0.08$ ft./sec. RUSHTON, GALLAGHER and OLDSHUE (50) confirmed the validity of Equ. 6.14 for turbine dispersers in the sulphite-air system for $3.08 < P_s < 28.9$ ft.lb./ft.^{3} (assumed, since the range of power input reported in the published paper was from 3080 to 28900 ft.lb./ft.^{3}!), and $0.025 < V_{sg} < 0.10$ ft./sec.

A reasonable comparison may be drawn between the results obtained with the pulsed column and those reported by CALDERBANK (47) for a stirred tank absorber, since in both cases a simplified form of baffle/disperser was used.

A summary of correlations reported by Sideman (49) is shown in Table 6.I.

Comparison of the exponents of equations 6.1 and 6.13 suggests that the pulsed absorption column is comparable with the stirred tank from the aspect of power utilisation to increase holdup.

6.2.2 Absorption Rates

SIDEMAN, HORTACSU and FULTON (49) in their review of published work upon gas-liquid mass transfer quote values for 'm' in Equ. 6.12 ranging from 0.43 (KARWAT) to 0.95 (COOPER, FERNSTROM and MILLER) and for 'n' ranging from zero (eg WESTERTERP, VAN DIERENDONCK and DE KRAA) to 1.0 (eg BARTHOLOMEW et al). A summary of reported correlations for '$k_L a$' in similar systems to the present work drawn from Sideman's paper is shown in Table 6.II.

The differences between reported values of the

Range of Experiments			Correlation: Exponent of			System			Investigator
V_{sg} ft./sec.	P_s ft.lb./ft^3.sec.	ϵ -	V_{sg}	N_i or ωA	P_s	Disperser	Liquid	Gas	
0.013 -0.053	3.9 - 19.8	0.009 -0.11	0.55	-	0.45	Vaned disc	Sulphite	Air	Gal-Or
0.005 -0.025	-	0.003 -0.05	0.49 -0.6	0.8 -0.6	-	Vaned disc	NaOH aq.	CO_2	Yoshida
0.005 -0.025	-	0.004 -0.05	0.75	0.8	-	Turbine	NaOH aq.	CO_2	Yoshida
0.01 -0.06	5.5 - 110	0 -0.08	0.5	-	0.40	Vaned disc	Water	Air	Calderbank
0.016 -0.083	3.9 - 11.0	0.02 -0.10	0.53	-	0.47	Turbine	Water	Air	Foust
0.039	-	0.03 -0.32	-	1.0	-	Turbine	Sulphite	Air	Westerterp
0.026 -0.085	0 - 35	0.03 -0.20	0.53	1.0	0.33	Pulse Column	Water	Air	Present Work

Table 6.I: Comparison of Present Results with Correlations of reported by Sideman (49)

Range of Experiments			Correlation: Exponent of				System			Investigator
V_{sg} ft./sec.	P_s ft.lb./ft.^{3}sec.	ε -	ε -	V_{sg}	N_i or ωA	P_s	Disperser	Liquid	Gas	
0.005 -0.18	0.2 - 50	-	-	0.67	-	0.95	Vaned disc	Sulphite	Air	Cooper
0.002 -0.2	2.5 - 75	-	-	0.76	-	0.71 -0.79	Multiple Turbine	Sulphite	Air	Rushton
0.0005 -0.004	0 - 300	-	-	-	2.4 -3.0	-	Turbine	Sulphite	Air	Elsworth
0.007 -0.07	-	-	-	0	1	-	Various	Sulphite	Air	Westerterp
0 -0.13	0 - 630	-	-	-	-	0.43 -0.95	Various	Sulphite	Air	Karwat
0.0003 -0.003	-	-	-	0.49 -0.75	0.70 -1.66	-	Paddle	Water	Air	Hortacsu
0.026 -0.085	0 - 35	0.03 -0.20	1.0	0.53	1.0	0.33	Pulse Column	Water	Air	Present Work

Table 6.II: Comparison of Present Results with Correlations of $k_L a$ reported by Sideman (49)

exponents in Equ. 6.12 are due to various reasons, including the geometry of particular systems used by the investigators, but the range of operating conditions is of prime importance (49). COOPER et al used superficial gas velocities in the range $0.005 < V_{sg} < 0.183$ ft./sec., and power inputs in the range $0.167 < P_s < 50.1$ ft.lb./ft.^{3}, obtaining values for the exponents (Equ. 6.12) of m = 0.95 and n = 0.67. The present results may be compared with these as being obtained within a similar range of experimental conditions, indicating that the pulsed column is less efficient than the stirred tank absorber in the utilisation of power to increase $k_L a$. The present results may be compared directly to the absolute values of '$k_L a$' obtained for a high efficiency gas-liquid contacting stage used by GAL-OR et al (39) since in this particular investigation the air-water system with a 'degree of contamination' (see section 5.1) was used in a similar range of superficial gas velocities. The data obtained in the present work are shown, together with those obtained by Gal-Or, in Fig. 6.5. The comparison is necessarily of a limited nature, no details of power input having been published in Gal-Or's paper. Shown together with Gal-Or's results are the best absorption rates obtained at values of V_{sg} = 0.027, 0.052 and 0.085 ft./sec. It will be seen that comparable absorption rates are obtained at high pulse velocities and low superficial gas velocities. Comparable '$k_L a$' values at high superficial gas velocities would be obtainable with the pulsed column, assuming that the linear relationship between '$k_L a$' and 'ωA' (Fig. 5.1) can be extrapolated to higher pulse velocities if the inlet/exhaust flow limitation of the present column is raised. The curve drawn in Fig. 6.5 is representative of the performance of the column extrapolated to ωA = 3.0 ft./sec.

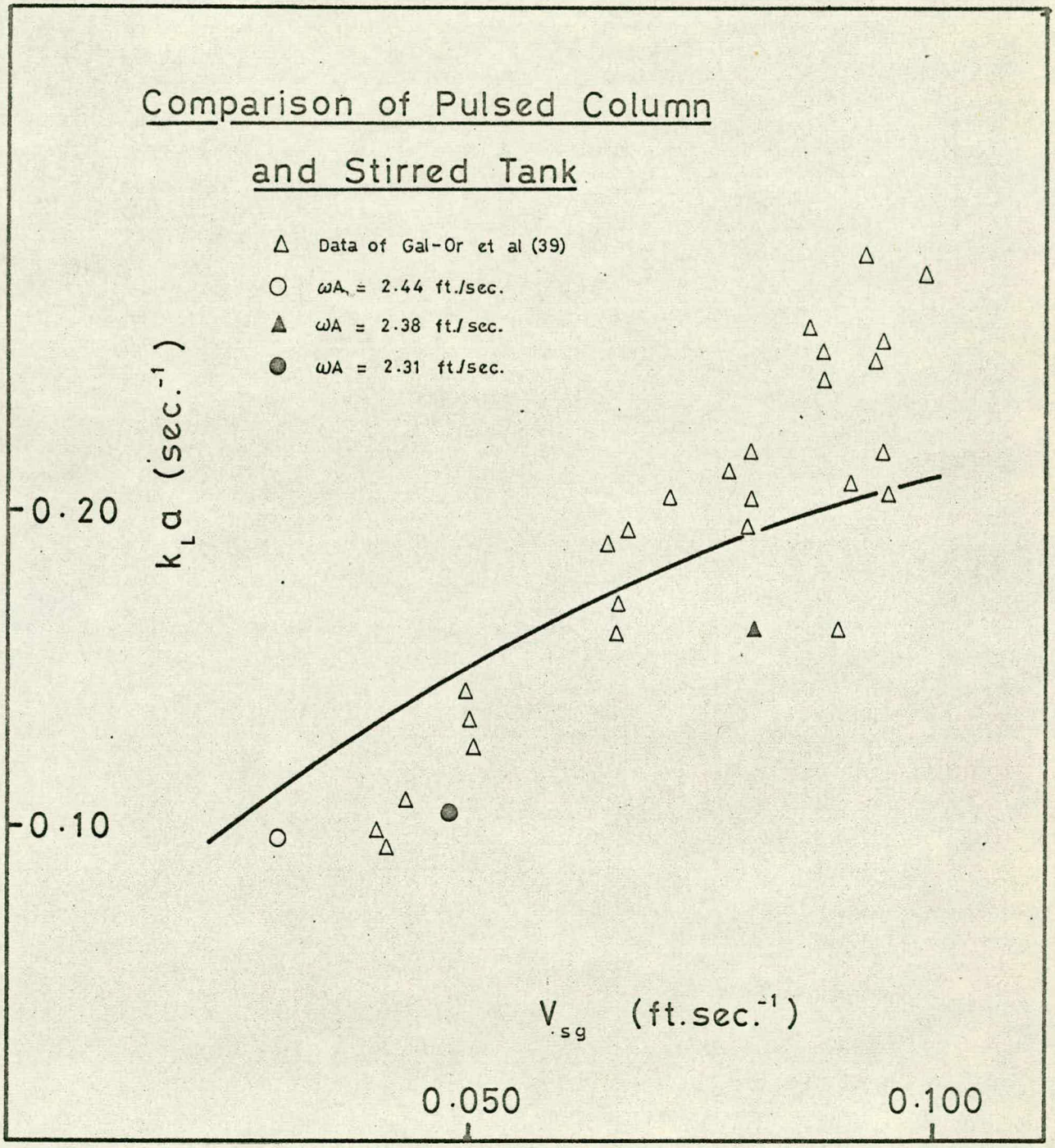
Comparison of Pulsed Column
and Stirred Tank
Data of Gal-Or et al (39)
ωA = 2.44 ft./sec.
ωA = 2.38 ft./sec.
ωA = 2.31 ft./sec.
$k_L a$ (sec.$^{-1}$)
0·20
0·10
V_{sg} (ft.sec.$^{-1}$)
0·050
0·100

Figure 6.5

The pulsed column exhibits an interesting correlation between '$k_L a$' and 'ϵ' (Equ. 6.10). Very few correlations between '$k_L a$' and 'ϵ' are found in the literature, although three are reported by Sideman et al between 'a' and 'ϵ', 'a' being found to be dependent upon 'ϵ' to the power of about 0.5. If, as is discussed in Sideman's paper, 'k_L' can be assumed to be essentially constant, then this relationship obviously also applies to '$k_L a$'. That '$k_L a$' is directly proportional to 'ϵ' in the pulsed column infers that there is little effect upon bubble size above the critical 'ωA' of about 0.8 - 1.0 ft./sec.

It is considered that the use of a more efficient disperser in the column such as a sieve plate in place of the simple baffles at present employed would yield absorption rates more favourably to be compared with stirred tank equipment.

The results show that the pulsed column is comparable to the stirred tank when operated batchwise. This would indicate that the column may have considerable advantages over conventional contacting equipment when operated countercurrently.

6.2.3 Experimental Errors

Scatter in the observed values of absorption rates due to random surfactant contamination was reduced as far as possible by the use of tap-water (39). Errors in the measurement of power dissipation, gas holdup and frequency of pulsations were negligible, the most significant observational error being introduced in the visual measurement of the amplitude of pulsation against a scale graduated in centimetres, the average position of the rapidly moving surface of the liquid in the column being somewhat difficult to assess. The maximum possible error in this

observation is estimated to be of the order of ±15% at the higher pulse velocities and superficial gas velocities, although in practice this magnitude of error does not appear to have been reached (see Fig. 4.6 for example). Comparison of the results for holdup (Fig. 4.6) and those for absorption rates (Fig. 5.1) indicates that a considerable amount of the scatter in the absorption rate results must be due to random surfactant contamination, notwithstanding the precautions taken. The scatter of absorption rate results is similar to that found by Gal-Or et al (39) using a similar system.

6.3 Conclusions and Recommendations for Further Work

From comparisons with published work it is concluded that, although the pulsed column in its present form is generally less efficient in terms of power utilisation than the stirred tank contacter, 'k_La' values comparable with a high efficiency gas-liquid contacter (39,60) using the same experimental conditions were obtained. The capability of the column to operate countercurrently would therefore offer great advantages in the gas absorption operation.

Indications are that the performance of the column would be improved through the use of more efficient dispersing units, such as packing or sieve plates, in place of the simple disc baffles used in this preliminary investigation.

It is considered that further work should also include an investigation into optimum baffle size and spacing with regard to the annular vortices observed in the region of the baffles.

Appendix I

Methods of Measurement

I.1 Measurement of Power Input

As described in the body of this thesis (Section 3.6.1), the method used to measure power consumption in the column was an adaptation of a long-standing procedure used in the testing of heat engines, known as 'the indicator diagram', and is here described in greater detail.

It was required that signals representing both the volume variation and the pressure in one of the gas spaces at the top of the column should be combined to yield a pressure-volume relationship during each cycle for the gas space.

The signal representing volume variation was obtained by use of a simple level metering device consisting of two parallel brass rods of 3/8th in. dia., one of the rods being the central baffle support of the leg. A constant voltage of 5 V. D.C. was applied between the two rods so that the current passed was proportional to the depth of immersion of the electrodes. The current developed a proportional voltage across a resistor placed in series circuit with the rods (Fig. I.1.(b)). This voltage was then applied to the Y amplifier of an oscilloscope.

Experiments showed that the rate of polarisation was negligible - the amplitude of the sinusoidal level signal as displayed on the oscilloscope did not vary appreciably from cycle to cycle, apart from a small (c. 5%) random change due presumably to actual variations in the liquid amplitude. The lack of polarisation was thought to be due to the fact that the surfaces of the electrodes were efficiently swept by the movement of the liquid surface. This supposition was confirmed when it was attempted to use the device as a level indicator for a static surface, when the current

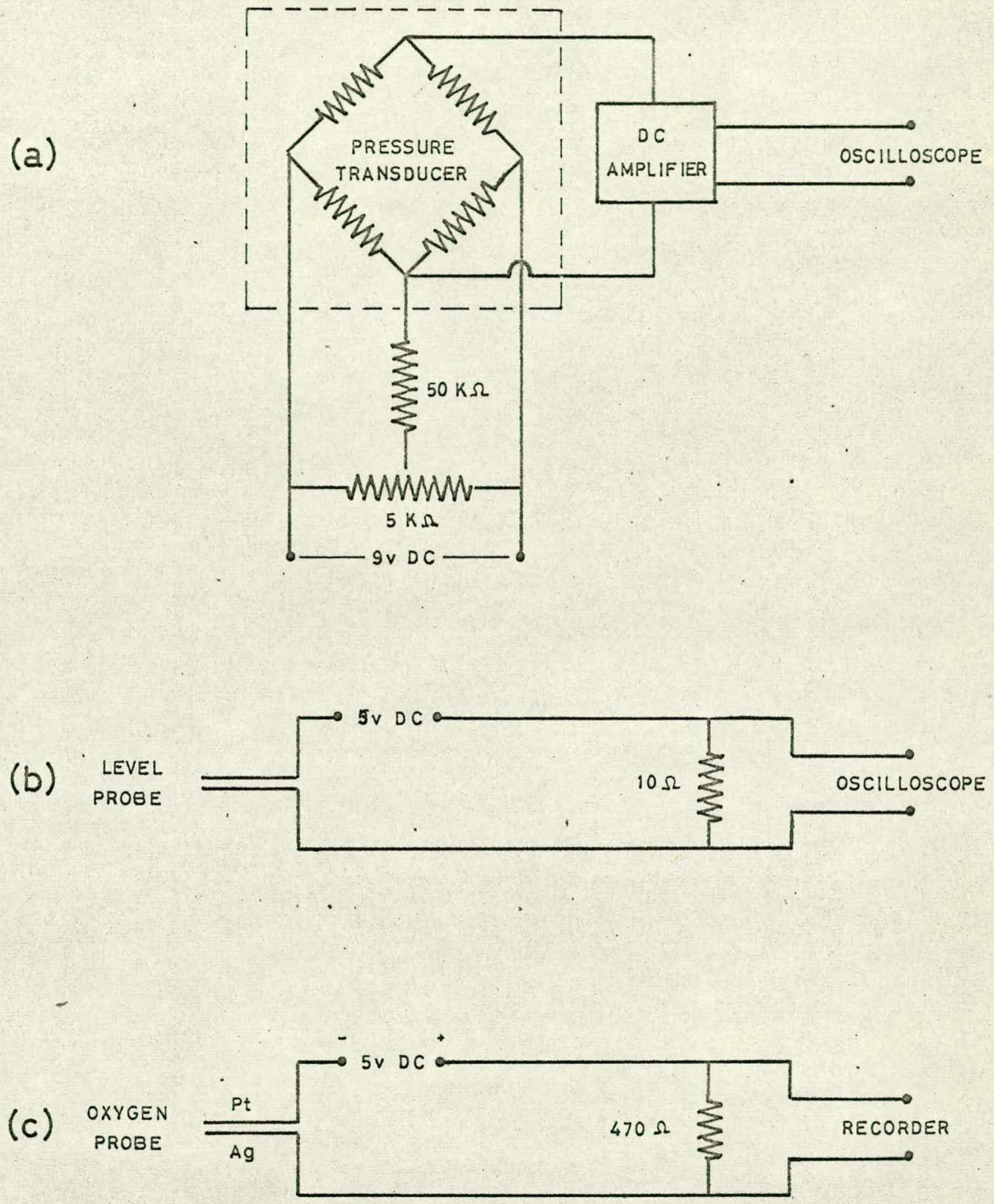
(a)
PRESSURE TRANSDUCER
DC AMPLIFIER
OSCILLOSCOPE
50 KΩ
5 KΩ
9v DC
(b)
LEVEL PROBE
5v DC
10 Ω
OSCILLOSCOPE
(c)
OXYGEN PROBE
Pt
Ag
5v DC
470 Ω
RECORDER

Figure I.1

passed between the electrodes rapidly fell on switching on the instrument. The level meter was in effect calibrated for each reading of the power input by measuring the amplitude directly on a centimeter scale attached to the external wall of the column.

The pressure signal was obtained from a Solartron pressure transducer mounted in the top plate of the column leg. The driving circuit for the transducer is shown in Fig. I.1(a). It was necessary to boost the signal obtained from the transducer by means of a D.C. amplifier before applying it to the X amplifier of the oscilloscope.

Typical traces obtained with this system are shown in Plate VII. Data obtained for each run and used in calculating the power consumption were as follows:-

f = frequency of pulsation;

A = amplitude of pulsation;

P_{cal} = transducer calibration (psig per unit deflection on oscilloscope grid).

Let us consider a general indicator diagram as depicted in Fig. I.2 below.

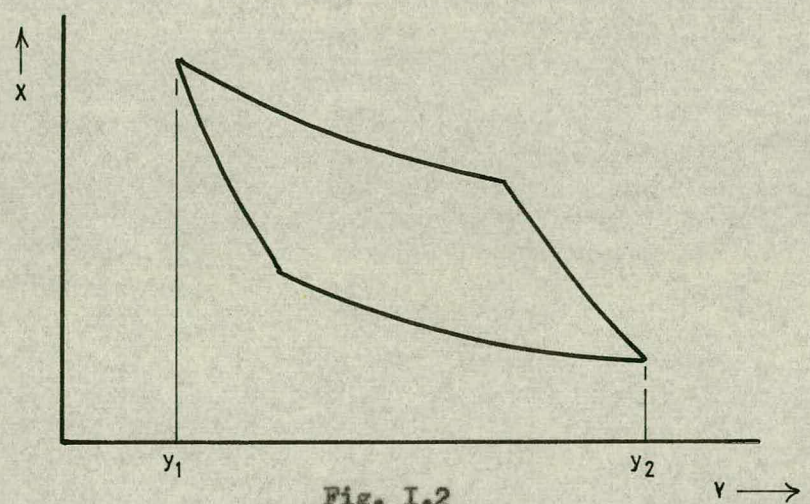

Fig. I.2

The area of the diagram, enlarged to a one inch square grid, was measured with a planimeter.

The volume scale is calculated as

$$v_{cal} = \frac{2A}{(y_2 - y_1)} \quad \frac{\pi D^2}{4} \text{ in}^3 \text{ per in. deflection}$$

where D = diameter of leg in inches

so that the energy dissipated per cycle per column leg is given by

$$\frac{(\text{Area of diagram})(p_{cal})(v_{cal})}{12} \text{ ft.lb.cycle}^{-1}$$

and the power dissipation is given by

$$\frac{(\text{Area})(p_{cal})(v_{cal})(f)}{12} \text{ ft.lb.sec.}^{-1}$$

for one leg of the column. It therefore follows that the total rate of consumption of power for the whole column 'P' is given by

$$P_{obs} = \frac{(\text{Area})(p_{cal})(v_{cal})(f)}{6} \text{ ft.lb.sec.}^{-1}$$

On a specific run (no. 74) the following data were observed:-

23.6 in. H_2O = 1 in. deflection on pressure scale

A = 2.65 in.

f = 1.30 cycles/sec.

Area of diagram = 3.22 in.^{2}

$y_2 - y_1$ = diagram stroke = 2.35 in.

Therefore:

$$v_{cal} = \frac{(2)(2.65)(\pi)(3.0)^2}{(2.35)(4)} = 15.9 \text{ in}^3\text{/in. deflection}$$

$$p_{cal} = (23.6)(0.0361) = 0.852 \text{ lb.in.}^{-2}\text{/in. deflection}$$

and $$P_{obs} = \frac{(3.22)(0.852)(15.9)(1.30)}{6} = 9.45 \text{ ft.lb.sec.}^{-1}$$

I.2 Measurement of Gas Holdup

Measurements of gas holdup were made quite simply by the following procedure.

The column was filled with tap water, air was injected at the bottom of the column at the required flow rate, and the pulsation generator was set in motion. The mean heights of dispersion in the two legs were then balanced by draining water from the base of the column, and at the same time the flow rates of air into the bottoms of the legs were equalised. When the column was in balanced operation, the amplitude of pulsation, frequency, mean height of dispersion, 'h_1', and air flow rates were noted. The pulsation generation system and the bubble air were switched off, and the dispersion was allowed to settle. The new height of the liquid surface in the column was then noted 'h_2'. It can be seen that the volume of gas held within the dispersion is equal to $2(h_1 - h_2) \times \frac{D^2}{4}$, less a small correction for the volume of baffles and the central support rod. The fractional gas holdup, 'ϵ', is then given by

$$\frac{2(h_1 - h_2)\frac{\pi D^2}{4} - c_1}{H_L \quad \frac{\pi D^2}{4} - c_2}$$

where c_1, c_2 are corrections for the volume of baffles and their support.

In a typical run the following data were recorded:-

Amplitude of pulsation A = 2.8 in.

Frequency = 1.25 Hz

$(h_1 - h_2)$ = 12.2 in.

c_1 = 6.230 in^2

c_2 = 31.86 in^2

$H_L = 168$ in.

$D = 3$ in.

Therefore:

$$\epsilon = \frac{(2)(12.2)(7.85) - 6.23}{(168)(7.85) - 31.86} = 0.144$$

I.3 Measurement of Mass Transfer Rates

Oxygen concentrations in the column were measured by means of polarographic cells.

The oxygen concentration probes were of simple construction (Fig. I.3), and consisted of two electrodes, one of 0.46 mm. diameter platinum wire and the other of 1.63 mm. diameter silver wire, embedded at one end in Araldite epoxy resin adhesive in a bored-out 3/8th in. Whitworth bolt. The gap between the electrodes was of the order of 5 thousandths of one inch.

The probe was prepared for a run as follows. A thin film of natural rubber latex (supplied by the North British Rubber Company) was drawn between the two electrodes and allowed to dry naturally in air. A thin membrane was then deposited on the assembly by dipping in a solution of polyethylene in toluene, and allowing it to dry. The thickness of the membrane thus produced was about 0.0004 in. (measured by micrometer). This method of production of the membrane is due to PROCTOR (38). The probes produced by this method are a hybrid between the standard polarographic cell, as used for example in Pye oxygen tension meters, and that developed by Proctor. The latter was a lead-silver cell which developed its own current proportional to the oxygen concentration, while the platinum-silver cell requires a driving EMF, and passes a current proportional to the oxygen

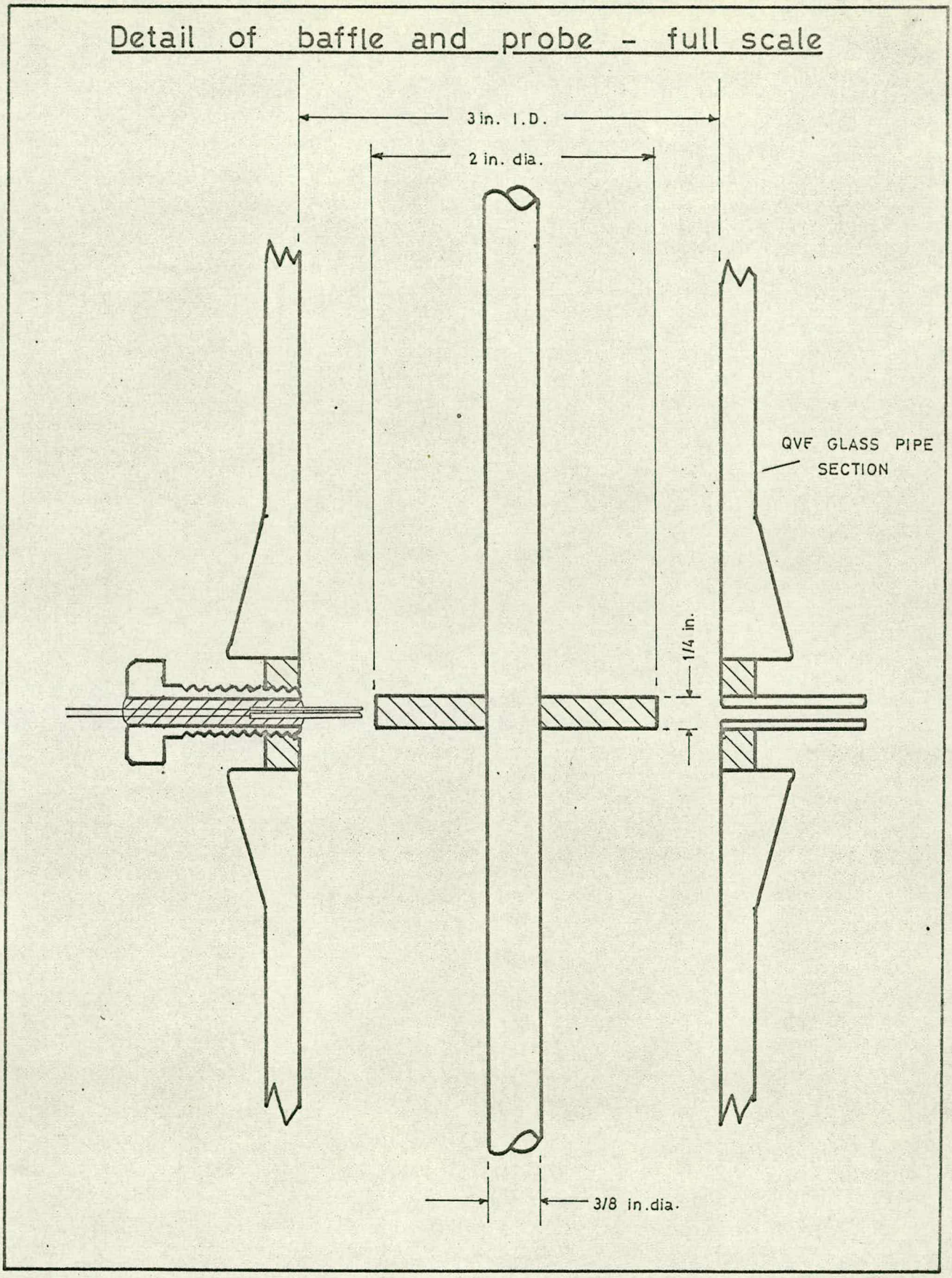
Detail of baffle and probe - full scale
3 in. I.D.
2 in. dia.
QVF GLASS PIPE SECTION
1/4 in.
3/8 in.dia.

Figure I.3

concentration. Attempts to use the lead-silver cell in the present work were unsuccessful due to the rather delicate construction allowing the membrane to rupture under the more rigorous conditions encountered in the pulsed column. However, the latex electrolyte and dipped polyethylene membrane were adapted to the platinum-silver electrode system to give a cell considerably smaller than the proprietary cells, and with a response time and lack of velocity sensitivity more suited to the present application.

The response times of the probes were measured in two ways, (a) by quickly removing all available dissolved oxygen in the region of the probe, and (b) by introducing a step increase in the oxygen concentration of the water surrounding the probe.

Method (a) was accomplished by immersing the probe in tap water in a well-stirred beaker, and injecting an amount of hydrazine hydrochloride to remove dissolved oxygen. The response to the step change in concentration was followed on a Servocord potentiometric recorder.

Method (b) required a specially constructed probe, mounted in the end of a Quickfit ground glass stopper. The geometry of the probe however was identical to those used in the absorption column. The stopper was fitted to a four-necked Quickfit reaction flask together with a stirrer and a dip tube to sparge nitrogen into tap water contained in the flask. The water was then de-oxygenated by purging with nitrogen. The purge gas was then turned off, and a quantity of water containing dissolved oxygen introduced. The response of the probe to the step change was again followed on the recorder.

Both the above methods showed response times for the measuring system varying between 0.5 and 1.0 seconds as compared with about

twenty to thirty seconds for commercial cells.

The cells were velocity sensitive to a small extent, this appearing as a 'noise' of about 5% of the total signal.

The circuit used for the employment of the oxygen concentration probes is shown in Fig. I.1(c). A constant voltage of about 5 V. was applied across the platinum-silver electrode pair, and the voltage across a 470 ohm resistor in series circuit with the electrodes was applied to the input terminals of a 'Servocord' potentiometric recorder.

The useful life of a probe depended upon the length of time for which the polyethylene membrane remained intact, and varied between one and eleven runs. That a membrane had ruptured was indicated by the sudden increase in velocity sensitivity, and the fact that during the desorption cycle it was not possible to bring the output of the probe to zero.

A certain amount of polarisation was noticeable with the probes, amounting to about 5% of the full scale signal per hour if the probe was left in water saturated with oxygen. The polarisation is thought to be due either to the fouling of the polyethylene membrane by dissolved species in the water other than oxygen, or to 'poisoning' of the surfaces of the electrodes. This rate of polarisation would make the use of the probes on long-term measurements questionable, but had negligible effect upon the measurement of absorption rates in the column.

For the measurement of absorption rates, the column was filled with tap water, the supply of air to the air distributors at the bottom of the column was turned on, and the pulsation generator was set in motion. After adjusting and balancing the air flow rates setting the pulsation amplitude, and balancing the mean levels of water in each leg, the

supply of gas to the bottom of the column was switched to oxygen-free nitrogen, and the equipment was run until all dissolved oxygen in the water was desorbed, as indicated by zero output from the oxygen concentration probes. The gas supply was then quickly switched to air and the oxygen concentration curve followed on the 'Servocord' recorder until saturation was achieved.

The instantaneous mass transfer rate is given by:-

$$N_{O_2} = \frac{dc}{dt} = k_L a\,(c_* - c)$$

where N_{O_2} = mass transfer rate, lb.moles/ft³sec.

c = oxygen concentration at time 't', lb.moles/ft³

c_* = equilibrium solute concentration, lb.moles/ft³

k_L = mass transfer coefficient, ft./sec.

a = specific interfacial area, ft²/ft³

t = time, sec.

transposing yields:-

$$\frac{dc}{(c_* - c)} = k_L a.dt$$

and integrating this:-

$$-\ln(c_* - c) = k_L a.t$$

Let $\sim$ = probe output at time 't', volts.

$\sim_*$ = probe output at time = ∞ (saturation), volts.

c_{cal} = probe calibration, lb.moles/ft³/volt.

then:

$$-\ln c_{cal}(\sim_* - \sim) = k_L a.t$$

or

$$-\ln c_{cal} - \ln(\sim_* - \sim) = k_L a.t$$

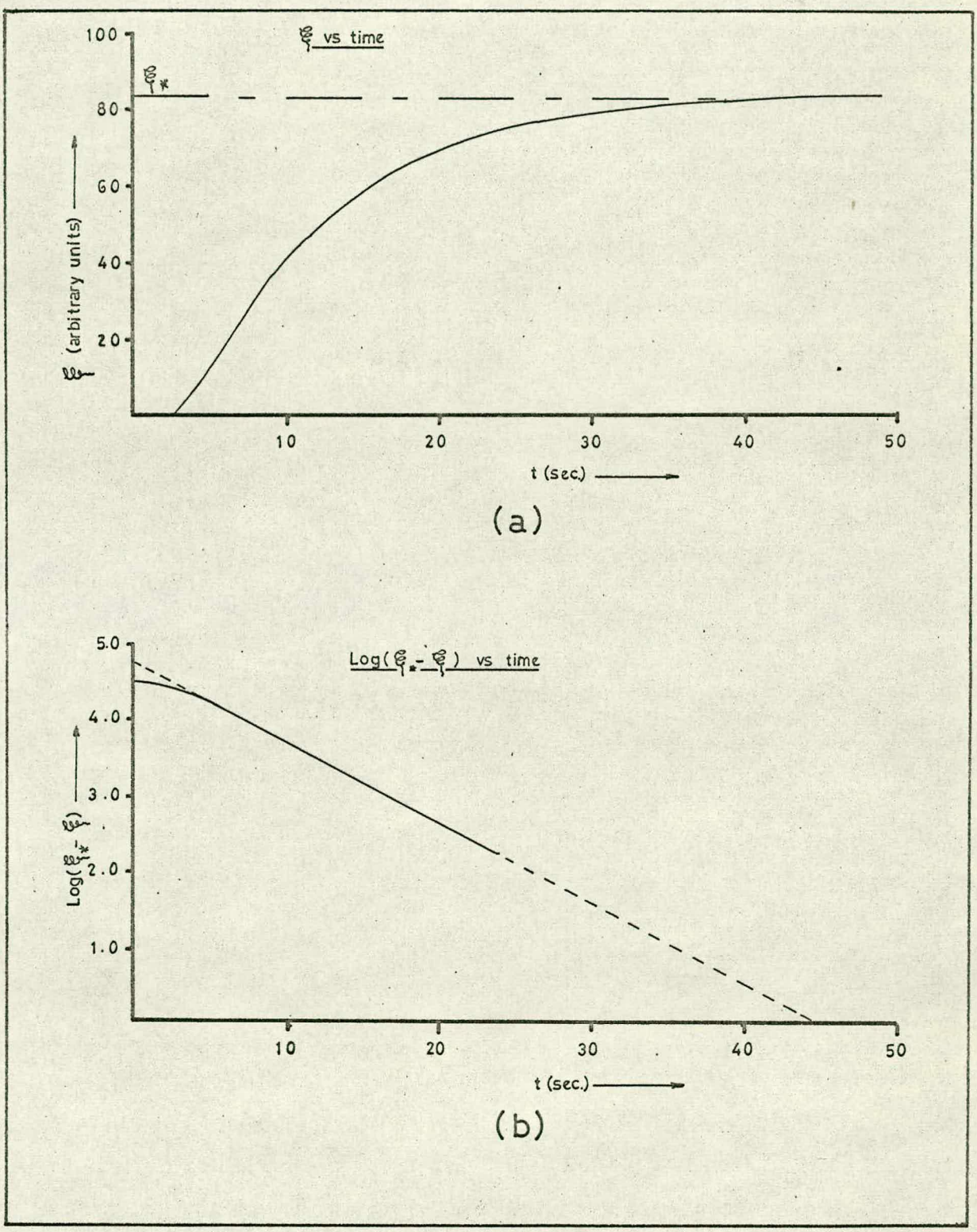
100
80
60
40
20
(arbitrary units)
vs time
10
20
30
40
50
t (sec.)
(a)
5.0
4.0
3.0
2.0
1.0
Log(-) vs time
10
20
30
40
50
t (sec.)
(b)

Figure I.4

Appendix II

Holdup - Tabulated Data and Results

II.1 Column Conditions

Number of baffles = 24

H_L = 168 in.

II.2 Holdup Results (1)

V_{sg} ft./sec.	Q SCFM	ωA ft./sec.	ε -
0.043	0	0	0.0625
0.043	0.67	0.73	0.0682
0.043	0.94	0.92	0.0761
0.043	1.04	0.98	0.0768
0.043	1.36	1.17	0.0803
0.043	1.49	1.22	0.0847
0.043	1.64	1.31	0.0940
0.043	2.02	1.51	0.0970
0.043	2.57	1.79	0.1091
0.043	2.97	1.95	0.1152
0.043	3.50	2.17	0.1220
0.043	3.93	2.32	0.1241
0.043	4.42	2.48	0.1324
0.043	4.88	2.60	0.1379
0.043	5.49	2.75	0.1422
0.025	0	0	0.0320
0.025	0.65	0.72	0.0395
0.025	1.48	1.22	0.0559
0.025	1.93	1.42	0.0640
0.025	2.20	1.61	0.0740
0.025	3.17	2.04	0.0809
0.025	4.04	2.37	0.0951
0.025	4.56	2.52	0.1009

V_{sg}	Q	ωA	ε
ft./sec.	SCFM	ft./sec.	-
0.013	0	0	0.0140
0.013	0.78	0.80	0.0160
0.013	0.93	0.89	0.0161
0.013	1.09	1.00	0.0196
0.013	1.28	1.12	0.0198
0.013	1.50	1.24	0.0209
0.013	1.84	1.34	0.0225
0.013	2.15	1.58	0.0260
0.013	2.64	1.82	0.0319
0.013	2.97	1.94	0.0378
0.013	3.46	2.15	0.0380
0.013	3.49	2.16	0.0429
0.013	3.85	2.30	0.0400
0.013	3.90	2.32	0.0402
0.013	4.39	2.43	0.0431
0.013	4.80	2.58	0.0440

II.3 **Holdup Results (2)**

V_{sg}	f	A	ωA	ε
ft./sec.	Hz	in.	ft./sec.	-
0.081	0.00	0.0	0.00	0.122
0.081	1.05	0.6	0.33	0.122
0.081	1.11	1.2	0.70	0.122
0.081	1.19	2.0	1.24	0.128
0.081	1.22	2.2	1.40	0.134
0.081	1.25	2.8	1.83	0.144
0.081	1.27	3.0	1.99	0.160
0.081	1.31	3.2	2.19	0.181
0.081	0.00	0.0	0.00	0.118
0.081	1.16	1.5	0.91	0.120
0.081	1.22	2.0	1.28	0.130
0.081	1.26	2.6	1.71	0.153

V_{sg}	f	A	ωA	ε
ft./sec.	Hz	in.	ft./sec.	-
0.081	1.22	2.9	1.85	0.146
0.081	1.25	3.1	2.03	0.172
0.081	1.40	3.5	2.56	0.195
0.051	0.00	0.0	0.00	0.074
0.051	1.07	1.2	0.67	0.074
0.051	1.13	1.6	0.95	0.077
0.051	1.15	1.8	1.08	0.084
0.051	1.20	2.0	1.26	0.102
0.051	1.21	2.4	1.52	0.106
0.051	1.23	2.8	1.80	0.121
0.051	1.26	3.1	2.04	0.142
0.051	0.00	0.0	0.00	0.076
0.051	1.16	2.0	1.21	0.100
0.051	1.23	2.6	1.67	0.117
0.051	1.24	2.9	1.88	0.132
0.051	1.25	3.3	2.16	0.162
0.051	0.00	0.0	0.00	0.067
0.051	1.17	1.8	1.10	0.087
0.051	1.20	2.2	1.38	0.107
0.051	1.23	2.6	1.67	0.118
0.051	1.25	3.1	2.02	0.136
0.027	0.00	0.0	0.00	0.036
0.027	0.89	0.6	0.28	0.037
0.027	1.13	1.8	1.06	0.047
0.027	1.17	2.2	1.34	0.066
0.027	1.21	2.8	1.77	0.085
0.027	1.24	3.1	2.01	0.095
0.027	1.25	3.7	2.42	0.120
0.027	0.00	0.0	0.00	0.038
0.027	0.90	0.3	0.41	0.038
0.027	1.04	1.0	0.54	0.038
0.027	1.08	1.3	0.73	0.040

V_{sg}	f	A	ωA	ε
ft./sec.	Hz	in.	ft./sec.	-
0.027	1.11	1.4	0.81	0.042
0.027	1.15	1.8	1.08	0.051
0.027	1.19	2.2	1.37	0.069
0.027	1.23	2.7	1.74	0.087
0.027	1.24	3.5	2.27	0.110
0.027	1.28	3.9	2.61	0.126

Appendix III

Power Dissipation and Air Consumption Tabulated Data and Results

III.1 Observed Data

III.1.1 24 baffles-no gas

Expt.no.	A	f	Area of diagram	$y_2 - y_1$	P_{cal}
-	in.	Hz	in^2.	in.	in.H_2O per in.
1	3.9	1.25	9.94	5.40	33.6
2	3.7	1.23	8.20	5.32	33.6
3	3.4	1.23	6.40	4.95	33.6
4	3.0	1.20	4.80	4.61	33.6
5	2.7	1.20	3.80	4.27	33.6
6	2.5	1.18	2.46	3.80	33.6
7	2.1	1.18	1.59	3.49	33.6
8	1.9	1.13	0.89	2.92	33.6
9	1.5	1.12	0.40	2.30	33.6
10	3.8	1.25	10.50	5.90	33.6
11	3.7	1.23	8.40	5.41	33.6
12	3.3	1.22	6.47	5.15	33.6
13	2.9	1.22	4.91	4.85	33.6
14	2.8	1.22	3.70	4.24	33.6
15	2.5	1.20	2.60	4.11	33.6
16	2.3	1.20	2.14	4.03	33.6
18	1.9	1.18	1.14	3.02	33.6
19	3.6	1.17	0.99	2.96	33.6

III.1.2 1 baffle-no gas

20	1.9	1.13	0.10	2.91	32.0
21	2.7	1.18	0.29	4.10	32.0
22	3.7	1.27	0.50	5.50	32.0
23	4.4	1.28	0.97	6.39	32.0
26	5.5	1.33	0.47	2.60	32.0
28	4.5	1.32	1.16	6.66	32.0

	Expt.no.	A	f	Area of diagram	$y_2 - y_1$	P_{cal}
	-	in.	Hz	in^2	in.	in.H_2O per in.
	30	3.0	1.23	0.16	3.17	32.0
III.1.3		1.5 ft. packed Raschig Rings-no gas				
	32	2.3	1.04	11.30	3.72	30.3
	33	2.2	1.03	10.49	3.65	30.3
	34	2.2	1.00	8.03	3.27	30.3
	35	2.0	1.04	3.05	3.24	67.0
	37	1.7	1.05	2.20	2.87	67.0
	38	1.5	1.07	1.66	2.50	67.0
	39	1.5	1.07	1.23	2.20	67.0
	40	1.2	1.09	0.89	1.93	67.0
	41	1.1	1.09	0.64	1.72	67.0
	42	0.9	1.09	0.38	1.46	67.0
III.1.4		3.3 ft. packed Raschig Rings-no gas				
	43	1.9	0.96	17.80	5.07	30.0
	44	1.9	0.96	15.25	4.71	30.0
	45	1.7	0.96	13.07	4.60	30.0
	47	1.5	0.98	9.65	4.07	30.0
	48	1.4	0.99	7.79	3.83	30.0
	50	1.2	1.01	5.20	3.36	30.0
	51	1.2	1.02	1.89	2.35	30.0
	52	0.9	1.03	2.69	2.61	30.0
	53	0.7	1.05	1.89	2.35	30.0
	54	0.6	1.05	1.19	2.00	30.0
	55	1.6	0.99	6.79	3.75	30.0
	56	1.2	1.00	6.79	3.75	30.0
III.1.5		24 baffles-V_{sg} = 0.025 ft./sec.				
	57	1.2	1.15	0.51	1.40	25.9
	58	1.7	1.20	0.75	1.79	25.9
	59	1.8	1.22	1.80	2.50	25.9
	60	2.1	1.22	2.10	2.31	25.9

Expt.no.	A	f	Area of diagram	$y_2 - y_1$	P_{cal}
-	in.	Hz	in^2.	in.	in.H_2O per in.
61	2.3	1.25	2.32	2.21	25.9
62	2.5	1.25	3.25	2.67	25.9
63	2.8	1.26	3.59	2.40	25.9
64	2.9	1.27	3.87	2.60	25.9
65	3.1	1.29	5.50	3.20	25.9
66	3.3	1.29	5.12	2.99	25.9
67	3.5	1.29	7.60	3.49	25.9
III.1.6	24 baffles-V_{sg} = 0.043 ft./sec.				
68	1.4	1.17	0.40	0.95	23.6
69	3.5	1.21	0.57	1.11	23.6
70	2.1	1.24	1.14	1.66	23.6
71	2.3	1.27	1.27	1.65	23.6
72	2.3	1.27	2.15	1.90	23.6
73	2.5	1.28	2.26	1.85	23.6
74	2.7	1.30	3.22	2.35	23.6
75	2.7	1.31	3.87	2.35	23.6
76	2.9	1.32	4.60	2.53	23.6
77	3.1	1.32	6.24	3.12	23.6
78	3.1	1.32	4.72	2.32	23.6

III.2 Power Dissipation - Tabulated Results

III.2.1 24 baffles-no gas

Expt.no.	$A\omega$	$(A\omega)^3$	P_{th}	P_{obs}	$\frac{P_{obs}}{P_{th}}$
-	ft./sec.	ft^3/sec^3.	ft.lb./sec.	ft.lb./sec.	-
1	2.55	16.63	36.79	25.68	0.70
2	2.42	14.20	31.42	20.40	0.65
3	2.20	10.58	23.42	15.51	0.66
4	1.88	6.70	14.82	10.73	0.72
5	1.67	4.62	10.21	8.10	0.79
6	1.52	3.50	7.74	5.37	0.69
7	1.30	2.20	4.87	3.24	0.66

	Expt.no.	$A\omega$	$(A\omega)^2$	P_{th}	P_{obs}	$\frac{P_{obs}}{P_{th}}$
	-	ft./sec.	ft^2/sec^2	ft.lb./sec.	ft.lb./sec.	-
	8	1.10	1.32	2.93	1.83	0.62
	9	0.85	0.61	1.35	0.81	0.60
	10	2.49	15.38	34.03	24.19	0.71
	11	2.36	13.10	28.97	20.00	0.69
	12	2.10	9.29	20.55	14.43	0.70
	13	1.88	6.64	14.68	10.40	0.71
	14	1.78	5.68	12.56	8.51	0.68
	15	1.54	3.65	8.07	5.32	0.66
	16	1.45	3.02	6.68	4.19	0.63
	18	1.18	1.63	3.61	2.43	0.67
	19	1.10	1.33	2.94	2.01	0.68
III.2.2			1 baffle-no gas			
	20	1.13	1.43	0.13	0.20	1.53
	21	1.67	4.68	0.43	0.62	1.43
	22	2.42	14.19	1.31	1.15	0.88
	23	2.96	25.84	2.38	2.34	0.98
	26	3.87	58.17	5.36	3.65	0.68
	28	3.14	30.86	2.85	2.84	1.00
	30	1.94	7.27	0.67	0.51	0.76
III.2.3			1.5 ft. packed Raschig Rings-no gas			
	32	1.23	1.85	17.62	18.37	1.04
	33	1.19	1.69	16.12	16.88	1.05
	34	1.13	1.45	13.79	13.69	0.99
	35	1.08	1.25	11.92	11.05	0.93
	37	0.93	0.79	7.55	7.73	1.02
	38	0.85	0.62	5.91	6.17	1.04
	39	0.82	0.55	5.24	4.99	0.95
	40	0.70	0.34	3.23	3.50	1.08
	41	0.62	0.24	2.28	2.52	1.10
	42	0.53	0.15	1.42	1.50	1.06
III.2.4			3.3 ft. packed Raschig Rings-no gas			
	43	0.97	0.91	19.21	16.62	0.87

	Expt.no.	$A\omega$	$(A\omega)^3$	P_{th}	P_{obs}	$\frac{P_{obs}}{P_{th}}$
	-	ft./sec.	ft^3/sec^3	ft.lb./sec.	ft.lb./sec.	-
	44	0.95	0.87	18.22	15.06	0.83
	45	0.87	0.67	14.05	12.12	0.86
	47	0.78	0.47	9.88	9.08	0.92
	48	0.72	0.37	7.87	7.15	0.91
	50	0.61	0.23	4.83	4.63	0.96
	51	0.57	0.18	3.84	3.63	0.95
	52	0.46	0.10	2.11	2.34	1.11
	53	0.41	0.07	1.49	1.62	1.09
	54	0.34	0.04	0.79	0.97	1.23
	55	0.83	0.58	12.22	10.59	0.87
	56	0.62	0.24	5.01	5.48	1.09
III.2.5		24 baffles-V_{sg} = 0.025 ft./sec.				
	57	0.72	0.38	0.81	1.11	1.37
	58	1.04	1.11	2.35	1.83	0.78
	59	1.15	1.50	3.14	3.47	1.10
	60	1.31	2.25	4.67	5.02	1.07
	61	1.50	3.38	6.95	6.64	0.96
	62	1.66	4.59	9.42	8.52	0.90
	63	1.85	6.30	12.84	11.64	0.91
	64	1.93	7.14	14.45	12.08	0.84
	65	2.13	9.71	19.53	15.45	0.79
	66	2.20	12.75	25.29	21.43	0.85
III.2.6		24 baffles-V_{sg} = 0.043 ft./sec.				
	68	0.86	0.63	1.30	1.39	1.07
	69	1.11	1.36	2.78	2.19	0.79
	70	1.34	2.39	4.83	3.52	0.73
	71	1.50	3.38	6.79	4.43	0.65
	72	1.56	3.83	7.61	6.80	0.89
	73	1.71	4.99	9.83	8.01	0.82
	74	1.80	5.85	11.43	9.48	0.83
	75	1.89	6.71	13.03	11.92	0.92

Expt.no.	$A\omega$	$(A\omega)^3$	P_{th}	P_{obs}	$\frac{P_{obs}}{P_{th}}$
-	ft./sec.	ft^3/sec^3	ft.lb./sec.	ft.lb./sec.	-
76	2.04	8.44	16.24	14.21	0.88
77	2.12	9.47	18.09	16.25	0.90
78	2.12	9.51	18.05	16.55	0.92

III.3 Compressed Air Consumption - Tabulated Results

III.3.1 24 baffles-no gas

Expt.no.	$A^2\omega^3$	Q_{th}	Q_{obs}	$\frac{Q_{obs}}{Q_{th}}$
-	ft^3/sec^3	SCFM	SCFM	-
1	51.17	6.62	4.61	0.70
2	45.44	5.88	4.11	0.70
3	37.36	4.83	3.57	0.74
4	26.79	3.47	2.89	0.83
5	20.90	2.70	2.38	0.88
6	17.13	2.22	1.95	0.88
7	12.59	1.63	1.62	0.99
8	8.58	1.11	1.25	1.13
9	5.04	0.65	0.89	1.36
10	48.58	6.28	4.64	0.74
11	43.05	5.57	4.09	0.73
12	33.78	4.37	3.36	0.77
13	27.00	3.49	2.87	0.82
14	24.32	3.15	2.50	0.79
15	17.87	2.31	2.10	0.91
16	15.75	2.04	1.89	0.93
18	10.30	1.33	1.43	1.07
19	8.86	1.15	1.25	1.09

III.3.2 1 baffle-no gas

20	9.05	0.05	0.74	15.15
21	20.81	0.11	1.08	9.59
22	46.64	0.25	1.47	5.86
23	70.49	0.38	1.82	4.79
26	125.77	0.68	2.40	3.54

Expt.no.	$A^2 \omega^3$	Q_{th}	Q_{obs}	$\frac{Q_{obs}}{Q_{th}}$
-	ft^2/sec^2	SCFM	SCFM	-
28	81.40	0.44	2.00	4.55
30	29.08	0.16	1.26	8.03
III.3.3	1.5 ft. packed Raschig Rings-no gas			
32	9.86	5.50	5.82	1.06
33	9.14	5.10	5.33	1.05
34	8.04	4.48	4.81	1.07
35	7.56	4.22	4.34	1.03
37	5.68	3.16	3.42	1.08
38	4.91	2.74	2.99	1.09
39	4.53	2.53	2.59	1.03
40	3.34	1.86	2.19	1.18
41	2.65	1.48	1.79	1.21
42	1.93	1.07	1.42	1.32
III.3.4	3.3 ft. packed Raschig Rings-no gas			
43	5.68	6.99	6.07	0.87
44	5.50	6.77	5.55	0.82
45	4.63	5.70	5.05	0.89
47	3.72	4.58	4.13	0.90
48	3.22	3.96	3.67	0.93
50	2.38	2.92	2.80	0.96
51	2.06	2.54	2.43	0.96
52	1.39	1.72	2.00	1.17
53	1.13	1.39	1.66	1.19
54	0.74	0.91	1.29	1.41
55	4.32	5.31	4.59	0.86
56	2.42	2.98	3.23	1.08

III.4 Data used in the calculation of P_{th} and Q_{th}

C = cross-sectional area of column leg = 0.0491 ft^2

C_D = coefficient of discharge = 0.70 (Ref. 41)

D_P = average particle diameter = 0.0725 ft. (Ref. 41)

F_m	= friction factor	= 1.0 (Ref. 41)
g_c	= acceleration due to gravity	= 32.16 ft./sec^2
L_g	= length of gas space	= 33.0 in.
L_p	= height of packing	= 1.509, 3.33 ft.
n	= exponent in expression for R	= 2.0 (Ref. 41)
ε_b	= voidage of packing	= 0.6114 (Ref. 41)
ρ_L	= density of water	= 62.35 lb./ft^3
ρ	= density of dispersion - obtained from holdup	= $\rho_L(1 - \varepsilon)$
ϕ_s	= shape factor of packing	= 0.3 (Ref. 41)
ψ	= fractional free area of baffle plate	= 0.556

Appendix IV

Absorption Rates - Tabulated Data and Results

Dependence of Absorption Rate upon Pulse Velocity

Expt.no.	A	f	ωA	V_{sg}	p_c	T_c	$k_L a$
-	in.	Hz	ft./sec.	ft./sec.	mm. Hg	°C	$sec.^{-1}$
57	0	0	0	0.027	75	19.2	0.0252
58	1.8	1.15	1.07	0.026	118	19.3	0.0401
59	2.6	1.22	1.38	0.027	135	19.2	0.0608
60	2.8	1.24	1.79	0.027	172	19.4	0.0763
61	3.2	1.25	2.06	0.026	200	19.5	0.0798
62	3.5	1.28	2.37	0.025	275	19.7	0.0879
63	0	0	0	0.026	75	19.7	0.0217
64	0.8	1.04	0.43	0.027	88	19.6	0.0258
65	1.1	1.09	0.62	0.027	95	19.6	0.0250
66	1.3	1.11	0.74	0.026	103	19.7	0.0250
67	1.5	1.14	0.88	0.026	110	19.8	0.0364
68	1.6	1.15	0.95	0.027	115	19.1	0.0355
69	1.8	1.20	1.11	0.027	120	19.3	0.0405
70	2.0	1.19	1.22	0.027	125	19.3	0.0463
71	2.2	1.21	1.37	0.027	130	19.4	0.0555
72	2.2	1.21	1.37	0.027	140	19.5	0.0539
73	2.4	1.23	1.52	0.027	145	19.5	0.0619
74	2.6	1.23	1.64	0.027	158	19.6	0.0685
75	2.8	1.24	1.79	0.027	172	19.6	0.0721
76	2.7	1.24	1.72	0.027	160	19.7	0.0755
77	3.0	1.26	2.01	0.027	192	19.6	0.0820
78	3.0	1.27	1.96	0.027	185	19.6	0.0825
79	3.1	1.27	2.09	0.026	210	19.6	0.0842
80	3.6	1.31	2.49	0.029	315	19.7	0.0934
81	0	0	0	0.028	75	19.3	0.0256
83	1.0	1.06	0.54	0.027	92	19.7	0.0217
84	1.1	1.07	0.61	0.028	95	19.9	0.0216

Expt.no.	A	f	ωA	V_{sg}	p_c	T_c	$k_L a$
-	in.	Hz	ft./sec.	ft./sec.	mm. Hg	°C	$sec.^{-1}$
85	1.3	1.09	0.73	0.028	100	19.6	0.0351
86	1.6	1.09	0.90	0.029	110	19.8	0.0309
87	1.7	1.13	0.99	0.028	117	19.9	0.0353
88	2.0	1.17	1.20	0.027	125	19.8	0.0424
89	2.1	1.19	1.29	0.028	130	19.8	0.0496
90	2.4	1.21	1.50	0.028	144	19.9	0.0574
91	2.5	1.21	1.56	0.028	147	20.0	0.0643
92	2.9	1.24	1.85	0.027	175	20.0	0.0743
93	3.0	1.24	1.91	0.028	180	19.8	0.0746
94	3.2	1.24	2.04	0.027	200	19.9	0.0818
95	3.3	1.27	2.22	0.027	255	19.9	0.0843
96	3.7	1.26	2.46	0.029	300	20.0	0.0915
97	3.7	1.25	2.44	0.029	295	18.8	0.0963
98	2.2	1.17	1.32	0.027	130	18.2	0.0466
99	2.4	1.20	1.48	0.028	143	18.3	0.0489
100	2.6	1.19	1.60	0.028	150	18.4	0.0521
101	2.7	1.22	1.70	0.028	158	18.7	0.0566
102	2.7	1.24	1.72	0.028	160	18.7	0.0643
103	2.8	1.23	1.77	0.029	172	18.9	0.0715
105	0	0	0	0.053	75	19.5	0.0411
106	0	0	0	0.051	75	19.5	0.0400
107	0.8	1.07	0.44	0.052	88	19.5	0.0435
108	1.2	1.13	0.70	0.052	100	19.5	0.0437
109	1.3	1.15	0.77	0.052	102	19.4	0.0495
110	1.5	1.17	0.90	0.051	110	19.5	0.0515
111	1.6	1.19	0.98	0.051	115	19.5	0.0564
112	1.8	1.21	1.12	0.052	120	19.5	0.0600
113	2.0	1.22	1.26	0.052	126	19.6	0.0711
114	2.1	1.23	1.33	0.052	132	19.5	0.0607
115	2.2	1.25	1.41	0.051	139	19.6	0.0711
116	2.4	1.25	1.54	0.051	148	19.6	0.0749
117	2.6	1.29	1.73	0.051	163	19.7	0.0855

Expt.no.	A	f	ωA	V_{sg}	p_c	T_c	$k_L a$
-	in.	Hz	ft./sec.	ft./sec.	mm. Hg	°C	$sec.^{-1}$
118	3.0	1.30	2.01	0.051	192	19.6	0.0929
119	3.3	1.32	2.31	0.048	263	19.6	0.1127
120	0	0	0	0.051	75	19.4	0.0411
124	0	0	0	0.052	75	19.4	0.0388
127	2.2	1.24	1.40	0.051	138	19.3	0.0742
128	2.1	1.23	1.33	0.051	132	19.3	0.0677
129	3.3	1.29	2.19	0.049	235	19.4	0.1018
130	3.1	1.30	2.08	0.050	203	19.4	0.0991
131	0.5	1.00	0.26	0.051	82	19.3	0.0371
133	0	0	0	0.052	75	19.5	0.0406
134	0.7	1.05	0.38	0.051	85	19.3	0.0408
135	0.9	1.08	0.50	0.052	80	19.3	0.0393
136	1.2	1.10	0.68	0.053	97	19.1	0.0435
137	2.2	1.22	1.38	0.051	135	19.1	0.0662
138	2.4	1.24	1.53	0.051	147	19.2	0.0702
139	2.6	1.26	1.69	0.050	160	19.3	0.0763
140	3.0	1.28	1.98	0.053	182	19.5	0.0929
141	3.3	1.33	2.26	0.049	260	19.5	0.1003
142	3.2	1.30	2.14	0.049	230	19.6	0.0984
143	0	0	0	0.089	75	18.9	0.0840
144	0.9	1.15	0.59	0.088	90	18.9	0.0821
145	1.6	1.18	0.97	0.086	115	18.9	0.0975
146	2.0	1.23	1.27	0.087	125	18.9	0.1002
148	0	0	0	0.082	75	19.0	0.0698
149	1.2	1.11	0.69	0.086	100	19.0	0.0835
150	1.7	1.19	1.04	0.087	118	18.9	0.1020
151	2.3	1.23	1.46	0.084	142	18.8	0.0977
152	2.4	1.25	1.55	0.085	147	18.9	0.1097
153	2.6	1.28	1.71	0.087	163	19.3	0.1488
154	3.0	1.30	2.01	0.084	190	19.2	0.1343
155	3.1	1.31	2.09	0.084	215	19.5	0.1345

Expt.no.	A	f	ωA	V_{sg}	p_c	T_c	$k_L a$
-	in.	Hz	ft./sec.	ft./sec.	mm. Hg	°C	$sec.^{-1}$
156	0	0	0	0.088	75	19.2	0.0845
157	1.4	1.17	0.84	0.086	108	19.4	0.0805
158	1.7	1.20	1.01	0.087	118	19.5	0.0896
159	2.0	1.25	1.29	0.084	130	19.5	0.0930
160	2.7	1.26	1.75	0.082	170	19.5	0.1096
161	2.5	1.24	1.60	0.084	150	19.5	0.1118
162	2.6	1.25	1.67	0.085	158	19.6	0.1307
163	3.4	1.32	2.38	0.080	285	19.8	0.1629
164	1.3	1.10	0.74	0.086	100	19.6	0.0728
165	0	0	0	0.081	75	19.5	0.0672
166	0	0	0	0.096	75	19.5	0.0650
167	0.7	1.09	0.39	0.086	85	19.4	0.0640
168	0	0	0	0.090	75	19.3	0.0649
169	2.2	1.26	1.43	0.083	140	18.6	0.1000
170	2.6	1.28	1.71	0.085	160	18.7	0.1196
171	3.0	1.30	2.00	0.084	190	19.2	0.1311
172	3.1	1.30	2.14	0.078	225	18.9	0.1345
173	3.3	1.31	2.29	0.081	275	19.1	0.1529
175	3.5	1.29	2.40	0.077	290	18.2	0.1500
176	3.7	1.34	2.63	0.085	360	18.3	0.1461

Appendix V

References

1.- Minnaert, M.; Phil. Mag. 16 235 (1933) (Ser. 7)

2.- Smith, F.D.; Phil. Mag. 19 1147 (1935) (Ser. 7)

3.- Bjerknes, V.; Die Kraftfelder, p.16 Vieweg, Braunschweig, 1909

4.- Van Dijck, W.J.D.; U.S. Patent 2,011,186 August 1935

5.- Jamrack, W.D.; "Rare Metal Extraction by Chemical Engineering Techniques" Pergamon Press, London 1963.

6.- Sege, G., and Woodfield, F.W.; Chem. Engng Prog. 50 396 (1954)

7.- Harbaum, K.L., and Houghton, G.; Chem. Engng Sci. 13 90 (1960)

8.- Harbaum, K.L., and Houghton, G.; J. App. Chem. 12 234 (1962)

9.- Pielemeier, W.H.; J. Acoust. Soc. Amer. 23 (2) 224 (1951)

10.- Bretsznajder, S., and Pasiuk, W.; Bull. Acad. Polon. Sci. (Ser. Sci. Chim.) 7 (8) 591 (1959)

11.- Bretsznajder, S, and Pasiuk, W.; Bull. Acad. Polon. Sci. (Ser. Sci. Chim.) 10 (3) 153 (1962)

12.- Bretsznajder, S., and Pasiuk, W.; Bull.Acad. Polon. Sci. (Ser. Sci. Chim.) 10 (11-12) 639 (1962)

13.- Bretsznajder, S., and Pasiuk, W.; Bull. Acad. Polon. Sci. (Ser. Sci. Chim.) 10 (11-12) 641 (1962)

14.- Bretsznajder, S., and Pasiuk, W.; Bull. Acad. Polon. Sci. (Ser. Sci. Chim.) 11 (2) 101 (1963)

15.- Bretsznajder, S., and Pasiuk, W.; Bull. Acad. Polon. Sci. (Ser. Sci. Chim.) 11 (2) 103 (1963)

16.- Bretsznajder, S., and Pasiuk, W.; Bull.Acad. Polon. Sci. (Ser. Sci. Chim.) 11 (2) 107 (1963)

17.- Baird, M.H.I.; Chem. Engng Sci. 18 685 (1963)

18.- Buchanan, R.H., Teplitsky, D.R., and Oedjoe, D.; Ind. & Engng Chem. (PD&D) 2 (3) 173 (1963)

19.- Buchanan, R.H., Jameson, G., and Oedjoe, D.; Ind. & Engng (Fund.) 1 82 (1962)

20.- Bretsznajder, S., and Pasiuk, W.; Int. Chem. Engng 4 61 (1964) (Prz. Chem. 42 435 (1963))

21.- Baird, M.H.I.; Can. J. Chem. Engng 41 52 (1963)

22.- Houghton, G.; J. Acoust. Soc. Amer. 35 1387 (1963)

23.- Jameson, G.J., and Davidson, J.F.; Chem. Engng Sci. 21 29 (1966)

24.- Jameson, G.J.; Chem. Engng Sci. 21 35 (1966)

25.- Rubin, E.; Can. J. Chem. Engng 46 145 (1968)

26.- Ziolkowski, Z., and Filip, S.; Int. Chem. Engng 5 40 (1965) (Prz. Chem. 43 328 (1964))

27.- Gorodetskii, I.Ya., Olevskii, V.M., Levitanaite, R.P., and Legochkina, L.A.; Khim. Prom. 41 834 (1965)

28.- Jackisch, D.A.; Dissertation Abstracts (Eng.) 26 5321 (1966)

29.- Bretsznajder, S., and Pasiuk, W.; Bull. Acad. Polon. Sci. (Ser. Sci. Chim.) 14 73 (1966)

30.- Jameson, G.J.; Trans. Instn. Chem. Engrs. 44 T91 (1966)

31.- Tudose, R.Z.; Int. Chem. Engng 4 219 (1964) (Studii si Certcetari Stiintifice 2 319 (1962))

32.- Beek, W.J.; Lecture - Mass Transfer with Stimulated Surface Renewal - Edinburgh University, 19th Jan., 1965

33.- Ziolkowski, Z., and Filip, S.; Int. Chem. Engng 3 433 (1963) (Prz. Chem. 2 99 (1963))

34.- Baird, M.H.I.; A.I.Ch.E. - I.Chem.E. Symposium Ser. 6, p. 53. London, Instn. Chem. Engnrs. (1965)

35.- Tudose, R.Z.; Rev. Roumaine de Chimie 11 621 (1966)

36.- Ziolkowski, Z., and Filip, S.; Chem. Stosow. IV 2B 189 (1967)

37.- Veviorovskii, M.M., Dil'man, V.V., and Aizenbud, M.B.; Khim. Prom. 42 783 (1966)

38.- Proctor, D.; Personal Communication and Ph.D Thesis, Dept. of Chemical Engineering, University of Edinburgh, 1968.

39.- Gal-or, B., Hauk, J.P., and Hoelscher, H.E.; Int. J. Heat & Mass Transfer 10 1559 (1967)

40.- Jealous, A.C., and Johnson, H.F.; Ind. & Engng Chem. 47 1159 (1955)

41.- Perry, J.H.; Chem. Engnrs. Handbook pp. 5.8, 5.50 (4th Edition)

42.- Vermijs, W.J.W.; A.I.Ch.E. - I.Chem. E. Symposium Ser. 6, p. 98, London - Instn. Chem. Engnrs. (1965)

43.- Rayleigh, Lord; 'Theory of Sound', Art. 306, Macmillan(1929)

44.- Baird, M.H.I.; Personal Communication

45.- Baird, M.H.I.; Personal Communication

46.- Baird, M.H.I., and Garstang, J.H.; Chem. Engng Sci. 22 1663 (1967)

47.- Calderbank, P.H.; Trans. Instn. Chem. Engnrs. 36 443 (1958)

48.- Valentin, F.H.H.; Brit. Chem. Engng 12 1213 (1967)

49.- Sideman, S., Hortacsu, O., and Fulton, J.W.; Ind. & Engng Chem. 58 32 (1966)

50.- Rushton, J.H., Gallagher, J.B., Oldshue, J.Y.; Chem. Engng Prog. 52 319 (1956)

51.- Foust, H.C., Mack, D.E., and Rushton, J.H.; Ind. Engng Chem. 36

517 (1944)

52.- Karwat, H.; Chem. Ing. Tech. 31 588 (1959)

53.- Cooper, C.M., Fernstrom, G.A., and Miller, S.A.; Ind. Engng Chem. 36 504 (1944)

54.- Westerterp, K.R., Van Dierendock, L.L., De Kraa, J.A.; Chem. Engng Sci. 18 157 (1963)

55.- Bartholomew, W.H., Karow, E.O., Sfat, M.R., and Wilhelm, R.H.; Ind. Engng Chem. 42 1801 (1950)

56.- Whitman, W.G.; Chem. and Met. Engng 29 147 (1923)

57.- Coulson, J.M., and Richardson, J.F.; 'Chemical Engineering' Vol. 2 p. 701 (Pergamon Press 1962)

58.- Calderbank, P.H.; Trans. Instn. Chem. Engnrs. 37 173 (1959)

59.- Coggins, J.; Ph.D Thesis, Dept. of Chemical Engineering, University of Edinburgh (1965)

60.- Resnick, W., and Gal-or, B.; Advances in Chem. Engng 7 295 (1968)

Appendix VI

Nomenclature

A	amplitude of pulsation
a	specific interfacial area
C	cross-sectional area of column leg
C_D	coefficient of discharge
c	solute concentration in the bulk liquid
c_∞	equilibrium solute concentration in the bulk liquid
D	column leg diameter
D_p	average particle diameter (packing)
d	bubble diameter
F_m	friction factor
f	frequency
f_r	resonant frequency
H_L	length of column of dispersion
HTU	height of transfer unit
H_1, H_2	lengths of columns of dispersion (section 4.6.2)
h	mean depth of bubble below liquid surface
I	mass transfer rate improvement factor
$K_g a$	volumetric mass transfer coefficient (33,36)
k	exponent in general equation of state pV^k = constant (equ. 2.1)
k_L	liquid film mass transfer coefficient
k_p	overall absorption coefficient under pulsed conditions (31,35)
$k_L a$	liquid film volumetric mass transfer coefficient
$(k_L a)_o$	transfer coefficient at zero power input
$k_G a$	gas film volumetric mass transfer coefficient

L_g length of gas space

L_p height of packing

M ratio of forces acting on bubble = $\frac{\text{nett downward force}}{\text{nett upward force}}$ (equ. 2.4)

N number of baffles

N_A mass flux of species A

N_i impeller speed

n exponent in equ. 4.13

P_s specific power input

P_{st} total specific power input

p_c time averaged pressure at probe level

p_{cal} oscilloscope pressure axis calibration factor

Q compressed air consumption referred to STP

R frictional resistance of packing and baffles

r radius of bubble

S_o surface area per unit volume of packing

t time

V_{sg} superficial gas velocity

V_G volume of gas space

v_{cal} oscilloscope volume axis calibration factor

γ ratio of specific heats

ε fractional gas holdup

ε_b voidage of packing

$\tilde{\varepsilon}$ oxygen concentration probe output

$\tilde{\varepsilon}^*$ oxygen concentration probe output at equilibrium

ρ density

ρ_L liquid density

ϕ_s shape factor of packing

ψ fractional free area of baffle plate

ω angular frequency = $2\pi f$

Appendix VII

Published Paper

Erratum

Superficial gas velocities are quoted in the paper as twice their actual values, i.e. the superficial gas velocities should be 0.043, 0.025 and 0.013 ft./sec., and not 0.085, 0.051 and 0.026 ft./sec.

Chemical Engineering Science, 1967, Vol. 22, pp. 1663–1673. Pergamon Press Ltd., Oxford. Printed in Great Britain.

Power consumption and gas hold-up in a pulsed column

M. H. I. BAIRD* and J. H. GARSTANG

Department of Chemical Engineering, University of Edinburgh

(*Received* 16 *June* 1967)

Abstract—A resonant air-pulsed water column has been developed for gas absorption experiments: its internal diameter is 3 in. and the effective inertial length of oscillating column is 14·17 ft. The amplitude is up to 6 in. at frequencies from 0·9 to 1·4 c/s and experiments have been carried out with the column unpacked, packed with random ½ in. rings and fitted with baffle plates. The quantities measured have included pulse air consumption, power dissipation and gas hold-up when air is passed through the water. The observed pulse air consumption and power dissipation are in approximate agreement with theoretical predictions based upon a quasi-steady-state model. The gas hold-up due to a separate air supply in the baffled column is increased as much as threefold by pulsations, which appear to be more effective than conventional stirring when the superficial gas velocity exceeds about 0·04 ft/sec.

SEVERAL workers [1–6] have found that gas absorption rates from bubble dispersions can be increased by the application of vertical vibrations. The largest effects have been found in the frequency range 10–150 c/s with well-defined maximum values at certain frequencies [4]. Measurements of gas hold-up as a function of frequency [4, 7] also show peak values at certain frequencies which are thought to be resonant frequencies [8] characteristic of the bubble dispersion. At high vibration intensities, gas bubbles may be prevented from rising altogether [4, 9, 10] or entrained downwards from the liquid surface [11]. Absorbers operated under such conditions require no submerged gas distributor and extremely high mass transfer rates have been reported [3, 5]. The retardation or halting of rising bubbles by vertical vibrations has been explained [11] as due to a Bjerknes force acting downwards on each bubble because of its volume pulsation and vertical oscillation. According to the simple theory [11] a bubble is halted by vibrations if M is unity, where

$$M=\omega^4A^2\rho h/2gP_0\,. \qquad (1)$$

Observations [12] confirm this theory at low vibrational Reynolds numbers, but as the Reynolds number increases the critical value of M rises to about 2.

Equation (1) implies that high frequencies are more effective than low ones in slowing down rising bubbles. However, if the applied frequency is higher than the resonant frequency of the dispersion [8] the vibrations are considerably attenuated within the dispersion. The effect of vibration upon hold-up has accordingly been found [4, 7] to diminish as the height of the bubble column is increased. The present author [13] developed an air-pulsed absorption column operating at a frequency of about 1 c/s. Although in this case the value of M was too low for the gas hold-up to be much affected by Bjerknes forces, the amplitude was high enough for considerable turbulence to be induced when baffle plates were mounted in the column. The low operating frequency permitted bubble columns up to 10 ft high to be pulsed without appreciable attenuation and preliminary experiments showed that mass transfer rates could be increased by up to 95% compared with the rates in unpulsed conditions.

This article describes a double-acting U-shaped column capable of much higher pulsation intensities than the earlier column [13] which was single-acting. Measurements of power dissipation and gas hold-up in the air–water system have been made as a preliminary to gas absorption experiments [14].

* Present address: Department of Chemical Engineering, McMaster University, Hamilton, Ontario, Canada.

EXPERIMENTAL

The pulsed absorption apparatus and ancillaries are shown in Fig. 1. The apparatus itself was constructed from 3 in. i.d. Q.V.F. glass tubing and consists of two vertical sections each 9 ft 10 in. high linked by a horizontal junction with an axis 5 in. from the bottom. The centre lines of the vertical sections are 10 in. apart and the sections are supported on a single base-plate of $\frac{1}{4}$ in. thick brass. The top plates are of $\frac{1}{2}$ in. PVC. Compressed air for pulsation is drawn from the 140 psi laboratory air supply, filtered, and reduced to 30 psi by a pressure control. At this pressure it is metered by a rotameter, the flow being controlled by a fine disk valve downstream of the rotameter. The pressure drop across the disk valve is always in excess of the critical pressure drop of about 13 psi, so the flow is independent of downstream pressure fluctuations. The air enters a 5-port solenoid valve by which it can be directed to either section of the column. The valve allows air to exhaust from the section which is not being supplied with air. The principle of operation is similar to the self-triggering principle described earlier [13].

The tower was operated in three conditions: unbaffled (open), baffled, and packed. The baffle plates are 2 in. disks of $\frac{1}{4}$ in. thick PVC mounted centrally at 6 in. intervals on two $\frac{3}{8}$ in. dia. brass support rods, one at the axis of each vertical section. The packing used is $\frac{1}{2}$ in. ceramic Raschig rings to a depth of 3·3 ft in one section only. In all cases the average liquid levels on each side were adjusted to leave a 2·75 ft long air space at the top. The equivalent length of liquid column being pulsed was estimated to be 14·17 ft so that the volume of pulsed liquid was 0·695 ft^3. Air for absorption or dispersion is supplied from the 30 psi line through a flow control valve followed by a rotameter. In this case, the effect of pressure fluctuation was almost eliminated by means of a 1 ft^3 surge tank connected in series. The absorption air enters the bottom of each section through a sintered polythene disperser, with a valve in one line to ensure a balanced distribution of air between the two sections.

The left-hand section is equipped with devices to measure variations in liquid level and column pressure. The level device is a simple conductivity meter consisting of a $\frac{3}{8}$ in. dia. brass rod mounted parallel to the axial rod and partly immersed in the liquid. A constant voltage of 5 V d.c. is applied between the rods so that the current flowing is proportional to the depth of immersion of the level device. Preliminary experiments had shown that there were no appreciable polarization effects. A

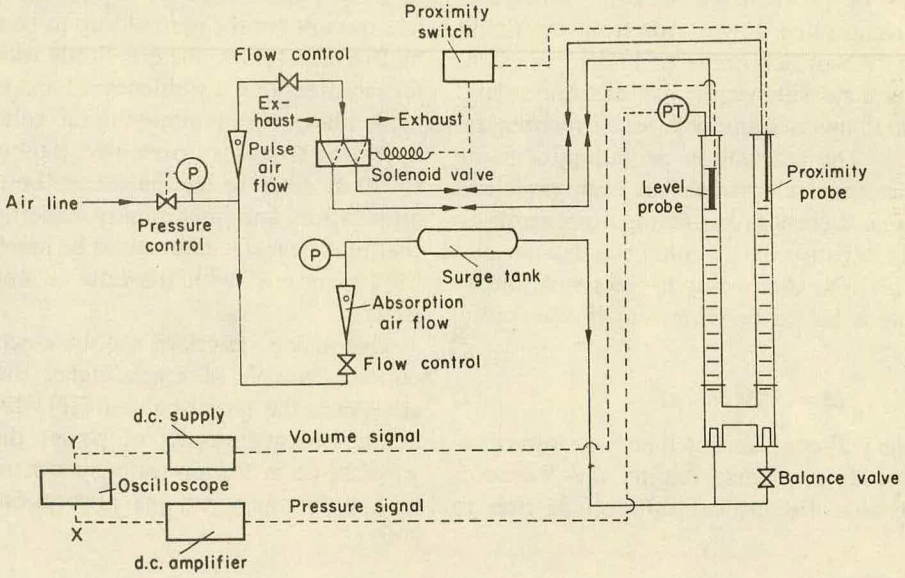

FIG. 1. Pulsation apparatus.

resistance was connected in series with the rods and the voltage across it was applied to the Y-amplifier of an oscilloscope. The airspace pressure is measured by a Solartron pressure transducer (shown as PT on Fig. 1) supplied with 9 V d.c. The pressure signal was boosted by a d.c. amplifier before being applied to the X-amplifier of the oscilloscope. The application of these two signals to the axes of the oscilloscope screen produces a pressure–volume diagram. The "volume" axis was calibrated for each measurement by comparing the length of the diagram with the observed stroke. The "pressure" axis was calibrated after each run by comparison with a constant head of water in the unbalanced columns.

The experimental procedure was as follows. Atmospheric pressure and temperature were noted and the pulsations were started. First, the mean liquid levels in each section were checked and adjusted if necessary by adding or removing some water. Then the "stroke" or end-to-end displacement of the liquid level was measured by means of a cm graduated scale attached to the column wall. The frequency was found by timing 60 cycles and the pulse air flow was found from the rotameter. Where dispersed air was also being added, the resultant increase in hold-up was found by measuring the volume of water which had to be removed to bring mean liquid levels to the datum value of 2·75 ft below the top. Finally, the pressure–volume diagram on the oscilloscope was photographed and its area was measured by a planimeter.

Prediction of Frequency

Consider a U-shaped column of liquid in an apparatus as shown in Fig. 1 with a closed gas space at each end. If the liquid level in one arm is displaced a small distance x below the equilibrium level, a restoring pressure acts upon the liquid column due to the compression/rarefaction of the gas spaces and to the difference between the liquid levels:

$$\Delta P = -2(\gamma P_0 S_0/V_G + \rho g)x. \qquad (2)$$

This expression is obtained assuming that $x \ll V_G/S_0$ and that the enclosed gas behaves adiabatically. The restoring pressure causes the column to accelerate towards the equilibrium position. For a column of uniform cross-sectional area the inertial balance of forces is:

$$\Delta P = \rho H_L \ddot{x} \qquad (3)$$

If, however, the column is made up of a number of sections having different cross-sectional areas, the balance of forces becomes:

$$\Delta P = \rho S_0 \ddot{x} \Sigma H_L/S \qquad (4)$$

From Eqs. (2) and (4):

$$\ddot{x}/x = -\frac{2(\gamma P_0 S_0/V_G + \rho g)}{\rho S_0 \Sigma H_L/S} \qquad (5)$$

Equation (5) is satisfied by a simple harmonic oscillation of the liquid column at a resonance frequency f, where

$$f = \frac{1}{2\pi}\sqrt{\left(\frac{2\gamma P_0}{\rho V_G \Sigma H_L/S} + \frac{2g}{S_0 \Sigma H_L/S}\right)}. \qquad (6)$$

If one arm of the U-tube is open to the atmosphere, the gas compressibility term in Eq. (6) is halved, giving:

$$f = \frac{1}{2\pi}\sqrt{\left(\frac{\gamma P_0}{\rho V_G \Sigma H_L/S} + \frac{2g}{S_0 \Sigma H_L/S}\right)}. \qquad (7)$$

Equations (6) and (7) do not take any account of damping effects, but a similar approach [13, 16] was found to be quite accurate in predicting the frequency of single acting pulsed columns.

The resonance frequency of the unobstructed column is readily calculated taking $S = S_0 = 0{\cdot}0491$ ft^2 and the data on gas and liquid column lengths given above. The mean gas pressure P_0 is taken as 1 atm and the frequencies according to Eqs. (6) and (7) are given in Table 1.

The cross-sectional area of the baffled column is obviously reduced by a factor of $\frac{5}{9}$ in the region of the 2 in. disks. The equivalent length of the constriction is estimated to be 2·01 in. per disk using Rayleigh's [15] expression for circular apertures. With 24 baffle plates, the liquid column therefore consists effectively of 4·02 ft having a cross-sectional area of 0·0273 ft^2 and the remainding 10·15 ft with

the full area of 0·0491 ft^2. The frequencies calculated on this basis are given in Table 1 and fall about 10 per cent below those for the unobstructed column.

Regarding the packed column, VERMIJS [16] has suggested that the acoustic impedance of a packed section is about 2·85 times that of a similar length of unobstructed column. In this investigation, 3·3 ft of packed section were used, so the total equivalent column length (assuming $S = S_0 = 0{\cdot}0491$ ft^2) is:

$$H_L = (14{\cdot}17 - 3{\cdot}3) + 3{\cdot}3 \times 2{\cdot}85 = 20{\cdot}27 \text{ ft}$$

This value has been used, with a small additional correction for the brass tube which was necessary to hold down the packing, in calculating the frequencies which are given in Table 1.

TABLE 1. CALCULATED RESONANCE FREQUENCIES (C/S)

	Both ends closed Eq. (6)	One end open Eq. (7)
Unobstructed column	1·455	1·055
Column with 24 baffles	1·31	0·955
Column with 3·3 ft. packing	1·19	0·863

OBSERVED FREQUENCY

Frequency and amplitude were first measured in the absence of dispersed air and the results are shown in Fig. 2. It will be seen that most of the frequencies are between the two theoretical values obtained from Eqs. (6) and (7). In unobstructed and baffled columns, frequency increases as the pulsing air supply is increased. At low air rates, the exhaust line offers little resistance to flow so that at any instant of column operation one arm of the U-tube is open to atmosphere. Equation (7) might be expected to apply in such cases. At high air rates, the back-pressure of the exhausting air tends to isolate the air space from atmosphere. This leads to an increase in the frequency, partly because Eq. (6) predicts a higher frequency than Eq. (7), and partly because the back-pressure raises the average column pressure P_0 substantially above atmospheric pressure.

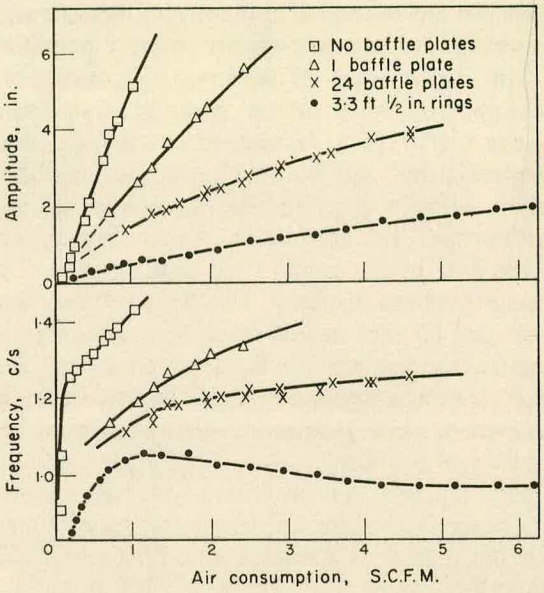

FIG. 2. Effect of air flow upon pulsation frequency and amplitude without dispersed air.

In the case of the packed column, the operating frequency shows a decreasing trend at high air rates. A probable factor here is the extremely damped nature of the system. It has been shown [17] that the natural frequency of an oscillatory system with square-law damping is decreased at high amplitudes. This effect would also be expected to a smaller extent in the baffled column, but is evidently masked by the back-pressure effect described above. A third feature of the frequency curves on Fig. 2 is the sharp drop in frequency at very low air rates. One frequency value in the unobstructed column is below even the prediction from Eq. (7). The sharp drop in frequency occurs at amplitudes below 0·5 in. and a possible explanation is that lag is introduced into the self-triggering system by the slow detachment of the meniscus from the capacitative probe as the water level moves downwards. Figure 2 includes data obtained with just a single baffle plate and it is curious that the frequency differs so much from the value for the wholly unobstructed column. Amplitude is also affected strongly, but this is more understandable. The frequency effect may well stem from the amplitude effect, bearing in mind that Eqs. (6) and (7) are valid only for very small amplitudes.

To summarize, the frequency is usually between the values predicted by Eqs. (6) and (7), but cannot be predicted with much accuracy. It is affected by many factors including air supply rate, the flow resistance of the air lines, the meniscus at the capacity probe and frictional forces which are approximately proportional to the square of the velocity.

Amplitude and Air Consumption

Vermijs [16] has proposed an expression for air consumption in terms of frequency, amplitude, etc. for a resonant air-pulsed column. His derivation is subject to some simplifying assumptions, namely:

(a) The gas in the gas spaces behaves isothermally.

(b) The injection–exhaust valve has a sinusoidal flow characteristic.

(c) The frictional force is proportional to the square of velocity.

(d) The usual assumptions that changes in pressure and displacement are relatively small.

The mean air consumption, referred to 1 atm, is given [16] by:

$$Q=\rho V_G F A^2\omega^3/\pi P_A\,. \qquad (8)$$

Although this expression was derived for a single-acting column, it can also be shown to apply to a double-acting unit, taking V_G as the volume of *each* air space.

The friction factor F relates to the pressure drop which would be obtained at a steady liquid velocity u:

$$\Delta P=\rho u^2 F\,. \qquad (9)$$

The value of F for the disk-shaped baffles may be estimated from data [18] on the pressure drop at heat exchanger baffles. The orifice coefficient for the flow apertures was found [18] to be 0·7, hence:

$$F=1{\cdot}02N(1-\sigma^2)/\sigma^2 \qquad (10)$$

where N is the total number of baffles and σ the fractional open area, 0·556 in this work.

Packed columns have also been subjected to steady-flow pressure drop measurements [19]. At high Reynolds numbers,

$$F=2(1-\psi)L/\phi\psi^3 D\,. \qquad (11)$$

The equivalent diameter D and the shape factor ϕ for ½ in. Raschig rings were obtained by the methods given in the literature [19], but the voidage ψ was found experimentally to be 0·611 compared with a quoted [19] value of 0·57

The air consumption in a baffled or a packed column may be calculated by substituting Eq. (10) or (11) (as appropriate) into Eq. (8). Figure 3 shows a comparison between the theory and observation. It will be seen that the observed air consumption is within ±20% of theory [16] in the case of the 24-baffle column and the packed column. This is a very satisfactory agreement in view of the several assumptions (a)–(d) on which the theory was based [16]. The data tend to fall below the theory at high amplitudes, but assumption (d) is no longer valid in such conditions. According to Eq. (10), the friction factor and hence the air consumption of the single-plate column should be $\frac{1}{24}$ of that for the 24-plate column. Figure 3 shows that the measured air consumption of the single-plate column is much higher than this prediction. The discrepancy may be explained by the relatively large additional drag due to wall effects and bends. These effects are less significant in heavily damped columns.

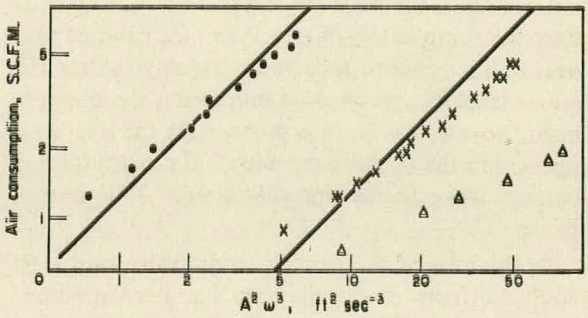

Fig. 3. Air consumption as a function of amplitude and frequency. Theory [16] shown as lines. Symbols: as in Fig. 2.

P–V DIAGRAMS

The power supplied to the column was measured by means of the indicator diagrams mentioned above, examples of which are shown in Fig. 4. The photographs obtained from the oscilloscope were enlarged to a 1 in. square unit grid and the areas measured by means of a planimeter. Pressure and volume waveforms varied from almost purely sinusoidal forms in the case of the unbaffled column, to the most heavily damped case (the packed column) shown in Fig. 4(a) and (b). The switching points in the pressure waveform are indicated by the discontinuities.

In all the examples of indicator diagram shown, pressure forms the vertical axis and volume the horizontal and time generally increases in a clockwise direction. In the diagram for the unbaffled column [Fig. 4(c)], an area of negative work may be seen at the high volume, low pressure end of the diagram. This is due to the practically undamped condition of the column, causing some of the work to be done by the column of liquid on the gas space at the end of the down stroke. The net area and hence the net power dissipated in the column is relatively small. In this condition the pressure and volume wave forms are almost 180° out of phase (cf. Lissajou's figures).

The baffled column diagram [Fig. 4(d)], represents a degree of damping intermediate between the unbaffled column and the packed column. Starting at the lower left-hand corner of the figure: the sudden rise in pressure is due to the opening of the inlet port, combined with a decreasing volume on the upstroke. As the surface passes through its maximum height, the pressure begins to fall, in spite of the continuing inflow of air. When the exhaust port opens, the pressure falls more rapidly. After the liquid level has reached its minimum, the pressure begins to rise slowly once more, until the inlet port opens and the cycle is repeated. The pressure and volume wave forms are still almost 180° out of phase.

In the case of the packed column diagram [Fig. 4(e)], the form of the diagram has been modified considerably. In this case, the pressure is leading the volume by about 90°. The exhaust and inlet opening points are very marked. The inlet port opens at the lower left-hand corner of the diagram and the pressure rises steeply until minimum volume, after which the rate of inflow of air is almost balanced by the rate of fall of the surface, until the exhaust port opens and the pressure falls quite rapidly. After the maximum volume, the rate of exhaust is almost balanced by the rate of rise of the surface, until the inlet port opens and the cycle is repeated.

An example of the diagrams obtained from the gassed, baffled column is shown in Fig. 4(f). As can be seen, the diagram is basically the same as Fig. 4(d), except for the small loop at the top left-hand corner. This is due not to negative work, but to random variations in the volume signal, caused by bubbling around the electrodes of the level meter and was not a reproducible feature of the diagram for any set of conditions in the gassed column. The bubbling effect reduced the accuracy of the power dissipation measurement.

POWER DISSIPATION

JEALOUS and JOHNSON [20] have calculated the power dissipation in a sinusoidally pulsed column with square-law friction. In the present notation, the average predicted [20] dissipation rate is:

$$J = 4\rho S_0 F A^3 \omega^3 / 3\pi . \qquad (12)$$

The experimental measurement of the work done by the air space on the water is described above. The experimental power dissipation rate was obtained as follows:

$$J = [\text{Area of } P\text{–}V \text{ diagram, ft lb}] \times 2f . \qquad (13)$$

The factor 2 is included because the apparatus contained two working gas spaces. The measured and predicted power dissipations are compared in Fig. 5. It will be seen that, whereas the packed column measurements are mostly within 10 per cent of the prediction [20], the data with 24 baffle plates are all about 30 per cent too low. The single-plate results appear to agree with the theory but this may not be significant because of the relatively large additional effect of wall friction and bends (see section on air consumption).

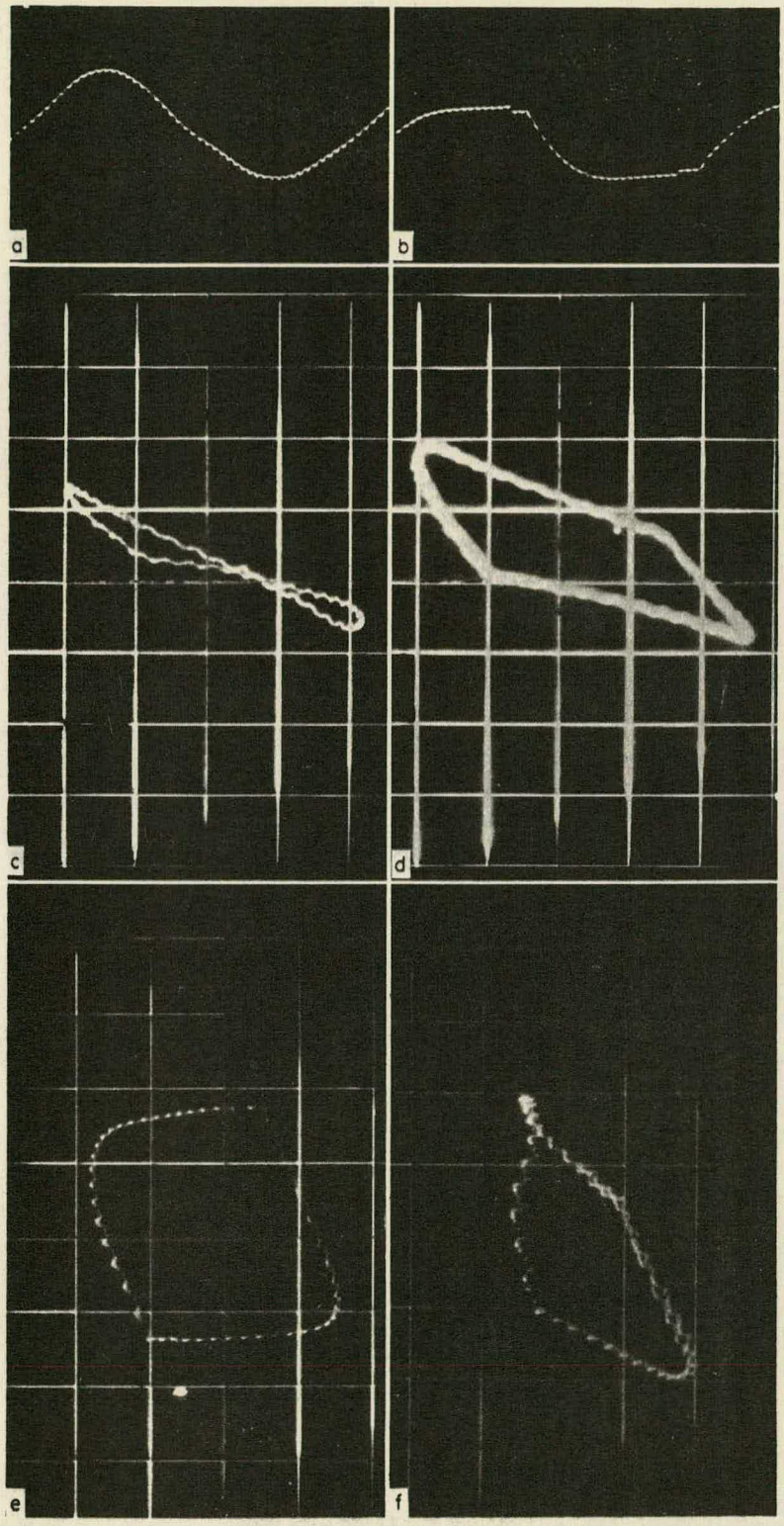

FIG. 4. (a) Volume vs. time for l.h. air space. (Packed column).
(b) Pressure vs. time for l.h. air space (packed column).
(c) *P–V* diagram for l.h. air space (Unbaffled column).
(d) *P–V* diagram for l.h. air space (Baffled column).
(e) *P–V* diagram for l.h. air space. (Packed column).
(f) *P–V* diagram for l.h. air space. (Gassed, baffled column).

Facing page 1668

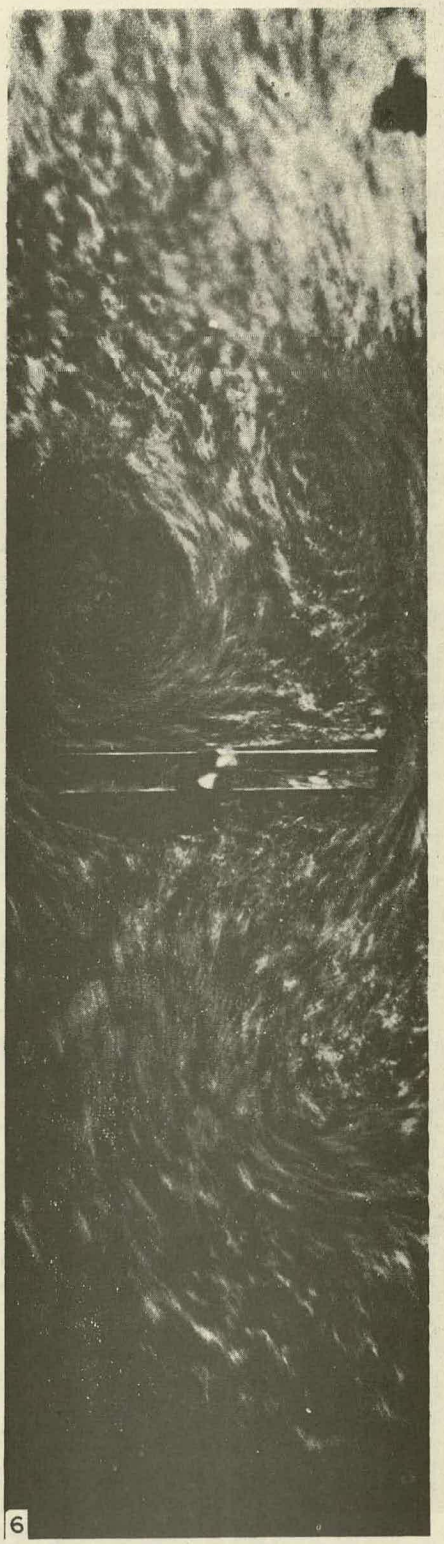

FIG. 6. Pulsating flow past a fixed plate.

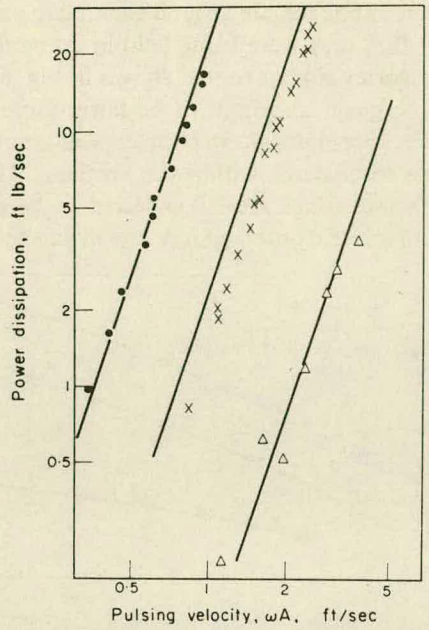

FIG. 5. Power dissipation as a function of amplitude × frequency. Theory [20] shown as lines. Symbols: as in Fig. 2.

The values assigned to F in Eqs. (10) and (11) are necessarily "steady-state" values as there is no relevant data on drag in unsteady flow. It was thought that the unexpectedly low power dissipation with baffle plates might be due to some unsteady-flow effect. An experimental pulsed column was accordingly constructed of perspex, with a rectangular cross section of internal width 4 in. and depth $\frac{1}{2}$ in. A brass plate was mounted centrally within the rectangular duct, leaving two apertures $\frac{2}{3}$ in. wide for the water flow. The dimensions were chosen for geometrical similarity to a section of the baffled column. Sinusoidal pulsations were applied at about 1 c/s and aluminium powder was added so that the flow patterns could be observed. Figure 6 illustrates the most striking feature of the flow patterns, namely, the large vortices which built up on the "downstream" side of the plate during each half-cycle. Similar flow patterns have recently been observed by MIYAUCHI and OHYA [21] in pulsed perforated plate columns. This is in sharp contrast to the situation in steady flow through an orifice, when only small vortices are formed before being shed into the fluid stream. It was observed that, in pulsed flow, the downstream vortex appeared to wind itself back through the aperture as soon as the flow was reversed. This unwinding process obviously involves the recovery of some kinetic energy which would have been lost in steady flow, and probably accounts for much of the 30 per cent discrepancy in the 24-plate results.

The packed column data agree better with the steady-state theory, as may be expected because vortices are less readily formed in the small, random interstices of the packing.

EFFECT OF DISPERSED GAS

Preliminary experiments were carried out without either baffles or packing in the column. The dispersed gas was found to slightly reduce the frequency in accordance with theoretical prediction [13]. However, the pulsations did not bring about any appreciable increase in the gas hold-up, nor was any disturbance of the rising bubbles noticed.

The characteristics of the packed pulsed column in the presence of a dispersed air flow are given in Fig. 7. Comparison of the frequency data with those in Fig. 2 shows that the dispersed air causes a slight increase in the operating frequency. This effect is further discussed in connexion with the baffled

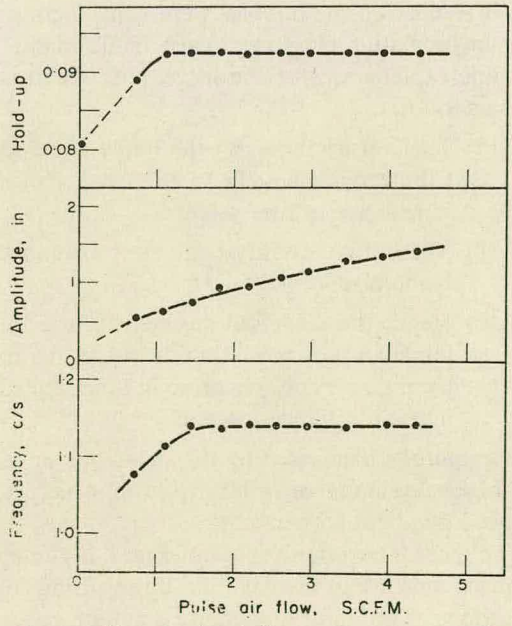

FIG. 7. Effect of pulse air flow on frequency, amplitude and gas hold-up at a superficial gas velocity of 0·0324 ft/sec, with 3·3 ft of packing.

column data (see below). The amplitude at a given pulse air flow is not appreciably different from that in the absence of dispersed air (Fig. 2). The variation of gas hold-up is shown at the top of Fig. 7 and indicates an increase at low pulsation intensities with a levelling off as the amplitude rises above 0·75 in. It was observed that pulsation reduced the average bubble diameter compared with that in the unpulsed column. The plateau in the hold-up curve probably corresponds to a limiting bubble size of the same order as the interstices in the packing. Because of the bubble size reduction, the increase in gas–liquid interfacial area is expected to be greater than the observed 15 per cent increase in the hold-up.

Figure 8 shows the effect of dispersed air upon the performance of the 24-plate column. The frequency of operation at a given pulse air flow tends to increase slightly with dispersed air flow. A comparison between the data for no dispersed gas (Fig. 2) and the points in Fig. 8 indicates that the frequency rises by about 5 per cent as the superficial gas velocity is raised from 0 to 0·085 ft/sec. This result contradicts previous theory and observations [13] showing that dispersed gas reduces the resonance frequency of a liquid column. However, the earlier work [13] concerned a *uniform* gas–liquid dispersion, whereas in this investigation the bubbles were seen to congregate in oscillating clusters at each baffle plate. A possible explanation for the increase in frequency runs as follows:

(a) The constrictions at each baffle plate contribute quite largely to the total acoustic impedance of the system.

(b) The bubble density is greatest around the baffle plates.

(c) Hence the dispersed gas reduces the total impedance by more than it would in a uniform dispersion, resulting in a net increase in the resonance frequency.

The amplitude is affected by dispersed gas only at the highest velocity of 0·085 ft/sec at which it is reduced by about 15 per cent.

The most interesting aspect of Fig. 8 is the pronounced increase in the gas hold-up resulting from pulsations. The factor of increase is as high as 3 and is almost independent of the superficial dispersed gas velocity. As already mentioned, the bubbles were seen to congregate around each plate and it is thought that they were being held in an oscillating annular vortex similar to that shown in Fig. 6. The bubble diameter appeared to be fairly uniform at 2–3 mm so presumably the bubbles would not have had time to coalesce within the vortices. The increase in interfacial area is expected to be of the same order as the observed increase in gas hold-up.

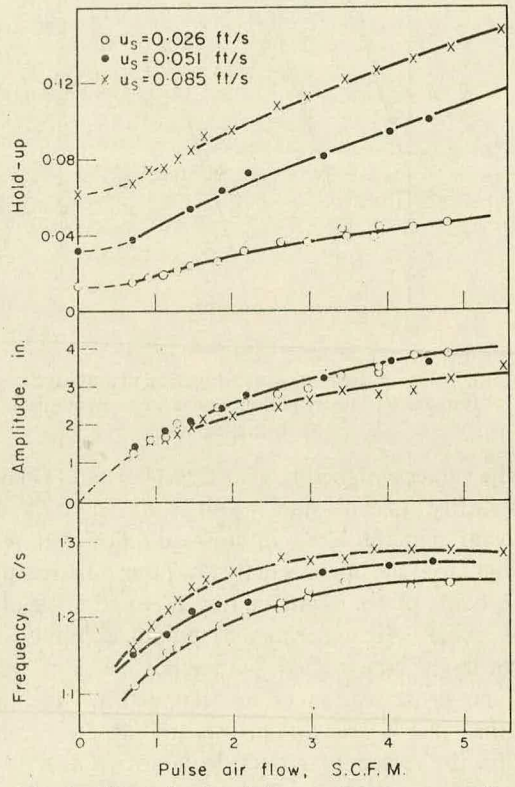

FIG. 8. Effect of pulse air flow on frequency, amplitude and gas hold-up with 24 baffle plates.

POWER DISSIPATION WITH DISPERSED GAS

Measurements were carried out at superficial gas velocities of 0·051 ft/sec and 0·085 ft/sec and the results are given in Fig. 9. Comparison between Fig. 9 and Fig. 5 shows that the power dissipation is not much different from that in the absence of dispersed gas. The data at a velocity of 0·051 ft/sec appear slightly higher than the ungassed values (Fig. 5), but the difference may not be significant. The trace of the P–V diagram became somewhat irregular at low amplitudes because of the effect of gas bubbles on the liquid level probe [see Fig. 4(f)].

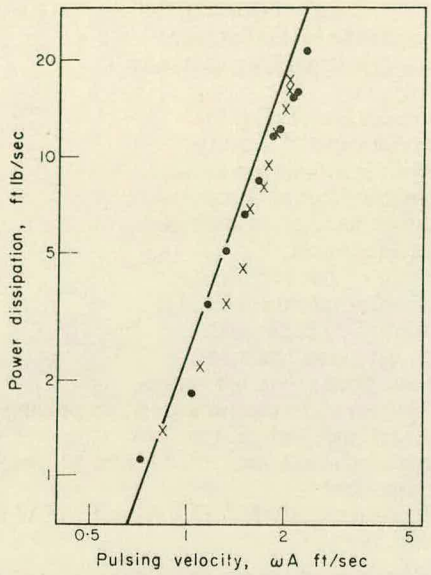

FIG. 9. Power dissipation in gas–liquid dispersions. Theory for no dispersed gas [20] shown as line. Symbols: as in Fig. 8.

It is interesting to compare the above results with those found for stirred tanks [22, 23] in which dispersed gas causes a marked reduction in power dissipation at a given impeller speed. The reduction in power has been attributed [23] to the "flooding" of the impeller by gas bubbles drawn in by its rotation. In the present apparatus, dispersed gas appeared to increase the power dissipation slightly at a given pulsing velocity, even though the bubbles tended to cluster around the baffle plates, leading to a flooding effect. The reason for the higher than expected power dissipation may lie in thermal losses by conduction from the pulsating bubbles. DEVIN [24] has reviewed past work on this effect which is well known at sonic and ultrasonic frequencies. It may be concluded that only part of the measured power in a pulsed gas dispersion is effective in producing turbulence, the remainder being converted directly to heat.

COMPARISON WITH STIRRED TANKS

The present data on hold-up may be correlated empirically with the specific power J_S (h.p./ft^3) and the superficial gas velocity u_S. Most of the data on Figs. 8 and 9 are approximately represented by:

$$\varepsilon = 4{\cdot}5 J_S^{0{\cdot}33} u_S \qquad (14)$$

This relation is shown in Fig. 10. The effectiveness of pulsation in increasing hold-up may be compared with the extensive data of FOUST *et al.* [25] on stirred tanks using the air–water system. Their results were correlated as follows:

$$\varepsilon = 1{\cdot}5 J_S^{0{\cdot}47} u_S^{0{\cdot}53} . \qquad (15)$$

Hence we can obtain a ratio, R, of the hold-up in the pulsed column to that in a stirred tank at the same values of J_S and u_S:

$$R = 3 J_S^{-0{\cdot}14} u_S^{0{\cdot}47} . \qquad (16)$$

Values of R for typical values of J_S and u_S are given in Table 2. It may be concluded that pulsation is more effective than stirring at high superficial gas velocities, but less so at low gas velocites. It should be emphasized that Table 2 applies only to gas hold-up, but it is hoped soon to obtain data on gas–liquid interfacial areas and mass transfer rates [14], which will allow a more thorough comparison to be made.

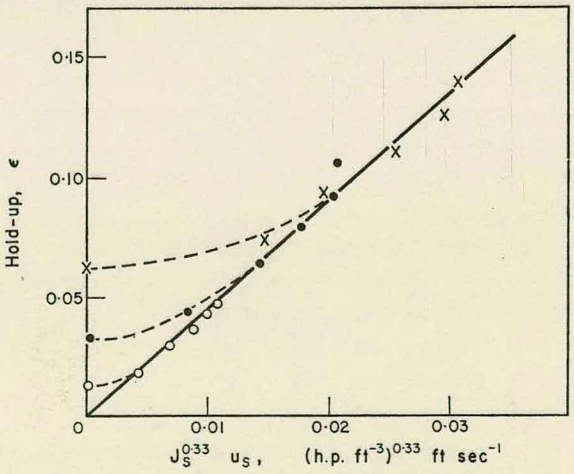

FIG. 10. Empirical correlation of gas hold-up. Symbols: as in Fig. 8.

TABLE 2. RATIO OF ADVANTAGE R OF PULSATION RELATIVE TO STIRRING [25]

J_S(h.p./ft^3)		0·01	0·02	0·05
u_S, ft/sec	0·02	0·91	0·83	0·72
	0·04	1·27	1·15	1·01
	0·08	1·76	1·59	1·40

CONCLUSIONS

This investigation has shown that low frequency pulsation is an effective means of agitating gas–liquid dispersions on a pilot scale. The observed increase in hold-up is similar to that found [4, 7] using higher frequency vibrations on a small scale. The measured air consumption and power dissipation agree very approximately with predictions based on steady-state models [16, 20], but there is some evidence that the pulsed flow around the baffle plates is not fully developed. The observed power dissipation is up to 10 h.p. per 1000 gal which is similar to the range obtainable in stirred tanks. As a means of increasing gas hold-up, pulsation is more effective than mechanical stirring [25] at superficial gas velocities above 0·04 ft/sec. Another possible advantage of pulsation might be in the agitation of non-Newtonian liquids such as fermentation broths, in which the turbulence due to a conventional rotating impeller tends to be localized [23]. With pulsation in a multi-baffled column, the agitation is more uniformly distributed.

Acknowledgment—One of us (J.H.G.) is grateful to the Science Research Council for financial support.

NOTATION†

A	amplitude (= half stroke)
D	equivalent packing diameter
f	frequency
F	friction factor, Eq. (9)
g	acceleration of gravity
h	depth below liquid surface
H_L	length of liquid column
J	power dissipation, ft lb/sec
J_S	specific power, h.p./ft^3
L	length of packed section
M	pulsation number, Eq. (1)
N	number of baffle plates
P_A	atmospheric pressure
P_0	mean pressure in air space
Q	volumetric air consumption for pulsing
R	ratio of advantage, Eq. (16)
S_0	cross-sectional area of U-tube at gas–liquid interface
S	cross-sectional area of non-uniform U-tube
u	velocity
u_S	superficial dispersed gas velocity
V_G	air space volume
x	displacement of liquid level from equilibrium
$\dot{x}$	velocity of liquid column
$\ddot{x}$	acceleration of liquid column
γ	ratio of specific heats (= 1·4 for air)
ΔP	pressure difference
ε	gas hold-up
ρ	liquid density
σ	fractional open area
ϕ	shape factor
ψ	voidage
ω	angular frequency

† Units are in ft lb sec absolute system unless otherwise stated.

REFERENCES

[1] BRETSNAJDER S. and PASIUK W., *Bull. Acad. Pol. Sci. Sér. Sci. Chim.* 1962 **10** 153.
[2] *Idem, Int. Chem. Engng* 1964 **4** 61.
[3] BUCHANAN R. H., TEPLITSKY D. R. and OEDJOE D., *Ind. Engng Chem. Process Design Devel.* 1963 **2** 173.
[4] HARBAUM K. L. and HOUGHTON G., *J. appl. Chem., Lond.* 1962 **12** 234.
[5] JAMESON G. J., Ph.D. Thesis, Cambridge 1963.
[6] MIREV D., BOYADZHIEV L. and BALAREV K., *Izv. Inst. Obshcha Khim., Bulgar., Akad. Nauk.* 1961 **8** 47, 83.
[7] VEVIOROVSKII M. M., DILMAN W. V. and AIZENBUD M. B., *Khim. Prom.* 1966 **42** 783.
[8] BAIRD M. H. I., *Chem. Engng Sci.* 1963 **18** 685.
[9] *Idem., Can. J. Chem. Engng* 1963 **41** 52.
[10] FRITZ C. G., PONDER C. A. and BLOUNT D. H., *N.A.S.A.* Memorandum TM X-53180 1966.
[11] BUCHANAN R. H., JAMESON G. J. and OEDJOE D., *Ind. Engng Chem. Fundls* 1962 **1** 82.
[12] JAMESON G. J., *Chem. Engng Sci.* 1966 **21** 35.
[13] BAIRD M. H. I., *Proc. A.I.Ch.E./I. Chem. E. Symposium on Transport Phenomena, London.* p. 53, 1965.
[14] BAIRD M. H. I. and GARSTANG J. H., To be published.
[15] LORD RAYLEIGH, *Theory of Sound*, Art. 306, Macmillan 1929.
[16] VERMIJS W. J. W., *Proc. A.I.Ch.E./I.Chem.E. Symposium on Transport Phenomena, London*, p. 98, 1965.
[17] VAN ZANDT J. P., *Phys. Rev.* 1917 **10** 415.

[18] PERRY J. H., CHILTON C. H. and KIRKPATRICK S. D. Eds., *Chemical Engineers Handbook*, 4th edn, 5–51, McGraw-Hill 1963.
[19] *Idem., ibid.* pp. 5–35.
[20] JEALOUS A. C. and JOHNSON H. F., *Ind. Engng Chem.* 1955 **47** 1159.
[21] MIYAUCHI T. and OHYA H., *Chem. Engng, Tokyo* 1965 **29** 125.
[22] COOPER C. M., FERNSTROM G. A. and MILLER S. A., *Ind. Engng Chem.* 1944 **36** 504.
[23] HAMER G. and BLAKEBROUGH N., *J. Appl. Chem., Lond.* 1963 **13** 517.
[24] DEVIN C., *J. Acoust. Soc. Am.* 1959 **31** 1654.
[25] FOUST H. C., MACK D. E. and RUSHTON J. H., *Ind. Engng Chem.* 1944 **36** 517.

Résumé—Une colonne d'eau résonnante à air pulsé a été réalisée pour expérimenter l'absorption de gaz: son diamètre intérieur est de 76mm et la longueur effective d'inertie de la colonne oscillante est de 4,28m à 5,18m. L'amplitude atteind jusqu'à 152mm à des fréquences variantes de 0,9 à 1,4 c/s et les expériences ont été entreprises sur des colonnes non garnies, garnies avec des anneaux de 12,70mm placés au hasard et munies de chicanes. On a mesuré la consommation d'air pulsé, la dispersion de puissance et la retenue de gaz quand l'air passe dans l'eau. La consommation d'air pulsé et la dispersion de puissance observées s'accordent approximativement avec les prévisions théoriques basées sur un modèle à l'état presque stable. La retenue de gaz qui accompagne une alimentation d'air indépendante dans la colonne à chicanes augmente du triple à chaque pulsation, ce qui apparaît donc comme étant plus efflcace que le brassage traditionnel au cours duquel la vitesse superficielle du gaz dépasse environ 12,19 mm/sec.

Zusammenfassung—Eine resonanzgebende Wassersäule mit Luftimpulsen wurde für Gasabsorptionsversuche entwickelt; sie hat einen Innendurchmesser von 76 mm (3″) und eine wirksame Trägheitslänge von 14,17 Fuss als Schwingungssäule. Die Amplitude beträgt bei Frequenzen von 0,9 bis 1,4 Perioden/Sek. bis zu 152,5 mm (6″). Versuche wurden mit einer lecren Säule, mit beliebig verteilten Ringen als Füllung und mit einer mit Prallblechen ausgestatteten Säule durchgeführt.

Zu den gemessenen grössen gehörten der Verbrauch an Impulsluft. Leistungsverbranch und Gasstanning beim Luftdurchgang durch das Wasser. Der beobachtete Verbrauch an Impulsluft und der Leistungsverbranch stimmen ungefähr mit theoretischen Vorhersagen überein, die auf der Basis eines quasi stanning beim Luftdurchgang durch das Wasser. Der beobachtete Verbrauch an Impulsluft und der Leistungsverbranch stimmen ungefähr mit theoretischen Vorhersagen überein, die auf der Basis eines quasi Stationär arbeitenden Modells gemacht wurden. Die Gasstanning infolge einer separaten Luftzufuhr stieg in der Prallblechsäule bis aufs Dreifache unter dem Einfluss der Schwingungen, die bei einer Oberflächen-Gasgeschwindigkeit von mehr als 0,04 Fuss/Sek. wirkungsvoller als normales Rühren zu sein scheinen.